




REVIEW

A survey on reconfigurable intelligent surfaces: Wireless communication perspective

Saber Hassouna  | Muhammad Ali Jamshed | James Rains | Jalil ur Rehman Kazim | Masood Ur Rehman  | Mohammad Abualhayja | Lina Mohjazi | Tei Jun Cui | Muhammad Ali Imran | Qammer H. Abbasi 

James Watt School of Engineering, University of Glasgow, Glasgow, UK

Correspondence

Saber Hassouna, James Watt School of Engineering, University of Glasgow, Glasgow, UK.
Email: s.hassouna.1@research.gla.ac.uk

Funding information

Engineering and Physical Sciences Research Council, Grant/Award Number: EP/T021063/1

Abstract

Using reconfigurable intelligent surfaces (RISs) to improve the coverage and the data rate of future wireless networks is a viable option. These surfaces are constituted of a significant number of passive and nearly passive components that interact with incident signals in a smart way, such as by reflecting them, to increase the wireless system's performance as a result of which the notion of a smart radio environment comes to fruition. In this survey, a study review of RIS-assisted wireless communication is supplied starting with the principles of RIS which include the hardware architecture, the control mechanisms, and the discussions of previously held views about the channel model and pathloss; then the performance analysis considering different performance parameters, analytical approaches and metrics are presented to describe the RIS-assisted wireless network performance improvements. Despite its enormous promise, RIS confronts new hurdles in integrating into wireless networks efficiently due to its passive nature. Consequently, the channel estimation for, both full and nearly passive RIS and the RIS deployments are compared under various wireless communication models and for single and multi-users. Lastly, the challenges and potential future study areas for the RIS aided wireless communication systems are proposed.

1 | INTRODUCTION

Although the evolutionary aspect of fifth-generation (5G) has acquired substantial traction, the promised revolutionary view of 5G, a system running nearly entirely at millimeter wave (mmWave) frequencies and enabling diverse internet of things (IoT) services, has remained a mirage so far [1, 2]. Although the 5G wireless network is still deployed around the world, both academia and industry are excited about the future beyond 5G (B5G) which seeks to satisfy more demanding requirements than 5G, such as ultra-high data rates, for example, Gigabit Per Second (Gbps), energy efficiency (EE), global coverage and connectivity, spectral efficiency (SE) as well as high reliability and low air latency [2, 3]. Figure 1 shows the vision and the expectation for the 6G [4] key performance requirements in comparison with 5G. Compared to 5G, 6G must offer a much higher data rate. While the peak data rate for 5G was intended to be 20 Gbps, the goal for 6G is to deliver a peak data rate of

1000 Gbps and a user experience data rate of 1 Gbps. The entire network performance must be enhanced in order to deliver advanced multimedia services to a large number of users, for example, by aiming to achieve spectral efficiency that is twice as high as 5G. As a result, it is critical to developing sustainably new and inventive technologies to enable future wireless network capacity increase at a moderate and manageable budget, complexities and power consumption with the widespread adoption of user devices that will form the future of IoT.

On the other hand, because of user mobility, time-varying wireless channels are a major challenge in building ultra-reliable wireless communications. Traditional ways to address this problem are either by using different modulation, coding and diversity plans to compensate for channel fading, or adjusting to it using modified power, rate management, and beamforming methods [5]. However, they require extra costs and have a restricted amount of influence over the essentially random nature of wireless channels, making the basic

This is an open access article under the terms of the [Creative Commons Attribution-NonCommercial-NoDerivs](https://creativecommons.org/licenses/by-nc-nd/4.0/) License, which permits use and distribution in any medium, provided the original work is properly cited, the use is non-commercial and no modifications or adaptations are made.

© 2023 The Authors. *IET Communications* published by John Wiley & Sons Ltd on behalf of The Institution of Engineering and Technology.

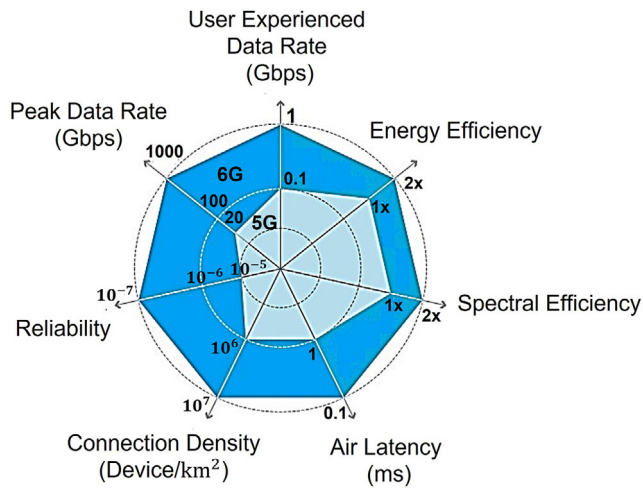


FIGURE 1 Comparison between 5G and 6G [4]

obstacle to establishing wireless communications with high capacity and reliability insurmountable. Moreover, signal transmission is subject to reflections, diffractions, and scattering before arriving at the destination, resulting in a plethora of arbitrarily degraded and deferred extra versions of the source waves along various paths owing to the unpredictability of the radio environment. This channel fading change becomes a fundamental restricting element in wireless network EE and SE performance optimization.

The existing modern physical layer solutions are insufficient, and overall progress is still modest, necessitating new and radical physical layer solutions. There is attracting attention in new communication patterns that exploit the propagation environment's extreme randomness to achieve the target of the simplicity of the transceiver components and the quality of service (QoS). The RIS has recently been added in the wireless communications by the academic researchers [6]. The RIS is a fundamental facilitator for achieving the concept of smart radio environments (SREs) by rendering the wireless environment configurable and adjustable.

RIS is an inexpensive adaptable surface, such as a smart lightweight composite structure layer, that can modulate wireless signals encroaching on it in ways that can be configured and modified using external inputs. As a result, one of the most important characteristics of RISs is their flexibility to be reconfigured after being deployed in a wireless environment. RIS is a metasurface, which is a two-dimensional (2D) electromagnetic (EM) material surface constitutes of multiple passive scattering units. Each unit in the surface can be modified in a method specified by software to change the EM characteristics of the incident signal's reflection on the scattering units. By heavily placing RISs in wireless networks and intelligently organizing their reflections, the propagating signals in wireless channels between sources and destinations can be freely reconfigured to obtain targeted realizations and distributions. Consequently, they introduce a better way to essentially address the fading channel deficiency, interference problem and potentially gives a practical solution.

RIS's aided future wireless networks have recently prompted substantial research. In the literature, a few publications have provided an overview of research on RIS and its variants from various perspectives. Realistic simulations and tests have shown the smart radio environment's potential to increase transmission performance in a variety of wireless networks by using the RIS's tunability. The author in [7] described the active wall, and how it works by manipulating the wireless environment via an active frequency-selective surface (FSS). The intelligent wall's major objective is to switch the active FSS on and off dynamically to modify its EM properties, which affects the propagation environment and hence, the system performance. More interestingly, in [8] the authors proved the advantages of deploying the low-cost devices into a building's walls to transmit and reflect wireless waves actively and passively, respectively. The paper [9] provides a novel technique for controlling the behavior of wireless environments that is predictable and programmable. The major enabler is the hypersurface tile, a novel class of planar meta-materials that can engage with encroaching EM radiation in a manageable way. EM waves may be re-engineered in many ways using hypersurface tiles, including total absorption, polarisation manipulation, and more. Multiple tiles are used to cover items in both indoor and outdoor conditions, such as facades of the buildings and other items. To better meet the demands of communication devices, an external software service determines and delivers the ideal interaction types per tile. Simulations are used to evaluate the new concept's potential. The researchers in [10] implement and evaluate many physical layer building-block solutions for a configurable wireless network and proposed the KPCONFIG method which is a new way to setting the programmable wireless environments (PWE), allowing for multi-user support and flexibility in expressing resource sharing policies and user communication goals. Furthermore, it uses an accessible model based on well-known ray-tracing principles to illustrate the underlying physics of hypersurfaces' unique ray-manipulation capabilities. The incident radio frequency (RF) waves may be configured with the desired response by regulating the distribution of the current over the hypersurfaces, resulting in a reconfigurable wireless environment. The programmable wireless environment can improve the performance of transmission relating to signal strength, communication coverage, EE, and SE performance by reducing signal pathloss, multi-path fading, and co-channel interference. Rather than using hypersurfaces, the authors in [11] proposed Scatter-MIMO, which employs a smart surface to maximize the scattering in the surroundings to give MIMO spatial multiplexing gain.

Wireless networks aided by the RIS are expected to change the existing network optimization patterns by incorporating the smart wireless environment into network optimization issues and are predicted to take a proactive role in the future wireless networks [16]. There have been several recent works reviewing the RIS based smart radio environment [3, 13] and repeating these reviews would not do a fair study however in comparison to prior publications, our work provides a thorough investigation of the RIS's theoretical foundations as well as a current evaluation of its most recent uses in wireless

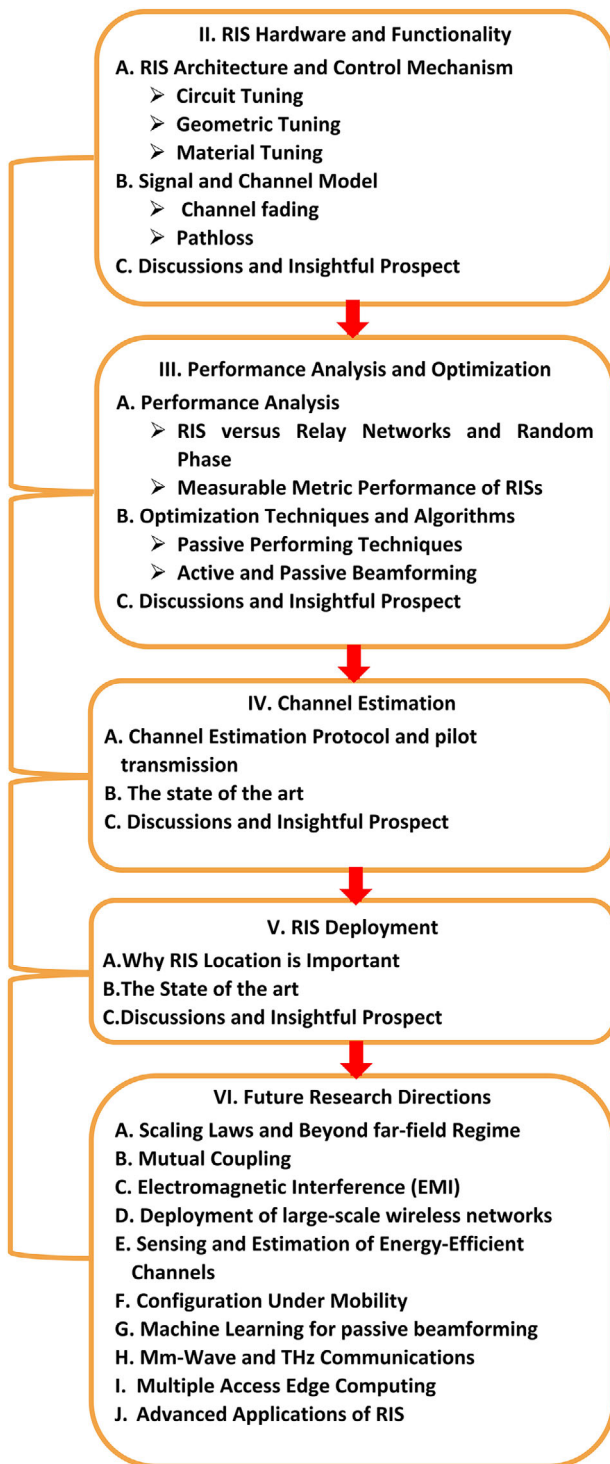


FIGURE 2 Structure of the paper

networks. The following are the highlights of our important contributions:

- An extensive study of the recent RIS works (as shown in Figure 2) including some areas of research that are not fully covered in the prior review publications in order to help the readers to grasp the RIS technology more deeply. We start

from the RIS architecture and control mechanism covering, the design and the types of tuning mechanism, circuit, geometric and material. We classify them from the perspective of research volume as per Figure 5 and by referring to different papers in Table 2 where the tuning method is shown for different publications in the literature. In addition to the channel correlation fading and practical pathloss models which characterize the signal and channel model in RIS-aided communication. Then, we concentrate on the performance analysis and optimization techniques by categorizing different papers according to their design goal, RIS functionality and the applied algorithms with their degree of conversion and optimality. For instance, the majority of the authors are relying on the alternating optimization (AO) method with sophisticated techniques and algorithms to maximize the data rate. Consequently, the need for low complex techniques and less elapsed time algorithms is becoming vital to jointly optimize the passive and active transmissions.

- We provide channel estimation methodologies that describe the estimation protocols and pilot transmission, which are not clarified in the other survey papers. Consequently, more advanced pilot transmission dedicated to aiding the RIS systems is still necessitating more exploration and investigation in the literature. Assuming the channel state information (CSI) availability at the transmitter and the receiver is impractical and a preceding channel estimation phase is required at the receiver. Furthermore, different RIS deployments methods were discussed to ensure that such passive RIS surfaces are deployed in a different way from the active networks that contain active nodes and relays.
- In the literature, the assumption of lossless amplitude and continuous phase yields encouraging analytical and simulation results. However, in actual hardware, energy loss is inescapable, and a practical phase shift model should take these losses into account.
- The shortcomings and the overoptimistic conclusions are discussed thoroughly in this review paper. For example, much research is considering certain system assumptions and dropping or ignoring other parameters that are vital for practical wireless systems, for example, mutual coupling, time-variant channels, Doppler shifts & mobility, discrete phase shifts models and electromagnetic interference are still needing more extended efforts and future exploration to enhance the research quality.

Table 1 illustrates the comparison of this work with the existing magazines/surveys/tutorials in the context of RIS. Compared with other surveys, we strive to reveal some important gaps which are not fully covered in the literature. The tuning mechanism are further explored to reflect the key feature in the RIS from communication perspective. The integration between the backscatter communication and the RIS is important to be more investigated to reap more rewards of power consumption systems and reduced power IOT technologies. Furthermore, new additions, such as pilot transmission and channel estimation for wideband communication are essential to look for refined communication models that leverage

TABLE 1 Comparison with other surveys/tutorials researches

Ref.	Description	Comparison to Our Work
[12] [3] [13] [14] [15]	<p>particularly interested in RIS operating principles, performance assessment, beamforming design, and resource management, as well as the integration of RISs with other developing technologies</p> <p>seeks to give an in-depth technical explanation to help and inspire future research in RIS-assisted wireless networks modelling, analysis, design, optimization, and implementation.</p> <p>Concentrates on the applications of the RIS in wireless communications and look at several performance metrics and analytical methodologies.</p> <p>provides an overview of the technical and crucial features of mathematical optimization and performance analysis of LIS systems, as well as a few potential research paths for the formulation of real challenges beyond 5G systems in the future. Outlines Capacity/data rate assessments, power/spectral optimizations, channel prediction, deep learning-based design, and reliability analysis.</p>	<p>Different from other surveys and overviews, our paper presents crucial and critical technical aspects of reconfigurable intelligent surfaces including the physical operational principle and channel model. It is then evaluates the performance metrics and optimization techniques in the literature taking into account the limitations, shortcomings and impractical assumptions that lead to overoptimistic results. The pilot transmission, channel estimation and different deployments methods for RIS are all topics that still need more investigations to the best of our knowledge. An outlook for the lessons learnt and summary is given at the end of each section. Finally, a proposal for future directions is highlighted to include the RIS applications not only from the channel and performance perspective but also when involving the RIS in digital information world.</p>

the electromagnetic properties to comply with realistic wireless communication applications. Moreover, lower computational complexity RIS-based algorithms that consider reduced number of operations and less elapsed run time are still requiring more investigations and thorough scrutiny

The remainder of this paper is structured as set out in Figure 2. The RIS hardware and functionality, including signal and channel models, hardware design, and control mechanisms are covered in Section 2. Section 3 considers the performance analysis and optimization of RIS-assisted wireless systems. We overview promising approaches for RIS channel estimates in Section 4, which apply to a variety of RIS topologies and communication settings. In Section 5, we look at how to deploy RISs at both the link and network level. We propose challenges and research direction for the future in Section 6. Finally, Section 7 brings this survey paper to a conclusion.

2 | RIS HARDWARE AND FUNCTIONALITY

In this section, we cover the fundamentals of RIS-assisted wireless communication, including the major RIS architecture, hardware, and control mechanism, as well as the signal and channel models presented in the existing works of literature.

2.1 | RIS architecture and control mechanism

Snell's law and the Fresnel equations control the intensities and directions of reflected and diffracted waves [17]. When the wave collides with a metasurface, the situation changes. A shifting in the resonance frequency and, as a result, changes in the boundary conditions might emerge from the periodic arrangement of the scattering components. Hence, extra phase shifts will be carried by the reflected and diffracted waves. The EM characteristics of the metasurface will be fixed once it is produced with a certain physical structure, allowing it to be utilized for a given aim, such as a ideal absorber working at a specific

frequency. The RIS is made up of a programmable metasurface that can completely regulate the phase changes that individual scattering components experience. This can be accomplished by applying outside stimulus to the scattering components, causing their physical characteristics to alter, resulting in a change in the metasurface's EM properties without refabrication [18].

Figure 3a depicts a typical RIS design, which includes three layers and a smart controller. The first layer (RIS layer) is made up of a dielectric substrate with several tunable and reconfigurable metallic patches put on it to directly regulate incoming waves. A copper substance is typically used in the second layer to avoid transmission power losses due to RIS reflection. The third layer is a control integrated board that is in charge of both excitation and real-time control of the reflecting elements' reflection amplitudes and phase shifts. Moreover, a smart controller linked to each RIS also activates and decides reflection adaptation, which may be done with a field programmable gate array (FPGA). Other network components such as base stations (BSs), and user terminals can link to each other over wired or wireless backhaul and control lines thanks to the RIS controller's role as a gateway. In practice, dedicated sensors can be deployed in the first layer, for example, interlaced with the RIS's reflecting elements, to detect the surrounding radio signals of interest and assist the smart controller in designing the reflection coefficients, to enhance RIS's environmental learning capability [3]. There are three basic categories for the different tuning processes that have been proven in the literature namely:

- 1) Circuit tuning comprises the integration or modification of individual impedance into the unit cell circuit model using changeable capacitors and switches inside and between unit cells.
- 2) Geometric tuning refers to techniques that change the form of the unit cell physically, causing the accompanying circuit model to change dramatically.
- 3) Material tuning is the process of modifying the material properties of a substrate or small section of a unit cell to change the responsiveness and characteristics of the substrate layer or small component of the unit cell.

TABLE 2 List of publications related to RIS from the smart radio environment (SRE) perspective

Reference	Surface architecture	Control Mechanism	System Setup	Achievement
[7]	Active frequency selective surfaces (FSS) with PIN diodes connecting metal parts of the FSS	ON-OFF PIN Diodes	Multi-user wideband indoor downlink OFDMA system	Surfaces that are fully reflected with proper coverage and can boost system performance by up to 80%
[8]	Programmable Radio Environment for Smart Spaces (PRESS) Low-Cost antenna elements connected to passive loads and embedded in the walls of a building	prototype PRESS elements equipped with (SP4T) RF switches change phase of each antenna by $\pi/2$	Multi-client's wideband system	Passively reflect or actively transmit radio waves, and so attenuate or enhance signal strength by up to 26 dB, to reconfigure multipath propagation
[9]	Hypersurface tile equipped with physical switch elements	Switch element Controllable state (ON/OFF)	12 receivers, in both microwave and mmWave frequency bands, are uniformly distributed in indoor space and are evaluated using a map-based ray-tracer	Re-engineering EM waves, including steering in any direction, complete absorption, polarisation modification, and other techniques. With maximum and minimum received power of 32.5 dBm and 12.4 dBm, respectively, and an average received power of 20.6 dBm, the results demonstrate Good Coverage.
[25]	Spatial microwave modulators (SMM) equipped with 102 controllable EM reflectors	Two states of resonant elements (the reflector and the parasitic strip), π state and 0 state	Two antennas source and receiver connected to network analyzer are located in a room that the spatial microwave modulator can be placed on the walls of the room	Increasing or cancelling the wireless transmission amplitude between two antennas (Shaping complex microwave field). SMM can perform wave front shaping and concealing the field around one single antenna on a correlation length wide area (6 cm at 2.4 GHz)
[26]	Reflect-array panel with totally 48 reflector units and its peripheral circuits and varactors	each reflector is controlled by a bias voltage to tune the varactors (0.6 – 8pF) for changing the capacitance and hence the phase of each unit	Two pairs of wireless users in a conference room where smart reflect array hung on the walls	Controlling the phase shift of each reflect-array element. The interference has been eliminated, and the interference-plus-noise ratio (SINR) has been enhanced to around 30 dB, according to the achieved results
[27]	Intelligent receiving antenna array	the information transfer capabilities of an intelligent surface for every m^2 deployed surface area	Multi-user narrow band system with ideal free space propagation	Active surface for transmission and reception. Consequently, the limit of the normalized capacity is enhanced when the wavelength approaches zero
[28]	Hypersurface tile with controllers that regulate the metasurface's switch components	Dynamic meta-atoms include phase switching components like MEMS, CMOS transistors, or microfluidic switches that can change the structure of the meta-atom	mm-wave setups that include a Rx-Tx pair situated in non-line of sight (NLOS) over a defined floorplan and walls covered with hypersurface	New physical layer security features can help avoid eavesdropping. Pathloss and multipath fading mitigation, as well as eavesdropping security, were proven in the 2.4 and 60 GHz configurations
[29]	Plasmonic antenna elements at each transceiver side	New intelligent plasmonic antenna arrays that can function in transmission, reception, reflection, and waveguiding, the mm-wave and THz-bands	Ultra-Massive MIMO (UM MIMO)	In the mm-wave and THz-bands, new intelligent plasmonic antenna arrays capable of communications and waveguiding have been developed. The results demonstrate a significant increase in transmission distance and data rate
[30]	RIS-assisted free-space optical (FSO) systems	Comparable mirror-assisted technology, which can be used to create a phase-shift profile that spans the IRS	A FSO communication system consists of a Tx with a Gaussian beam-emitting laser source (LS), an IRS, and a Rx with a lens and a photo detector (PD)	FSO systems with IRS assistance can compensate the need for a line of sight (LoS) between Tx and Rx. The effect on the end-to-end channel varies depending on where TX, RIS, and RX are in relation to each other

(Continues)

TABLE 2 (Continued)

Reference	Surface architecture	Control Mechanism	System Setup	Achievement
[31]	102 phase-binary components make up the metasurface	The phase shift of the reflected wave may be electrically controlled for each element using a PIN Diode bias voltage from an Arduino microcontroller to be either 0 or π	The transfer of an RGB colour image across a 3-3 MIMO system was simulated using wireless image transmission in an office room	The benefit of shaping wireless channels. Physical shaping of propagation media with simple metasurfaces may achieve complete orthogonality of wireless channels and excellent channel diversity and low crosstalk
[32]	RIS with 16 elements	A method of encoding information in both the sent signal and the RIS configuration	SIMO over a quasi-static fading channel	To boost capacity, a method is utilised that encodes data in the sent signal as well as the RIS configuration. Three times quicker than max-SNR encoding is the joint encoding.
[33]	RIS with large reflecting elements	The best RIS phase shift configuration	Multiple antennas at the transmitter and receiver in a point-to-point RIS-based system	Developing an overhead-aware resource allocation framework where RIS used to improve the performance SE/EE of the system
[34]	256 unit cell programmable surfaces based on varactor diodes	A digital to analogue converter generates an external control signal that controls the phase response of the unit cell	RIS-assisted MIMO wireless system	The proposed prototype implements real-time RIS based MIMO-QAM wireless communication with less power consumption and achievable data rate 20 Mbps

2.1.1 | Circuit tuning

The EM behaviour of actual, passive transmission lines, antennas, and metamaterials may be modelled as a lumped inductive, capacitive, and resistive equivalent circuit. This way of breaking down complex geometric shapes into a known circuit model is highly useful for predicting how updated designs would behave. Metamaterial circuit tuning is described as methods for introducing, altering, and controlling specific components in the metamaterial's equivalent circuit. Due to their ease of combination into a variety of metamaterials, varactor diodes are the most often used tuning method [19]. The incorporation of a varactor in a metamaterial design is frequently referred to as active metamaterial despite the fact that the device remains inactive for RFs and is only active in its desire for a DC bias [20].

The varactors in most cases have been considered as perfect or nearly ideal linear capacitors with good accuracy, although numerous researches have looked at the nonlinearity aspect of the varactor at various power levels [21]. In terms of applicability and simplicity of integration, the use of PIN diodes [22] in a metamaterial is comparable to the use of varactors, although these actuators influence resistance rather than capacitance. In practice, independent amplitude and phase shift control of every RIS element are preferable for superior reflection design, but this needs more intricate architectural patterns and design elements [23] than those listed above for their independent control alone. While continually adjusting the reflection coefficient is advantageous for improving communication performance, it is challenging to put into practice because better quality reflective components need not only more expensive but also more complicated hardware architecture. For instance, at least $\log_2(8) = 3$ PIN diodes are required to allow 8 levels of phase changes per RIS unit. By properly quantizing the intervals $[0,1]$ and $[0, 2\pi]$,

we can calculate the discrete amplitude and phase-shift values, respectively. Even though phase-shift control or phase beamforming can achieve better passive beamforming performance than amplitude control or amplitude beamforming, phase-shift control or phase beamforming for RIS is more expensive to construct when the number of control bits and discrete levels for each reflective element are the same. The authors in [24] proposed a practical reflection model by simulating every reflective component as a resonant circuit with specific inductance, capacitance, and resistance values and depending on his prototype, it was discovered that the reflecting element's amplitude response and phase shift are in general non-linearly linked, and hence are not separately controllable. The reflection amplitude achieves a minimum value at zero phase shift, as shown in Figure 4, but rises uniformly as the phase shift approaches 180 or -180, asymptotically approaching one.

2.1.2 | Geometrical tuning

Many metamaterials depend on conductive components that may combine with encroaching EM signals to produce the required electric or magnetic resonance or other beneficial behaviour. Because metamaterial characteristics are generally influenced by the form, size, direction, and closeness of conducting components, methods that change the geometric features of the conductive elements can be a powerful tool for adjusting or switching metamaterial response. By shifting conducting components in respect to each other, metamaterials may be geometrically adjusted. Micro electromechanical systems (MEMS) are often used in THz metamaterials to accomplish the mechanical movement of conducting components. The coupling between conducting components varies when they are

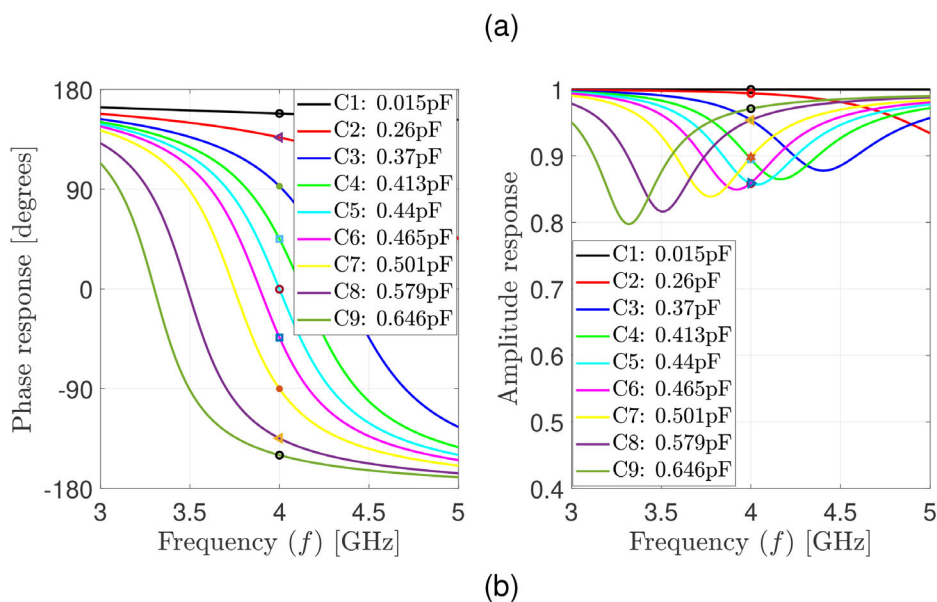
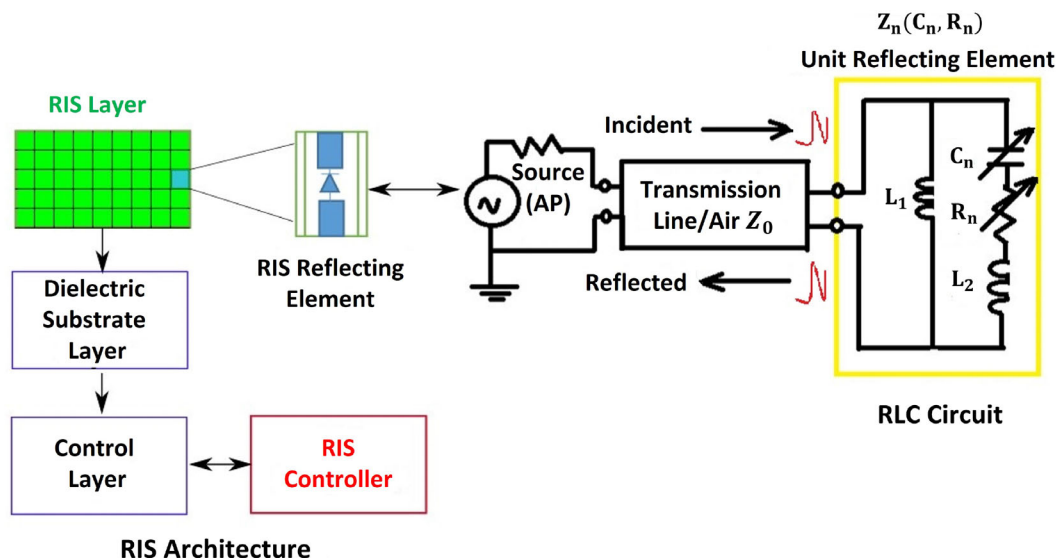


FIGURE 3 (a) the structure of the RIS including its reflecting element and the equivalent RLC circuit model and (b) the amplitude and phase responses for different elements and their corresponding capacitance values.

pushed closer or farther away, resulting in variations in resonance frequency or resonance strength. Moving conducting elements can also alter the shape of the element. Stretching the substrate to further separate the elements on the substrate, resulting in significant variations in the resonance frequency of the elements, is a unique approach for moving conducting components in a metamaterial. Several tunable high impedance surfaces (HIS) have been shown to alter the phase of the reflected wave by mechanically sliding an upper plate of elements along the surface or vertically [19]. Geometrical tuning may result in substantial variations in metamaterial features since the geometry of the conducting elements has such a large influence on the related resonant frequency. Geometrical tuning, on the other hand, is difficult to execute since it necessitates a physical control mechanism.

2.1.3 | Material tuning

While changing the structure of resonant components provides for a number of tuning possibilities, the metamaterial's properties are ultimately determined by the constituent materials used to create the unit cell. Various constituent materials have been examined and used in the literature for tuning metamaterials by changing the permittivity, permeability, and conductivity of unit cell sections. Several candidate materials, such as $\text{Ba}_{0.5}\text{Sr}_{0.5}\text{TiO}_3$ (BST) ferroelectric films, liquid crystal, and Ga-Sb-Te (GST) phase-change materials, have been used to tune the permittivity of metamaterials. More details about the material tuning subject can be found in [19, 35, 36].

The purpose of presenting the three tuning approaches in this review study is to mention that due to its rapid

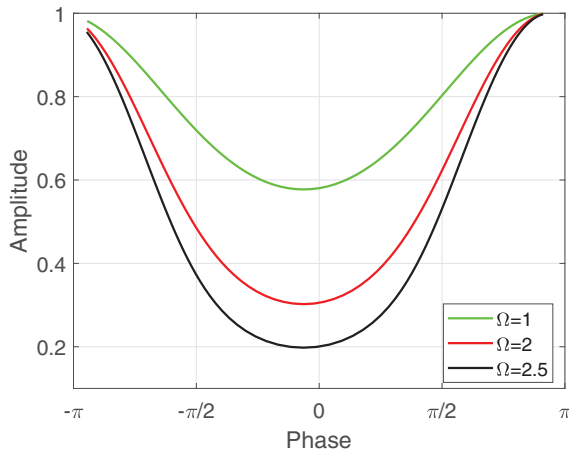


FIGURE 4 Reflected amplitude vs. phase shift for RIS element

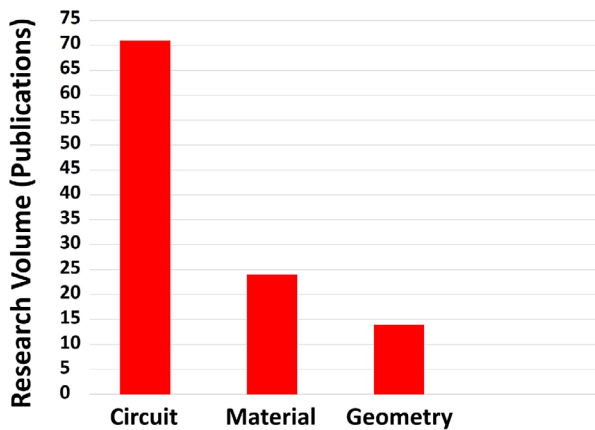


FIGURE 5 Tuning mechanism comparison

reaction time, minimal reflection loss, low power consumption and cheap equipment price, the first technique (circuit tuning) has been widely used in actual applications and implementations. Figure 3a depicts an example of a reflecting element and its corresponding RLC circuit based on a PIN diode installed in the centre of the element. Such illustrations of RLC circuit equivalence have been used widely in the literature. Table 2 provides an overview of the most updated and recent concepts and realizations for a smart radio environment taking into account essential parameters such as surface architecture, control mechanisms, system setup and ending with the outcomes and work achievements. We noticed that high volume of researches depend on the circuit tuning more than the other two tuning methods which coincides with Figure 5 survey.

2.2 | Signal and channel model

2.2.1 | Channel fading

RIS can be coated on the front of buildings in the wireless environment, such as solid structures and top surfaces of

rooms, or carried on aerial vehicles, such as not fixed balloons in the air and UAVs [37], to achieve the idea of the smart radio environment. As a result, for modelling and performance analysis of RIS-aided wireless communication, scientific analysis models that consider the geographical placements of RIS elements, the RIS's EM characteristics, and the wave modifications utilized by adjacent RIS elements in the environment are necessary. A transmitted radio signal in a typical wireless communication environment contacts many objects along the route, resulting in duplicates of the transmitted wave which comes across reflection, diffraction, and dispersion. Multipath components are signal copies that reach the receiver with randomly and unexpectedly different amplitudes, phase shifts, and signal delays, causing considerable distortions in the received signal due to their relative constructive or destructive addition. This is termed as fading in wireless communication systems, and it is a critical parameter in existing and future wireless communication systems.

The basic goal of RIS is to establish a controllable wireless communication in which the extremely unpredictable radio channel is turned into a controllable space by carefully modifying EM signal propagation in a software-controlled manner. A channel model that captures the key characteristics of any wireless technology is required for an accurate performance assessment. The most theoretical work on wireless systems technologies in scattering conditions has been and continues to be based on the independent and identically (IDD) distributed Rayleigh fading channel model [39–41]. When using a rectangular RIS, the authors in [38] shows that such a paradigm does not exist realistically, and present an equivalent physically valid Rayleigh fading model that may be used as a reference for evaluating RIS-assisted communications. The received signal $z \in \mathbb{C}$ can be represented as in literature:

$$z = (V^T \theta G + b_d)x + w, \quad (1)$$

where, x is the transmitted signal with power $p = \mathbb{E}\{|x|^2\}$ and $w \sim \mathcal{N}_{\mathbb{C}}(0, \sigma^2)$ is the noise variance. The configuration of the RIS is given by the diagonal matrix $\theta = \Gamma \Phi$ with $\Phi = \text{diag}(e^{-j\theta_1}, \dots, e^{-j\theta_N})$ and $\Gamma = \text{diag}(\gamma_1, \dots, \gamma_N)$. The direct path $b_d \in \mathbb{C}$ has a Rayleigh fading distribution. However, the fading distribution of the channels $V \in \mathbb{C}^N$ and $G \in \mathbb{C}^N$ is independent and distributed as $V \sim \mathcal{N}_{\mathbb{C}}(0, AD_V C_V)$ and $G \sim \mathcal{N}_{\mathbb{C}}(0, AD_G C_G)$ where A is the area of the RIS element, D is the average attenuation intensity and C is the spatial correlation matrix. Figure 6 shows that non of the cases $d_H = d_V = d \in \{\lambda/8, \lambda/4, \lambda/2\}$ resemble The I.I.D. Rayleigh fading. More details can be found in [38]

2.2.2 | Pathloss

The authors [42] evaluated the two-ray channel model as per Figure 7. In the most perfect propagation scenario, with no user movement and no unanticipated environmental consequences, a single uncontrolled ground reflection might cause substantial signal degradation. The authors assumes that a changeable

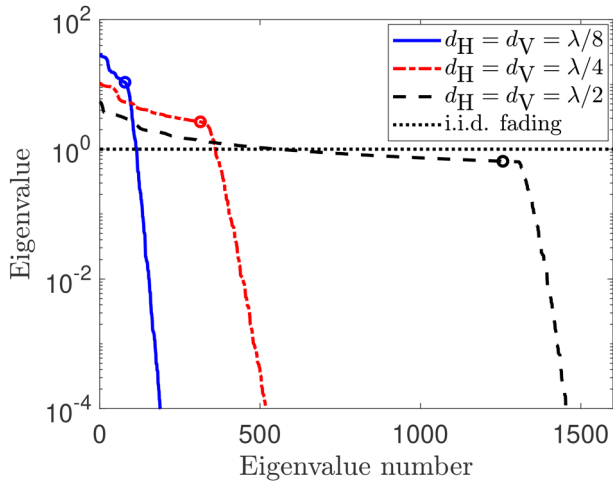


FIGURE 6 The eigenvalues of R in decreasing order for an RIS with $N = 1600$ and $d_H = d_V = d \in \{\lambda/8, \lambda/4, \lambda/2\}$. please, refer to [38] for simulation parameters

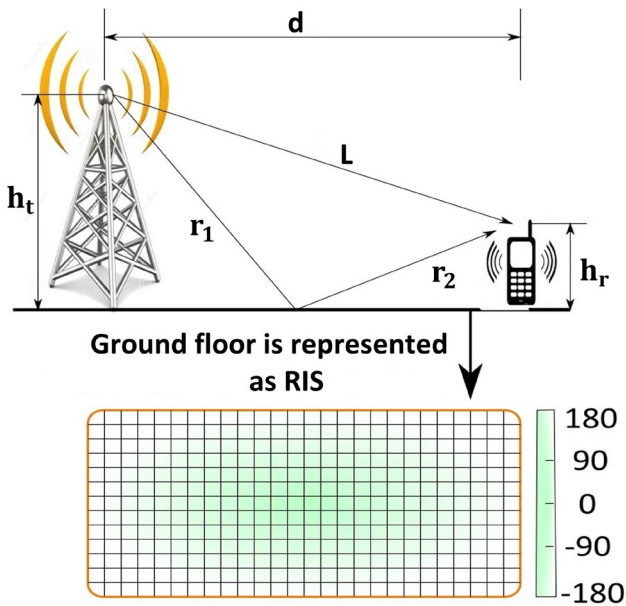


FIGURE 7 Illustration of the pathloss of 'Two Rays' Propagation Model

metasurface covers the whole ground. The RIS may be thought of as a perfect phase shifter, designed to change the reflected signal phase such that the LOS and reflected radiations add up constructively, increasing signal strength. It has been shown that the usage of programmable intelligent surfaces has the possibility to change the scaling rule that regulates the received signal power with distance. Despite the results concluded by [42] are promising, they are not realistic and practical because they were based on several assumptions including the ability to tune the reflected phases without any analogue to digital conversion error and for any incident and scattered angle, as well as the lack of reflection impairments and comprehensive awareness of the phases status at the RIS. Furthermore, for more actual system models, optimizing the phases is typically not a simple process.

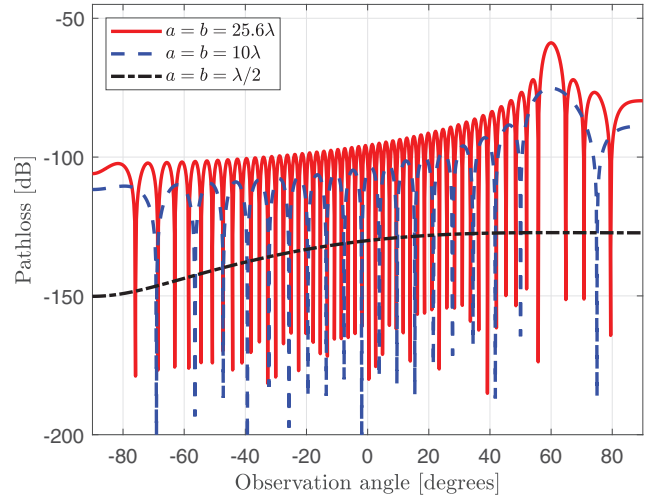


FIGURE 8 Pathloss of the reflected path. Refer to [45] for simulations parameters

By researching the physics and EM characteristics of RISs, the author in [43] develops free-space pathloss models for RIS-assisted wireless communications for various circumstances which can be divided into two groups: RIS-assisted beamforming and RIS-assisted broadcasting. The proposed models reveal the relations between the free-space pathloss of RIS and distances from both the transmitter and receiver to the RIS. To explain the free-space pathloss of RIS-assisted beamforming and broadcasting, three perceptive free-space pathloss models were developed: the far and near fields beamforming equations and the near-field broadcasting equation. The authors in [44] improved the pathloss models derived in [43] by formulating joint radiation pattern of antennas and unit cells in addition to clarifying the relation between the scattering gain of the unit cell and its size.

The authors in [45] calculates the far-field pathloss using physical optics methods and explain why the surface consists of multiple reconfigurable elements that individually behaves as diffuse scatterers but may collectively beamform the signal in a desirable direction with a certain beamwidth. As a result, an RIS can be thought of as an array of sub- λ -sized diffuse scatterers that aiming the phase of their reflected signals at the receiver, resulting in anomalous reflection. Figure 8 depicts the pathloss as a function of observation angle for various RIS sizes. The main beamwidth narrows as the RIS surface area grows. The RIS virtually functions as a diffuse scatterer when the dimension is sub-wavelength (less than $\lambda/2$). The authors proved that the power of the received signal is proportional to the square of the RIS area and to $1/(r_1 r_2)^2$, where r_1 is the distance between the transmitter and the RIS and r_2 is the distance between the RIS and the receiver. This refutes [42] hypothesis that the received power is proportional to $1/(r_1 + r_2)^2$. To compensate for the enormous power loss caused by twofold attenuation, a significant number of RIS reflecting components must be employed to combine their reflection magnitude and phases to obtain higher passive beamforming gains. RIS is made up of several sub-wavelength components that scatter incident waves with distinct

phase shifts in order to perform constructive beamforming in a certain direction.

Using the scalar theory of diffraction and the Huygens-Fresnel principle, the authors in [46] describe pathloss in RISs in both the near and far fields. RISs are represented as homogeneous sheets of EM material with negligible depth. The authors reveal the regimes in which the pathloss relies on the summation and multiplication of the distances between the RIS and the source, as well as the RIS and the destination, using the stationary phase technique. The analytical technique provided is proven to be sufficiently generic for use with a consistent reflecting surface, anomalously behaving reflectors, and lenses with highly concentrating and reflecting features.

The authors in [47] have provided a viewpoint that unites RIS opposing behaviour as a scatterer and as a mirror. It has been proven that the RIS may be seen as a zero, one, or two-dimensional object, depending on its size and distance and its radiated power exhibits a dependency on the fourth, third, or second power of the distance, respectively. In addition, the Fresnel zone decomposition is used to gain a better understanding of how the various variables interact. More precisely, the importance of phase in determining the eventual pathloss exponent is discovered and demonstrated how free space propagation may be outperformed via smart dephasing. The findings are calculated numerically, and the received signal in terms of distance has no clear analytical meaning. [48] reports similar observations.

2.3 | Discussions and insightful prospect for section II

- Figure 5 shows the volume of research (paper publications) using the three approaches of tuning however in this paper we will not list the publications [19] to avoid repeating what other authors have done and worth mentioning that the reasons stated above for the more widespread usage of the first approach is not enough and more research still has to be conducted on the other two approaches to be parallel with the circuit tuning method.
- We have noticed a disagreement between the authors in [45] and the authors in [42] regarding the reflected power in the far-field region as a function of the distance between the transmitter to the RIS and the RIS to the receiver while other researches are in agreement with [45]. Moreover, the correlation fading revealed in [38] clarifies that using the iid fading channel is not encouraged to be modelled in the RIS wireless systems analysis which opens the door for reconsidering previous works depending on the IDD fading models. Table 3 offer a comparison for different pathloss models in the existing literature. The purpose of narrating the previous work is to investigate the pathloss derivations based on strong foundation presenting all the scenarios bearing in mind that pathloss due to distance, large and small scale shadowing and multipath fading are all factors that affect channel coefficients. The pathloss of an RIS reflected channel, in particular, represents the average power of the channel and is therefore

critical for link budget analysis and performance assessment of RIS-assisted wireless systems.

3 | PERFORMANCE ANALYSIS AND OPTIMIZATION

This section is divided into two parts. In the first part, we present the performance analysis of the RIS using different performance metrics like bit error probability and sum rate for evaluating the overall behaviour of the wireless systems aided RIS and under various channels and environments. Furthermore, the second part will concentrate on the RIS reflection optimization techniques and algorithms.

3.1 | Performance analysis

In this study, we will present the RIS advantages and performance comparisons with other wireless systems. furthermore, we show the behaviour and the usage of the RIS as reflector, receiver and transmitter taking into consideration the performance metrics proposed in the literature for RIS supported wireless communication systems like coverage or outage probability, bit error probability, Ergodic capacity, and achievable data rate.

3.1.1 | RISs versus relay networks and random phase surfaces

We first present the following unique advantages of RIS-assisted wireless communications:

- **Densely deployed and sustainable operation:** If RISs are formed of smart metasurfaces, there are a lot of sub-wavelength unit cells in them. Such sub-wavelength heavy installations of small sub-wavelength dispersing devices are not typically used in radio communications, where mutual coupling among the reflecting elements is frequently prevented by design, by confirming that the scattering units are sufficiently far apart. This paves the way for the development of novel wave and propagation scenarios that may have an impact on wireless networks' ultimate performance limits, as well as the introduction of new scenarios in design in which wireless systems are built to be mutual coupling fully cognizant. RIS is easily applied and removed from a variety of surfaces, including front of buildings, interior walls, and top ceilings. The RIS can be battery-free and remotely powered thanks to RF-based energy harvesting, which eliminates the need for active equipments that require signal processing methods and power consumption.
- **New signal processing is not required for RIS-aided communication:** The semi-passive feature of RISs opens new possibilities for re-defining communication, allowing data to be transferred without the use of EM waves, instead

TABLE 3 Pathloss comparison for the existing literature

Reference	Concept	Field	Goal	Notes
[42]	LoS and ground-reflected rays in a two-ray propagation model	Far-field regime	Beamforming	The received signal power is proportional to the square of the RIS area N^2 and inversely proportional to the square sum of the distances between the TX and the RIS and the RIS and the RX $1/(r_1 + r_2)^2$
[43]	The physics and the EM nature of the RIS	Far and near field regime	Beamforming and broadcasting	The received signal power is proportional to the square of the RIS area and inversely proportional to the square product $1/d_1^2 d_2^2$ of the distances between transmitter and RIS and between RIS and receiver
[45]	Physical optics techniques and Antenna Theory	Far-field regime	Beamforming	The received signal power is proportional to the square of the RIS area and inversely proportional to the square product $1/(r_1 r_2)^2$ of the distances between transmitter and RIS and between RIS and receiver
[46]	The Huygens-Fresnel concept and generalized scalar diffraction theory	Far and near field regime	Anomalous mirrors and scatterers	RISs act like anomalous mirrors in the short distance domain while they behave as scatterers in the long-distance regime.
[47]	The Fresnel zone decomposition	Far and near field regime	Anomalous mirrors and scatterers	The RIS can be seen as a zero, one, or two-dimensional object, depending on its size and distance, and its radiated power exhibits a dependency with the fourth, third, or second power of the distance, accordingly.
[49]	Metallic reflectors using measurements, analytical expressions, and ray-tracing simulations	Near field regime	Anomalous mirror	Over the same link distance, the reflected received power is the same as the LoS free space received power for millimetre wave communications

of reprocessing existing EM signals. This may be extremely useful in terms of minimizing EM pollution and lowering human EM exposure, which is often raised by deploying more network equipment and utilizing more spectra. This might be crucial for the effective installations of wireless technology in areas that are vulnerable to EM fields (e.g. in hospitals).

- Highly focusing capabilities:** This high focusing capability could be used for a variety of purposes, including firstly, it enables interference-free communication in densely populated areas, secondly, enabling accurate radio identifications of users and environment modelling, and lastly, fill the batteries of limited power equipment by means of transfer the power wirelessly. The intelligent wireless wall (IWW) is a real-world example of this high focusing characteristic. The IWW consists of a reconfigurable intelligent surface that does beam steering and beamforming, as well as machine learning algorithms that can accurately and automatically identify human activity [50].
- Flexible reconfiguration and enhanced capacity:** The RIS may be used to configure the wireless channel to provide a larger link capacity while consuming less power for point-to-point communications. When the RIS is used, interference reduction becomes more effective, resulting in improved signal performance for end users at the cell's edge. Scattering components in multi-user cellular networks can be separated and shared to optimise data transfer for multiple users. As a consequence, the RIS-assisted wireless network may be able to improve QoS provisioning as well as sum-rate performance or max-min fairness amongst users.
- Investigating of new wireless application:** The RIS's advancement is likely to open the door for new and exciting research avenues. The RIS, for example, was recently presented as a unique technique for avoiding wireless eavesdropping assaults by regulating the transfer at the source and the optimized reflections at the RIS at the same time. The achievable secrecy rate is greatly enhanced by deploying the RISs close to the legitimate or eavesdropping user and

appropriately configuring the RIS passive beamforming to raise or lower the achievable rate of the legitimate or eavesdropping user [51]. Despite the said feature in RIS-aided secrecy communication, the channel state information CSI is still needed between the AP and eavesdroppers as well as between the RIS and the eavesdropper. The challenge is obvious when the eavesdroppers intentionally continue to be covert, secret or hidden due to the fact that their CSI link cannot be estimated properly from their signal leakage, and this thus requires new channel estimation methods and robust RIS beamforming taking into account the imperfect CSI of the eavesdropper [52]. Furthermore, in large-scale secrecy wireless communication networks with thousands of users whether legitimate or eavesdropper as well as highly dense RIS deployments, RIS is a key to increase the network security throughput and enhance the physical layer security for future 6G wireless modern systems where 1000x, as per Figure 1, increase in the data rates yielding a target of 1 Terabit/sec is required. Consequently, meeting these challenges of channel estimations and robust RIS beamforming in 6G massive networks deserve further investigations. Many other developing research fields, including wireless power transfer, UAV communications, and MEC take the advantages of RIS technology.

In order to assess the advantages of RISs technology, it should be compared with different types of relay networks and surfaces which are not coated with RIS. The SNR for RIS and DF relay as per Figure 9 can be represented as follows:

$$SNR_{RIS} = \frac{p}{BN_0} |b_d + V^T \theta G|^2, \quad (2)$$

$$SNR_{DF} = \min \left(\frac{p_1 G}{\sigma^2}, \frac{p_1 b_d}{\sigma^2} + \frac{p_2 V}{\sigma^2} \right), \quad (3)$$

where, p is the transmit power, B is the bandwidth and N_0 is the noise power spectral density. Consequently, the spectral efficiency \mathcal{R} can be calculated for RIS and relay supported network as follows:

$$\mathcal{R}_{RIS/DF} = \log_2 (1 + SNR_{RIS/DF}). \quad (4)$$

Figure 9a shows a typical RIS-assisted wireless communication system model. An RIS controller is used to program the RIS reflecting elements. Furthermore, the controller communicates with the BS by another wireless signal in order for the BS to control the RIS reflections by creating a phase shift matrix θ that results from modifying huge cheap passive reflecting elements to configure the channel, and thus the concept of passive signal reflections is introduced in the research. As per Figure 9d, AF repeater simply amplifies and sends the received RF signal, including noise, to the users located in a dead spot. By introducing amplifying channel coefficient β . Repeaters are commonly employed in places where signal coverage is a problem and to extend the cell coverage however, it has a drawback of amplifying the noise as well which by return will degrade the received signal to interference and noise ratio. Repeaters work in the AF

mode, whereas relays work in DF mode. In comparison to AF repeaters, DF relays, as per Figure 9c, can provide superior noise immunity and intercell interference mitigation. The DF relay, on the other hand, necessitates a complex transceiver and might add to the transmission latency [54, 55]. In RIS-assisted and AF/DF relay-assisted communications, the receiver decodes the source information symbols, but in wireless backscatter communications, it seeks to decode the piggybacked information symbols from the strong interference signal. Backscatter, as per Figure 9b, reflects an incoming RF signal while also modifying and modulating it for secondary transmission, or backscatter. There is no need to deploy and maintain separate RF sources because already-available RF sources are used, resulting in cost and power savings. Impedance mismatching is the fundamental concept behind altering and reflecting RF signals [56]. It uses the impedance of an antenna to encode data into previously existing waves, however it has low data rate transmission speeds and lacks data security. Massive backscatter communication [57] is a new idea that uses a programmable metasurface to alter the propagation environment of stray ambient waves. The metasurface's huge aperture and many degrees of freedom allow for exceptional signal control and, as a result, safe and high-speed data transmission. The proposed backscatter wireless communication strategy in which the transmitter depends on a programmable metasurface to modulate the propagation environment rather than a single or a few impedance-modulated dipole antennas open the door for significantly larger control over the wave. More interestingly, Ambient backscatter communication (AmBC) was designed to solve communication and power consumption concerns in indoor and limited power IoT technologies. The authors in [58] presents a novel Ambient backscatter communication approach in the frequency domain using ambient OFDM subcarriers in combination with the RIS. The higher performance in terms of BER and data rate is demonstrated by analytical and numerical analyses.

The comparison between the RIS and relay assisted networks has been studied in the literature. The power transmission needed for achieving a certain rate has been studied in [53, 59] and a comparison between the RIS and the DF relay was investigated. Figure 10 shows that the transmit power required in the RIS case reduces as the number of elements grows, and the distance to the DF relaying scenario is lowest when the receiver is either near to the transmitter or the RIS. When the distance is 80 (Mtrs), the RIS must have around or fewer than 100 elements to outperform DF relaying, demonstrating the RIS importance technology in future wireless generations. The data rate of RIS and relay are compared as a function of distance in Figure 11 [59]. The RIS, for example, is setup to work as an adjusting lens as well as an irregular reflector. The diagram indicates that an RIS may achieve a rate comparable to that of an ideal FD relay without the use of a power amplifier. This is possible due to the RIS's size effective length. For distances up to 25-50 (Mtrs), the RIS under analysis acts as an anomalous mirror, and for distances larger than 75-100 (Mtrs), it behaves as a diffuse scatterer. Figure 11 further illustrates that over long transmission lengths, more than 150 (Mtrs) in the case study, an ideal FD relay

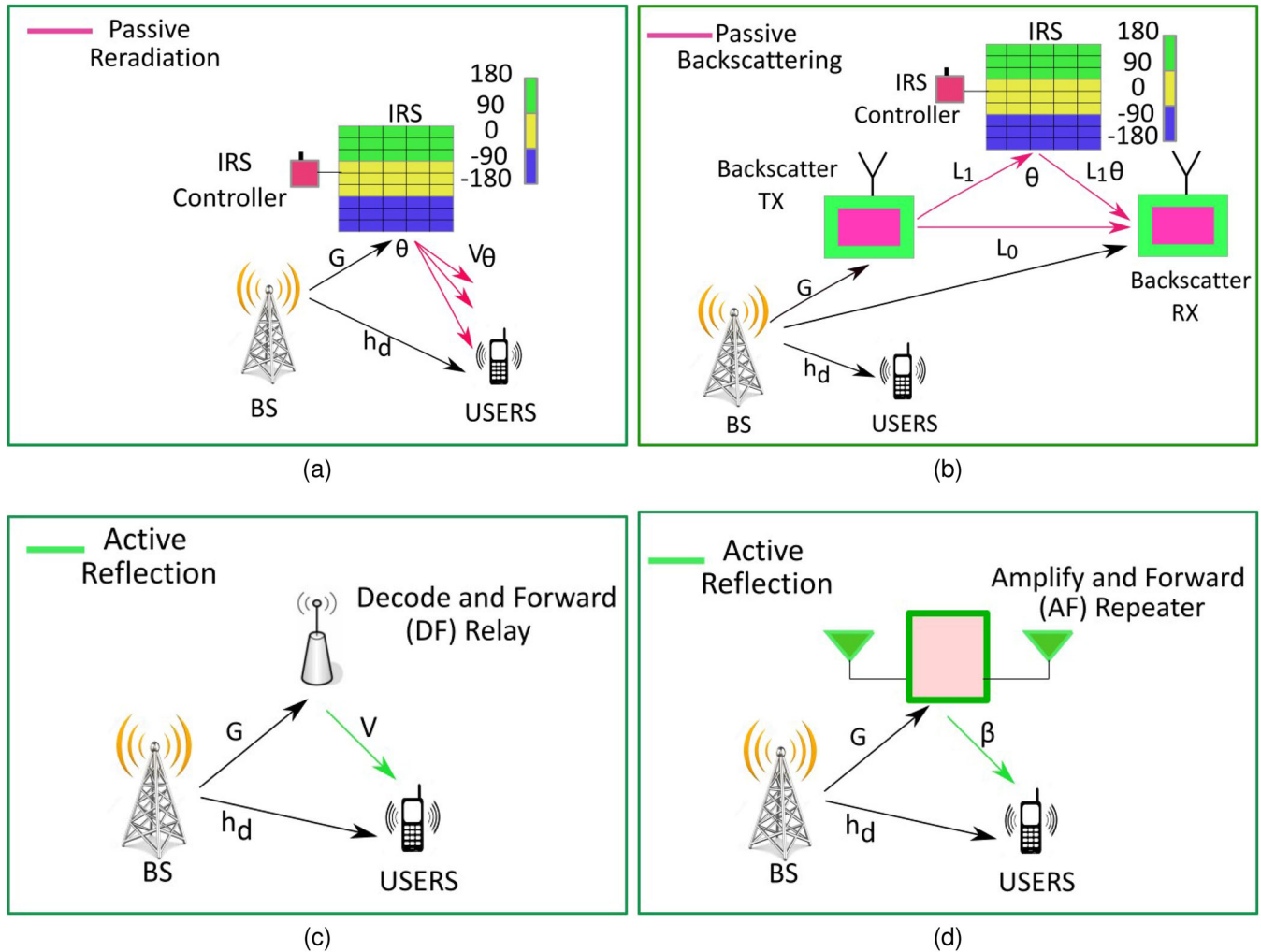


FIGURE 9 Comparison of Different Wireless Systems. (a) RIS assisted wireless communication, (b) wireless backscatter communication, (c) Decode and forward (DF) Relay assisted wireless communication, (d) Amplify and Forward (AF) Repeater Assisted wireless communication. G , h_d , and V_θ represent the BS-RIS, BS-user, and RIS-user channels, respectively

beats a RIS. To outperform a perfect FD relay across extended transmission distances, a bigger RIS may be required.

3.1.2 | Measurable metric performance of RISs: The state-of-the art

The authors in [60], with the help of RISs, has proposed new models for MIMO systems. The schemes of vertical Bell Labs Layered Space Time (VBLAST) and Alamouti have been presented. Both schemes have shown improved BER performance gains and spectral efficiency and do not require significant changes to existing MIMO models, particularly in their receiver design, making them workable and viable options for future wireless communications. However, the authors did not consider a workable phase-shift setup, which take into considerations phase-dependent amplitude differences, in the model of the suggested schemes.

The authors in [61] determined the precise probability that a randomly located RIS may reflect for a certain transceiver using

generalised rules of reflection. The analytical findings reveal that the length of a randomly positioned reflector has no effect on the possibility of reflecting. This approach, however, implies that all RISs have the same length, which does not reflect the real-world network situation. Furthermore, the authors focus just on reflection likelihood, with no assessment of how the large-scale RIS can increase transmission performance.

The researchers in [62–66] studied the outage probability of RIS-assisted wireless systems. The first authors proposed that The RIS could be used to increase the LoS likelihood for indoor mm-Wave setups. The authors derive a formula for the outage probability and then optimizes the RIS’s deployment position to further reduce the outage probability while the second authors mentioned that for non-LoS components, the outage performance is initially assessed and optimized in the slow fading scenario. The optimal outage probability declines with the size of the RIS when the LoS components are bigger than the non-LoS components. The authors next describe the asymptotically ideal outage probability in the high SNR zone, showing that it decreases as the LoS component powers grow.

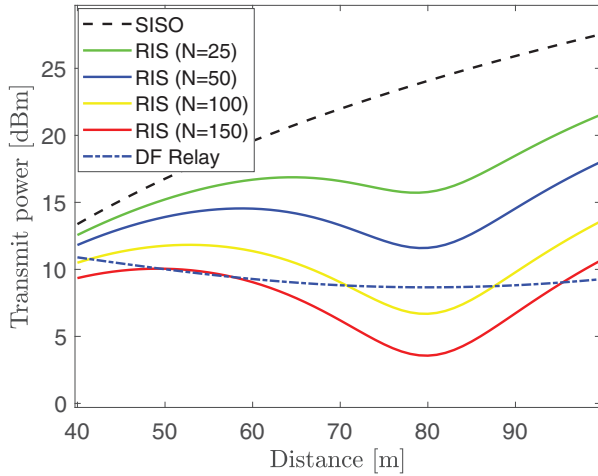


FIGURE 10 The transmit power to achieve the rate 6 bit/s/Hz [53]

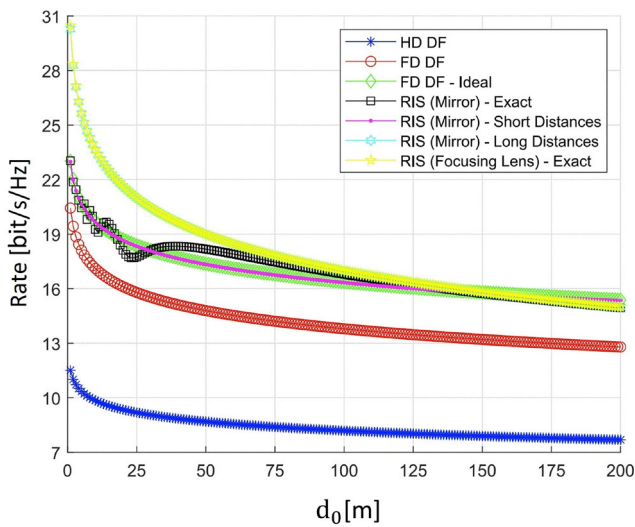


FIGURE 11 Data rates of RIS and relaying versus distance [59]

Unlike the authors in [62], who look at point-to-point mm-Wave communications, the authors in [64] consider a generalized mm-Wave downlink cellular network with random barriers and reflectors. According to the findings, only the placement of high-density reflectors can result in a considerable increase in mm-Wave coverage while reflected signals must travel greater distances than direct signals in low-density networks, and coverage probability does not differ from that of blockages. A restriction on this work is that the authors did not take into consideration the optimized deployment for the reflectors consequently, the performance coverage of the network was not promising.

The performance of outage probability in RIS-assisted vehicular communication networks is examined in [66]. Using series expansion and the central limit theorem, the authors derived the expression for outage probability. The RIS can greatly lower the probability of outages for vehicles in its area, according to numerical results. However, the authors in [65] investigated the outage probability of intelligent reflecting surface aided

full duplex two-way communication systems which characterizes the performance of overcoming transmitted data loss induced by extended deep fades. The authors computed the probability distribution of the cascaded end-to-end equivalent channel using an RIS beamformer of his choice. The number of reflecting components has a considerable influence on system reliability, according to both authors [65, 66]. A shortcoming of their work is that the analysis was shown under the assumption of continuous amplitude and phase shifts.

For calculating the BER of the LIS-assisted systems, the authors in [67] suggested an approximation and upper bound equation. Under the influence of Nakagami- m fading channels, the author looked at BPSK and M-QAM modulations. For number of elements $N < 4$, the authors derived the exact distribution of the channel coefficient and used a Gaussian approximation for the in-phase and quadrature components because the exact calculation becomes too complicated for large values of N . However, the exact derivation for the BER was only for two and three elements and the scenario is more sophisticated when the number of elements is huge.

Unlike the authors in [67], the researchers in [68] established a broad mathematical model for calculating the SEP by determining the distribution of the received SNR, and the number of elements used in the simulations was in terms of hundred. On the other hand, the exact BER analysis of a two-user NOMA system utilizing square QAM is discussed in [69]. Unlike previous work, there are no restrictions on the modulation order of QAM symbols for any user. In Rayleigh fading channels, closed-form formulas for the BER of the successive interference cancellation (SIC) receiver are developed. The BER performance of an RIS-assisted NOMA downlink system is derived in closed form in [70].

In [72], the researchers examine a reconfigurable intelligent surface aided wireless system with and without a direct link between the AP and the user, using a finite number of RIS elements. The authors give a BER and average achievable rate (AAR) study of RIS-based systems, assuming maximum received power. The authors constructs a closed-form BER approximation that allows forecasting asymptotic performance variation as SNRs and RIS elements increase. Simulation results show more accurate BERs than previous studies [68]. However, the performance of RIS-assisted wireless communications over Rician fading channels is discussed in [73]. For numerous performance metrics, such as outage probability, average SEP, and channel capacity, the authors construct new accurate closed-form approximations. Asymptotic equations for the outage probability at high SNR levels, as well as closed-form formulations for the system diversity order and coding gain are provided to give a better explanation of the system behavior. The performance analysis in the previous works did not consider practical implementations like imperfect CSI.

The asymptotic optimality of achievable rate in a downlink RIS system is investigated in [71], which takes place in a real-world RIS environment with all of its limitations. Under practical reflection coefficients, a passive beamformer is proposed that can attain asymptotic optimal performance by manipulating the incident wave characteristics. To enhance

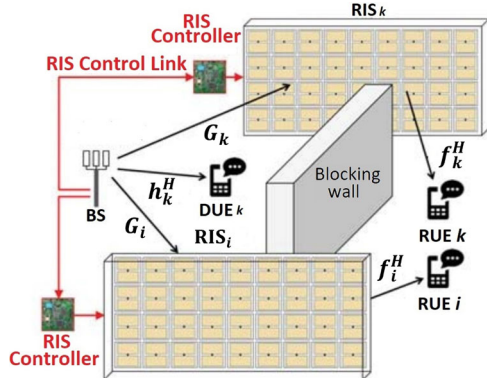


FIGURE 12 System model for RIS-based MISO [71]

the feasible system sum-rate, a modulating mechanism that may be applied in a RIS without interacting with current users is provided, and its average symbol error rate is asymptotically determined. Simulation findings show that the proposed methods are in close agreement with their upper bounds in the presence of multiple RIS references. An obvious concern about this work that a RIS cannot coherently align with all users connected to BS via RIS (named RUE users as per Figure 12) RUEs' intended channels at the same time, which limiting system performance in addition to the highly dense individual RIS surfaces needed per each user.

In an RIS-assisted mm-Wave MIMO system, the authors in [74] define the RIS's ideal phase shifts based on limited feedback from the mobile user to describe the possible data rate from the BS to the user. In addition to improving data throughput, simulation results demonstrate that by deploying the RIS with perfect CSI, the positioning and orientation error bounds can both be decreased while the authors in [75] show the way that RIS can be employed and optimized to boost the rank of the channel matrix, resulting in significant capacity improvements. Because the previous works make use of a perfect RIS with unlimited phase resolution, the capacity related study that arises has an undefined mismatch with practical systems. The authors in [76] produce an approximation of the feasible data rate and discuss performance deterioration when a practical RIS is implemented with constrained phase shifts.

The authors in [77] employ a basic receiver architecture to explore the deterioration of attainable rate and discuss the correlation design of equipment deficiencies as a function of the distance between reflective elements.

The authors in [78] specified the spatial throughput of a single-cell multiuser system supported by numerous RISs that are randomly placed in the cell, in contrast to earlier works that concentrate on link-level performance optimization for RIS-aided wireless applications. When the number of RISs surpasses a specific value, the simulations show the analysis is correct, and the RIS-aided system outperforms the full-duplex relay-aided counterpart system in terms of spatial throughput. Furthermore, it is demonstrated that alternative deploying procedures for RISs and active relays should be used to maximize their respective throughput. It is discovered that when fewer RISs are

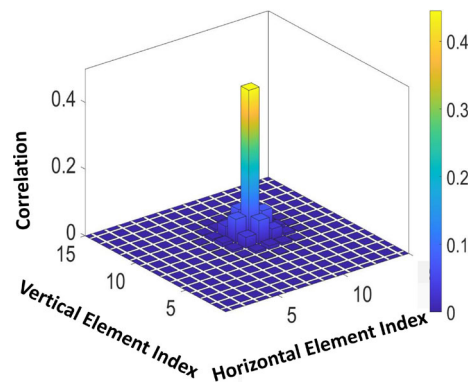


FIGURE 13 The actual capacitance of the RIS element at row 10 and column 10 is correlated with the intended capacitances of itself and the neighbouring elements

deployed, each with more reflecting elements, the system spatial throughput increases, but at the cost of greater spatially varied user rates and this is met with the research article in [79] when the author deployed one RIS only consisting of 4096 elements to enhance the communication data rate for 50 users distributed randomly in a room of 13(Mtrs) \times 14(Mtrs) and far from the RIS 16.5(Mtrs).

The authors in [77] studied the hardware impairments and its impact on the performance data rate while in [79] the authors analyzed in his system model the effect of mutual coupling between the adjacent reflecting elements on the achievable data rate per each user as per Figure 13 and then the authors represented the mutual coupling per RIS elements statistically as follows:

$$C_n = \sum_{i=1}^N C_{i,\theta} \frac{100^{-\frac{d_{n,i}}{\lambda}}}{\sum_{j=1}^N 100^{-\frac{d_{n,j}}{\lambda}}} \quad (5)$$

where $d_{n,i}$ is the distance between element n and element i , $C_{i,\theta}$ is the capacitance that we assign to element i and C_n is the actual capacitance of element n . Hence, we may expect that studying parameters like hardware impairments, mutual coupling, and discrete phase shifts in the wireless communication aided RIS will not only enhance the system performance in general but also establish a new era of communication research based on robust foundations that will end eventually with reliable technology.

The deployment of the RIS in [79] was near the user equipment's however, the authors in [80] studied the distributed and centralized deployments of the RIS in the wireless network. Under symmetric channel topology, it has been proved that centralised deployment outperforms scattered deployment in terms of achievable user rates. Nevertheless, the authors in [81] analyzed and compared two interesting scenarios in a SISO system, namely a finite number of big RISs and many finite-size RISs, to illustrate which implementation technique is more favourable. Using the deterministic equivalent (DE) approach, the authors calculate the coverage probability in closed form for both instances based on statistical CSI. The ideal coverage

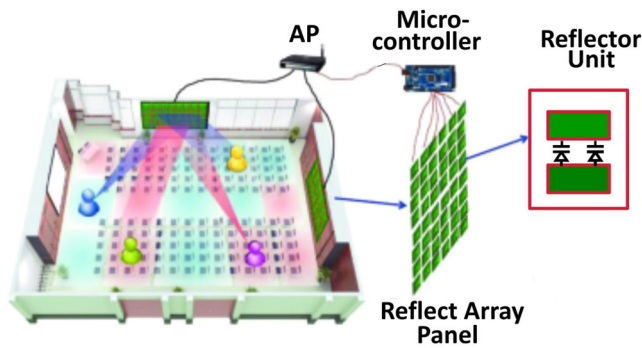


FIGURE 14 Spectrum sharing using reflect-array [26]

probability is then calculated. Numerical results show, among other things, that adding more surfaces beats the design strategy of adding more elements per surface.

In contrast to the early works, [26] presents a collaborative analytical and empirical investigation to introduce a new spectrum sharing solution for interior situations based on the use of a reconfigurable reflect-array in the wireless channel. The relevant signals for each transmission pair could be improved while interferences would be suppressed by managing the phase shift of each element on the reflect-array optimally. As a result, numerous wireless users in the same room can simultaneously access the same spectrum band without interfering with one another. Consequently, network capacity can be significantly boosted. The smart reflect-array panels are hung on the walls in the indoor setting, as shown in Figure 14. Even though the reflected array does not buffer or process any incoming signals; it can alter the phase of the reflected wireless signal.

The authors in [82] studied the uplink rate in the presence of restrictions such as hardware flaws, inaccurate channel estimation, and interference caused by device-specific spatially correlated Rician fading. The authors has demonstrated that studies can reliably predict the performance of a LIS surface without the use of large simulations. Furthermore, it is shown that in a LIS-based system, a channel hardening occurs, and the authors also found the asymptotic bound for the uplink data rate and demonstrated that as the number of elements rises, hardware impairments, noise, and interference due to channel estimation errors and the NLoS path become insignificant. In comparison to conventional massive MIMO, the simulation results show that a large-scale RIS can achieve greater reliability in terms of capacity expectation and variation. We noticed that the number of elements that have been used in the simulations is huge in the order of thousands (10000) which raise our concern about the mutual coupling between the adjacent elements and the practical phase-shift model considerations. In LIS systems, the authors in [83] looked at the capacity impacts of hardware impairments (HWI). The authors created a general model of the HWI based on the distance between a considered point on the LIS and its Centre, with the latter serving as a reference point in hardware design. To limit the negative impacts of hardware deficiencies, the analytical and simulation results suggest dividing a largescale RIS into a succession of smaller RIS units.

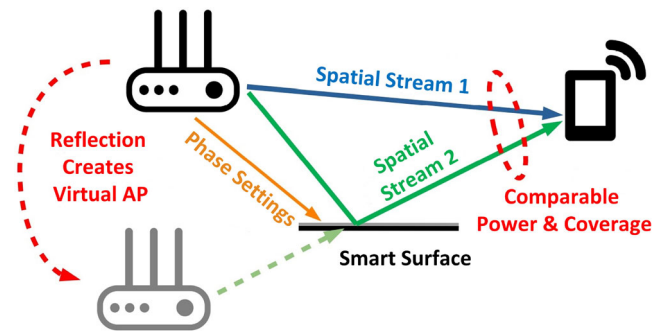


FIGURE 15 Scatter MIMO creates virtual AP for MIMO streams via phase shift reflection and its optimization algorithm [11]

Similar to [83], the authors in [84] not only did investigate the effects of transceiver hardware impairments (T-HWIs) and reconfigurable intelligent surfaces hardware impairments (RIS-HWIs) on a general RIS-assisted MU-MISO system with imperfect CSI and correlated Rayleigh fading, but also proposed a novel optimization methodology for reflecting beamforming matrices (RBM) optimization with low computational cost, which is particularly useful in RIS-assisted systems with many elements. The authors were able to get the channel's linear MMSE estimate with T-HWIs and RIS-HWIs. Furthermore, using just large-scale data, the uplink attainable sum SE with MRC was calculated in closed form and performed high computationally efficient optimization about the RIS RBM. In general, the authors presented an approach that produced analytical and tractable formulations that were superior to prior efforts, as demonstrated by simulation results.

Unlike other studies that focus on capacity, the paper in [85] looks into the feasibility of employing an RIS with a large number of scattering components for terminal location. The author goes into details about the effects of deployments with a single centralized LIS and numerous smaller distributed LISs constrained to the same total surface area. Splitting the LIS into 16 smaller LISs results in minor benefits, but it also increases the overheads for different small LISs to collaborate with one another.

Scatter-MIMO is a method for delivering MIMO spatial multiplexing gain that use a smart surface to enhance scattering in the surroundings [11]. Smart surface connects to a wireless transmitter device, such as an active AP, and re-radiates the same amount of power as any active AP, resulting in virtual passive APs as per Figure 15. By employing virtual passive APs, Scatter-MIMO eliminates the synchronization, interference, and power requirements of traditional dispersed MIMO systems, allowing its smart surface to give spatial multiplexing gain at a cheap cost. According to the simulation results, Scatter-MIMO gives a median throughput gain of 2 over the active AP alone.

From the above-mentioned references and different illustrations, we would like to refer that the RIS aided wireless communication systems can be used as a reflector, receiver and transmitter [13] by modifying the phase shifts of the RIS's scattering units. The RIS's outgoing waves can generate different radiation paradigms that can convey data if these patterns

can be identified and distinguished at the receiver. This is the basic design concept of spatial modulation, which is commonly implemented using programmable antennas [86, 87]. This is very similar to wireless backscatter communications, which use load modulation to adjust the antenna's reflection coefficients [88]. It's difficult to get a high rate for SU user in CR communication systems when there is a lot of cross-link interference with the PU user. The authors in [89] used the recently developed RIS to solve this problem in their research. In particular, the authors investigate an RIS-assisted CR system, in which an RIS is used to help with spectrum sharing between a PU and an SU link. By combining SU transmit power and RIS reflect beamforming to optimise the feasible SU rate for a particular SINR target for the PU connection. The authors used the AO algorithm to solve the SU rate maximization problem via the joint transmit power control and RIS reflect beamforming. Simulation findings demonstrate that the RIS-assisted CR is effective for secondary transmissions, even in the tough scenario when the secondary transmitter is much closer to the primary user.

RIS-enhanced energy detection is investigated in depth in [90] for single-user spectrum sensing, cooperative spectrum sensing, and diversity reception. For each example, a performance analysis is presented, as well as an analysis for the average probability of detection and false alarm. Monte Carlo simulations are used to verify the validation of his results. It is believed that RIS can significantly increase detection performance.

The authors in [91] investigate RIS concept in the UAV enabled communications to expand network coverage and improve communication reliability and spectral efficiency of IoT networks. The authors also show that RIS-assisted UAV communication systems may achieve ten times the capacity of traditional UAV communication systems in terms of achievable ergodic capacity. The impact of imperfect phase knowledge on system capacity and BER analysis for UAVs communications assisted by flying intelligent reflecting surfaces is examined in [92, 93]. The authors in [93] takes into account a multi-layer UAV network with several hops, whereas [92] only addresses a single-hop case. The obtained results demonstrate the need of correct phase estimation for RIS-based systems, especially for systems with a limited number of reflecting elements. The results are also demonstrating the importance of the number of elements in getting a reliable performance.

3.2 | Optimization techniques and algorithms

The impact of multipath on the received signal is determined by how great or small the spread of time delays associated with the LoS and other multipath components are concerning the inverted signal bandwidth. The LoS and other multipath components are often non-resolvable if the channel delay spread is minimal, leading to the narrowband fading model. The LoS and all multipath components are often resolvable into several discrete components if the delay spread is large, resulting in the wideband fading model [5]. The reflected signals can be merged coherently at the intended receiver to boost the received signal

strength or destructively at the non-intended receiver to limit interference by smartly altering the phase shifts of all scattering elements, as shown in Figure 9. The experimental demonstration and channel measurements in [43] support this, paving the road for more theoretical research and system optimization. In the following section, we go over the most common optimization formulations and solutions for RIS-assisted narrow and wideband wireless systems for single and multi-users.

3.2.1 | Passive beamforming techniques

In this part, we will investigate the passive reflection optimization for RIS-assisted wireless communications. We will assume the knowledge of direct and indirect channels for the purpose of exposition however, the channel estimation will be discussed in Section 4. The optimization problem can be expressed generally as follows:

$$\begin{aligned} \text{(OP)} \quad & \max_{\mathbf{Q}, \boldsymbol{\theta}} f(\mathbf{Q}, \boldsymbol{\theta}) = \left| (V^T \boldsymbol{\theta} G + b_d) \mathbf{Q} \right|^2 \\ \text{s.t:} \quad & \\ \text{(C1)} \quad & \|\mathbf{Q}\|^2 \leq p \\ \text{(C2)} \quad & \phi_1, \dots, \phi_N \in [0, 2\pi) \\ \text{(C3)} \quad & \gamma_1, \dots, \gamma_N = 1 \end{aligned} \quad (6)$$

where \mathbf{Q} is the transmit beamforming vector, $\boldsymbol{\theta}$ is the RIS matrix with unit-modular constraint on each element and $f(\mathbf{Q}, \boldsymbol{\theta})$ denotes the objective function. We envision that the joint beamforming optimization problem is a non-convex problem due to the fact that both \mathbf{Q} and $\boldsymbol{\theta}$ are linked to each other. Furthermore, RIS elements need unit magnitude since, unlike relays, they do not amplify or decode then transmit a received signal. The necessity for suboptimal tractable rate optimization solutions is motivated by the non-convex unit modular constraints in the above mentioned optimization issue. Previous works on narrowband [94–107] and wideband [108–113] RIS-assisted wireless communication systems attempt to solve the non-convex problem where the main challenge includes the unit modulus constraint. Several techniques have been used in the literature to address this constraint.

- **The alternating optimization method:**

The famous alternating optimization method is examined extensively in the literature. The method style of switching between the active transmit beamforming and passive reflection gives it an advantage to deal with the active transmit beamforming as a conventional problem when the passive beamforming is fixed; however, under the given active beamforming the passive beamforming is still a non-trivial exercise to tackle including the unit modular constraint on each element of the RIS. There are possible ways have been shown in the literature to deal with this constraint. For example, the SDR method is applied to relax the non-convex

rank-one constraint to a standard convex semidefinite program (SDP). The SDP is used then to solve the formulated non-convex quadratically constrained quadratic program (QCQP) problem. However, the relaxed problem may not result to a rank one solution which by return require obtaining the eigenvalue decomposition by using circularly symmetric complex Gaussian (CSCG) distribution methods. The SDR with Large number of gaussian randomizations will lead eventually to approximation of $\pi/4$ of the optimal objective value [100]. Consequently, the SDR approach can only provide an approximation and solving an SDP program is computationally expensive for large number of antennas and RIS elements.

- **The iterative methods:**

The concept of the iterative algorithms is to find a locally or near optimal solution for the objective problem at a reasonable computational complexity and acceptable run time. For example the low-complexity successive refinement algorithm [94, 98] to determine the optimal discrete phase shifts of different elements at RIS one by one in an iterative way. Another technique based on the fixed point iteration and manifold optimization is investigated [99]. The authors in [107] used the projected gradient method (PGM) to jointly optimize the covariance transmitted matrix and the phases of the RIS elements. The PGM method achieved the same data rate as the alternating optimization method but with less number of iterations and lower computational complexity. The authors in [113] extended the work of [107] in the wideband MIMO communication. The paper in [109] proposed the low complexity power method to compute the dominant eigenvector of the reflection coefficient matrix to configure the RIS phases. In general, all these iterative methods have shown good system performance with acceptable computational complexity and reasonable run time.

3.2.2 | Active and passive beamforming: The state-of-the art

The authors in [114] investigate an RIS-assisted point-to-point MISO wireless system in which one RIS is used to aid transmission from a multi-antenna access point AP to a single-antenna user. As a consequence, the user simultaneously receives both the signal directly from the AP and the signal reflected by the RIS. By combining the active transmitted beam at the AP with the passive reflected beam at the RIS using phase shifters, the authors aimed to optimize overall received signal power at the user. Assuming that the RIS contains global CSI, a centralised solution based on the SDR technique was proposed. Because the centralised approach includes excessive channel estimation and signal exchange overheads, a low-complexity distributed technique is used, in which the AP and RIS modify the transmit beamforming and phase shifts in alternating fashion until convergence is achieved. When compared to benchmark systems, simulation results suggest that the proposed techniques can obtain high performance gains. Furthermore, it has been proven that the RIS can significantly improve link quality and

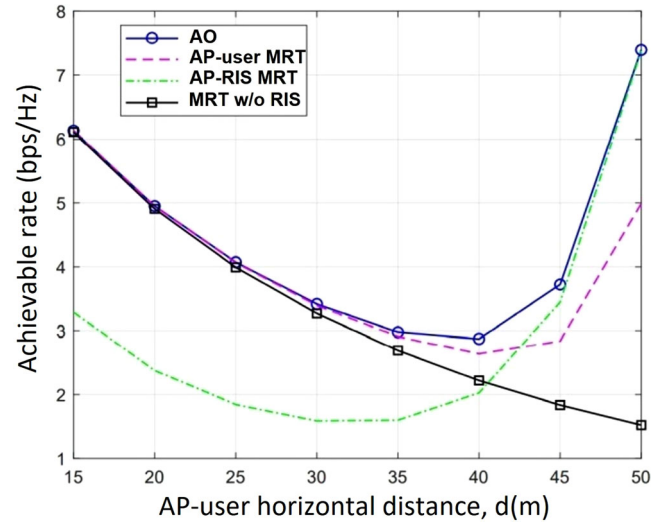


FIGURE 16 Achievable rate of RIS-aided MISO system versus AP-user horizontal distance, d [11, 114]

coverage when compared to a traditional setup without the RIS. For example, Figure 16 [3, 114] investigates four schemes (1) AO's joint transmit and passive beamforming design, (2) AP-user MRT transmission, (3) AP-RIS MRT, and (4) MRT without RIS. When the user is near to the AP, the AP-user MRT system works similarly to the AO method, but suffers a considerable rate loss when the user is nearer to the RIS, as illustrated in Figure 16. This is to be expected, given the AP-user direct link dominates the user received signal in the former scenario, but the RIS-user link dominates in the latter. Furthermore, the AP-RIS MRT system operates in the opposite manner when compared to the AP-user MRT counterpart. Consequently, as shown in Figure 16, if the transmit beamforming is not adequately built according to the whole channels, the attainable rate utilizing the RIS may be poorer than the conventional MRT without the RIS, for example, in the application of the AP-RIS MRT scheme for distance $d \leq 40$ (Mtrs). This emphasises the significance of combining active and passive beamforming to achieve the best balance of direct transmission to the user and indirect transmission via RIS reflection in order to maximise the received signal strength at the user. For a desired SNR of 8 dB, the network coverage without the RIS is roughly 33 (Mtrs), but when the suggested combined beamforming designs with an RIS are utilised, this value is increased to about 50 (Mtrs) [114]. Another important result in [114] is that the user's receive power grows quadratically as N grows, by a factor of $\mathcal{O}(N^2)$. The transmit power can be reduced at the AP in the order of $1/N^2$ without sacrificing the receive SNR. This is due to the fact that the RIS catches an extra aperture gain of $\mathcal{O}(N)$ in the AP-RIS link in addition to the reflect beamforming gain of $\mathcal{O}(N)$ in the RIS-user link.

The power scaling in reconfigurable intelligent surfaces and its comparison with m-MIMO, are studied in the reference [115] in which the authors proved analytically that the gap between m-MIMO and RIS is enormous; an RIS requires a high number of reflecting elements to achieve SNRs equivalent to massive

m-MIMO and by concluding such solid fact the authors disapproves of the myths and the wrong understanding of the RIS fundamental concepts.

A point-to-point MISO communication system with RIS assistance is also investigated in [116]. The beamformer at the AP and the RIS phase shifts are tuned simultaneously to improve spectral efficiency. The resultant non-convex optimization problem is handled with the help of two efficient methods that employ fixed-point iteration and manifold optimization approaches, respectively. The proposed techniques not only improve spectral efficiency but also reduce computational complexity as compared to the current state-of-the-art approach. The RIS-assisted MISO downlink model described above, as well as the heuristic alternating optimization described in [114, 116], provide a generic framework for the optimum design of RIS-assisted systems that may be used in a variety of network scenarios. Despite the fact that RISs with continuously phase shifts and maximum reflection magnitudes were explored, it was discovered that realistic RIS with discrete phase shifts and discrete reflection amplitudes satisfied the hardware criteria.

Different from the preceding sections, the authors in [117] look at an RIS-based wireless communication, in which an RIS with a limited figure of phase shifts at each element is used to enhance communication between a multi-antenna AP and many individual-antenna users. Particularly, the continuously transmitted precoder at the AP and the discrete phase shifts at the RIS were tuned together to lower transmit power at the AP while still achieving user SINR requirements. For single-user and multiuser instances, both optimum and successive refinement based suboptimal solutions were investigated. Furthermore, when the figure of reflecting elements gets asymptotically large, the performance degradation of RIS due to discrete phase shifts against the ideal scenario with continuous phase changes was investigated. Surprisingly, it was discovered that utilizing RIS with even 1-bit phase shifters can attain the same asymptotic squared power increase as continuous phase shifts when only a constant power loss in dB is applied. In comparison to the situation without RIS, simulation results revealed that employing RIS with discrete phase shifts can save significant transmit power. Furthermore, it was shown that immediately quantizing the optimised continuous phase shifts to generate discrete phase shifts offers near-optimal performance in the single-user scenario, but that performance is significantly reduced in the multiuser case owing to substantial co-channel interference. Eventually, owing to the multiuser channel rank enhancement provided by the RIS's extra signal routes, it was proved that the ZF precoder-based algorithm performs almost as well as the MMSE precoder-based method.

We looked at narrow-band communication systems with frequency-flat fading channels and a single and multiple antenna for the AP and user in the aforementioned works. Consequently, the wideband communication is important to explore in the literature. Passive RIS reflection optimization problems for MIMO systems with multiple antennas at both the AP and the user, as well as broadband OFDM systems with frequency-selective fading channels, must cater to multi-antenna channels and multi-path channels with different delays, making

them more complicated and challenging to solve. The fundamental capacity limit of RIS-assisted point-to-point MIMO communication systems with multi-antenna transmitter and receiver is quantified in general by simultaneously optimising the RIS reflection coefficients and the MIMO transmit covariance matrix, which differs from previous MISO systems [118]. For frequency-flat channels, an alternate optimization approach was devised to discover a locally optimum solution by optimising one of the reflected coefficients or transmitted covariance matrix at a time while leaving the others constant, and the best possible solution were found in closed-form. Alternative, less difficult algorithms for asymptotically low and high SNR circumstances, as well as MISO and SIMO channels, were devised. Furthermore, for frequency-selective channels, a MIMO-OFDM system was investigated, in which a collection of reflection coefficients for all subcarriers must be designed. A novel alternating optimization approach used the convex relaxation technique to successively optimise a set of transmitting covariance matrices across multiple subcarriers or a common reflection coefficient for all subcarriers. Extensive numerical results reveal that the suggested algorithms outperform several benchmark methods with and without RIS in terms of rate performance. The performance gain improves as the number of elements increases.

The authors in [119] make the first efforts to investigate the wideband beamforming for RIS-assisted mm-Wave massive MIMO using a different design. For RIS-assisted millimetre-wave (mm-Wave) hybrid MIMO systems, the authors present a geometric mean decomposition-based beamforming method. With the help of RIS, simulation results show that the proposed strategy can achieve good BER performance in a wideband hybrid MIMO system. To increase the system sum-rate, the authors [120] updated the source precoders and RIS phase shift matrix in the full-duplex MIMO two-way communication system. To maximise the system sum rate, the RIS phase shift matrix and source precoders are tuned jointly. The Arimoto-Blahut approach is used to divide the non-convex optimization issue into three sub-problems that are tackled alternately. Closed-form solutions can be used to solve all the sub-problems quickly. RIS provides a performance boost equal to a relay operating at a transmission power of only 40 dBm to 35 dBm. This is related to the RIS's concern with double-fading. It's worth noting, though, that RIS does not need any transmission power.

All of the aforementioned research studies in [116, 118–120] rely on an ideal RIS with infinite phase resolution, that is, each scattering element's phase shift may be entirely controlled. However, this is difficult to accomplish in practice, and devising precise phase control algorithms is similarly tough. Furthermore, for the RIS controller to provide precise phase control, full CSI is usually required. This implies that data sharing might be incredibly expensive, particularly for RIS that is self-sustaining due to wireless energy harvesting.

The authors in [121] presented a novel way to use the RIS to improve the attainable rate of an OFDM system. The authors developed a workable transmission protocol by assembling the RIS elements as shown in Figure 17 and calculating the joint channel for every group, with data transfer based on a

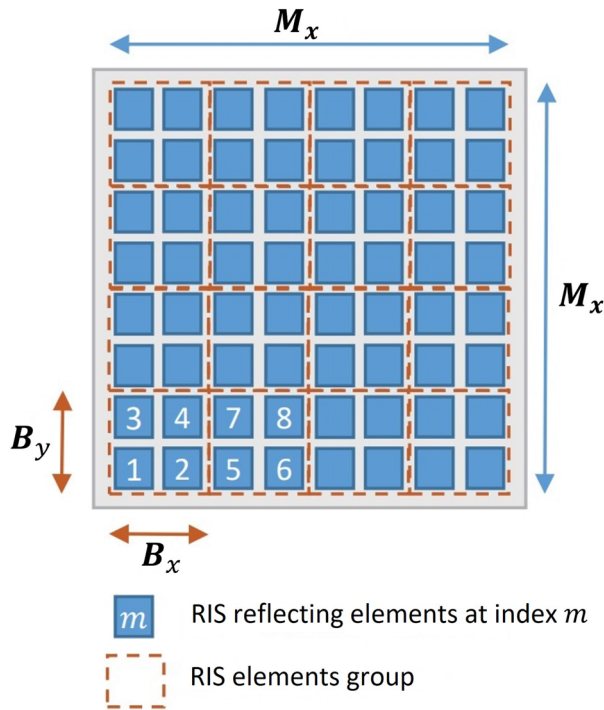


FIGURE 17 Illustration of the RIS reflect array and proposed elements grouping [121]

shared RIS reflection coefficient. Then, based on the predicted channels under the recommended protocol with any defined grouping, the authors constructed a combined optimization problem of transmit power allocation and RIS reflection coefficients. The non-concave rate function was estimated utilising its concave lower limit based on the first-order Taylor expansion in an efficient sequential convex approximation (SCA)-based technique. The SCA-based approach guarantees that the RIS's combined reflection and transmission power optimization issue will converge to a stationary point, and it only has polynomial complexity over the number of elements and sub-carriers. The simulation results show that the improvements in the data rate is connected with the selection of the group ratio and the coherence time of the channel however, we have seen a performance degradation in the low SNR regime as the design parameters are adjusted based on the calculated CSI, the CSI obtained at low SNR is inaccurate, resulting in a larger performance degradation at both low and high grouping ratios so, we think that to maximize the obtainable rate, the grouping approach as well as the training sequence can be further improved. In addition, the author considers continuous phase and maximum amplitude equal one in the optimization schemes rather than proposing practical discrete phase shift.

To reduce complexity even more, the authors in [122] proposed a simpler approach called highest channel impulse response (CIR) maximisation, in which RIS phase changes are only aligned with the time-domain channel with the strongest path power. The authors proposes a feasible transmission protocol for an RIS-enhanced OFDM system that conducts channel estimation and reflection optimization sequentially. The

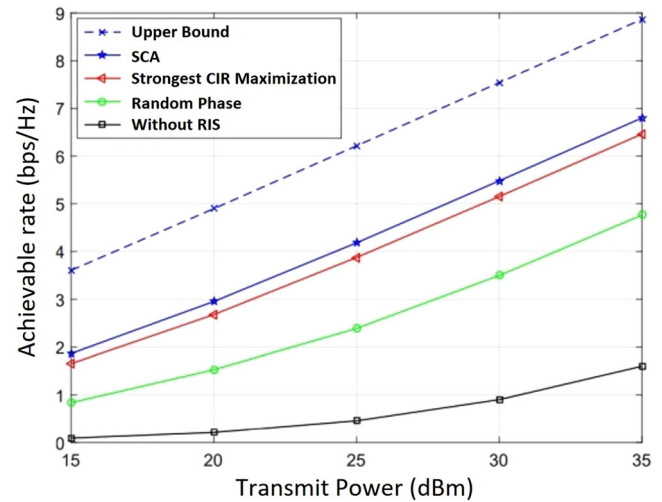


FIGURE 18 Achievable rate versus transmit power for RIS-aided OFDM system [122]

RIS proposes a unique reflection pattern to facilitate channel estimation at the AP based on received pilot signals from the user, for which the channel estimation error is calculated in closed-form under the unit-modulus constraint. After that, the reflection coefficients are optimised using the estimated CSI and a low-complexity approach based on the temporal domain's resolved strongest signal route. It is observed from Figure 18 that in comparison to the OFDM system without RIS and the OFDM system with random RIS phase shifts and the related optimal transmit power allocation, the SCA-based algorithm suggested in [121] achieves a much higher rate. Furthermore, the most powerful CIR maximization algorithm provides similar results to the SCA-based method, making it a cost-effective and low-complexity option. The figure also sets a possible upper rate limit by proposing that various RIS reflection coefficients can be created ideally for various sub-carriers, resulting in a frequency-selective RIS reflection system. With the realistic frequency-flat RIS reflection, this upper rate limit greatly outperforms the SCA-based approach, and the rate difference expands as the number of sub-carriers rises. As a result of its passive functioning, RIS-aided OFDM systems have a basic weakness in the absence of frequency selectivity of the RIS reflection. Due to the necessity to cater to additional channels in both space and frequency, the RIS reflection design for rate increase is entailed in more general RIS-aided MIMO-OFDM systems where the user and AP are kitted out with more antennas. Additionally, numerous transmit covariance matrices at distinct sub-carriers must be optimised together with the RIS reflection. Consequently, the authors in [118] expanded the narrow-band MIMO situation and using the convex relaxation technique, the authors suggested an effective AO-based solution. Despite the absence of frequency selectivity, the results in [118] revealed that RIS is still useful in enhancing the systems rate of MIMO-OFDM with well-planned RIS reflection coefficients when compared to a typical system without considering RIS.

Different from the above researches, the authors in [79] investigated a wideband OFDM system supported by a

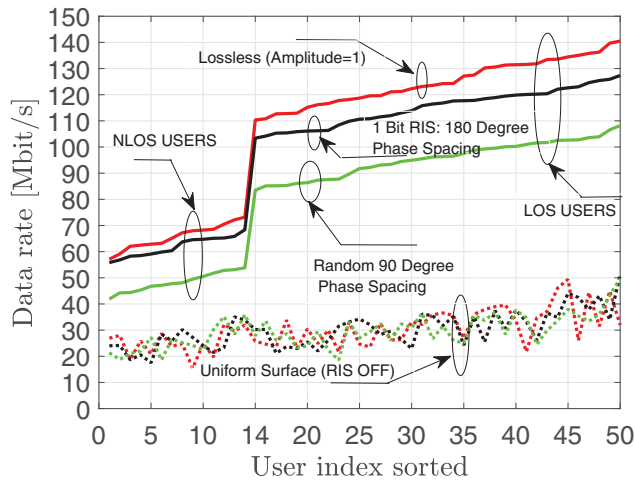


FIGURE 19 Achieved Data Rate using dataset in [123]

practical RIS configuration with two binary states per each element as well as mutual coupling between adjacent elements. Using the dataset from [123], new channel estimation and configuration techniques have been proposed and analyzed. Because of the tradeoff between multiple subcarriers, finding a good RIS configuration with reasonable complexity is difficult in OFDM systems.

In [122, 129], the strongest tap maximization approach is studied, to maximize the magnitude of the channel's greatest entry. This works well for LoS channels but not for NLoS channels [16] and extending it to the scenario where each RIS element has just two states is difficult. Instead, the authors aimed to optimize the total signal power received by creating a heuristic algorithm based on the iterative power method, which finds the dominating eigenvalue by iterating the computation until it converges. The simulation results show the rates achieved by the 50 Users in dataset as per Figure 19, which are arranged by increasing rates using the proposed technique. Two benchmarks are used: (1) choose the best configuration from among the N examined during pilot transmission; and (2) turn off all coefficients to simulate a uniform metal surface. For all Users, including NLoS, the suggested technique gives higher rates. When compared to a uniform surface, the sum rate with an optimized RIS is 3.3 times higher, demonstrating the technology's considerable benefits even in complex configurations.

Similar to [79], the authors in [130] investigated a wideband orthogonal frequency-division multiplexing OFDM system for MISO multi-users, the authors first look at the dual-phase and amplitude squint effect of reflected signals before presenting a simplified RIS reflection model for wideband signals. Then, a wideband RIS enhanced MU MISO-OFDM system is examined. When using both continuous and discrete phase shifters, the transmit beamformer and RIS reflection are developed jointly to maximise the average sum-rate over all subcarriers. The original problem is turned into a multi-block variable problem that may be solved effectively using the block coordinate descent (BCD) approach by leveraging the relationship between

sum-rate maximization and MSE minimization. In Both scenarios complexity and convergence are explored. When compared to the ideal RIS reflection model, simulation results demonstrate that the proposed technique may provide considerable average sum-rate augmentation, underscoring the importance of using the realistic model in wideband system design. However, the authors put the assumption that the channels were well known, but in practice, a channel estimating phase is required. Because the RIS is a passive device, the estimation must be done at the receiver which was not considered in addition to the proper employment of the RIS.

3.3 | Discussions and insightful prospect for section III

- In summary of the performance analysis, we would like to refer that the bulk of the research papers presume that the channel state information and discrete phase shifts are known at both transmitter and receiver [68]. As a result, more practical setups are needed to evaluate the effectiveness of implementing large-scale RIS cellular communications networks in practice. Furthermore, neither for indoor nor outdoor communication setups, the above-mentioned literature pays little attention to user mobility. User mobility causes not just handoffs between RIS units, but also a geographical correlation in user distribution, which could have a significant impact on system performance. Consequently, incorporating various mobility models into performance will become a crucial study path in the future. Furthermore, the maximization of performance gain for a certain network structure problem involves a combined tuning of active transceivers and RIS passively scattering components. Passively reflected signals, which are intimately related with the active transceivers' control variables, can be thought of as the combined phase control of scattering components. Because the scattering objects in wireless environment scenarios are unpredictable and omnipresent, performance evaluation of RIS-assisted wireless systems is complicated, but it also generates new optimization challenges that demand creative methods to account for active-passive device communication [3, 16]. Table 4 is a summary of some of the work done in the performance system analysis considering the usage of the intelligent reflecting surfaces as a reflector, receiver, and transmitter in addition to the design objectives. We believe that in order to construct genuinely widespread wireless networks that can provide continuous wideband communication and good quality of service (QoS) to numerous users in such a challenging wireless environment, new and radical solutions are still required.
- In summary of the optimization techniques and algorithms, we have presented the different optimization techniques used in the literature for both narrow and wideband systems taking into consideration many communication systems parameters like capacity, rate, sum rate and SNR to study the performance and efficiency. Different system models were illustrated using single and multi-users under various channels and environments however, there are still huge subjects

TABLE 4 Summary of existing work in the field of RIS systems performance analysis

Reference	Communication setup	IRS functionality	Criterion for measuring performance	Design goal
[60]	MIMO	Transmitter	BER	Enhance the performance and boost the spectral efficiency
[61]	SISO in the presence of random objects	Reflector	Probability of being a reflector	If an item is coated in meta surfaces, the chance that it is a reflector is unaffected by its length, but it is strongly affected if Snell's law of reflection must be applied
[62]	SISO mm-wave communications with Blocked LoS	Reflector	Outage probability	Even when the links are impeded by barriers, a reflect-array deployment may provide reliable mm-Wave connections for indoor communications
[63]	MISO	Reflector	Outage Probability	The effects of several critical system factors on the ideal outage probability are analysed to uncover crucial design insights
[64]	SISO in the presence of both line-of-sight signal blockages and reflectors	Reflector	Coverage probability	Improving the coverage in high-density networks
[67]	SISO under double Nakagami-m channels	Reflector	Bit error probability	Performance improvement
[68]	SISO under Rayleigh fading channel	Reflector and Transmitter	SEP	Increasing the received SNR
[70]	Multi-users NOMA system	Reflector	BER	Improving system performance and reliability
[71]	Multi-users MISO	Reflector	SER	Optimal SNR and increase Sum rate
[74]	mm-wave MIMO	Reflector	Achievable Rate	High rate in low SNR
[75]	Point to point MIMO	Reflector	Achievable Rate	Rate by choosing proper RIS deployment and phases
[76]	Narrow band SISO	Reflector	Achievable data rate	Maximize data rate
[78]	Single BS-Multiusers	Reflector	Spatial throughput	Maximize spatial throughput for users
[79]	Single BS-Multiusers	Reflector	Achievable data rate	Sum Rate enhancement
[80]	Single AP- Multiuser	Reflector	Achievable user Rate	Superior rate performance of centralized over distributed
[81]	SISO	Reflector	Coverage Probability	Increasing the number of surfaces surpasses the design technique of increasing the number of elements per surface.
[82]	Uplink LIS-based large antenna-array system for single Antenna multiusers	Receiver	Ergodic Rate	Produce performance comparable to traditional massive MIMO
[83]	Uplink single user to signal processing unit	Receiver	Capacity	Reducing the impact of hardware impairments
[84]	MU-MISO	Reflector	Sum SE	Enhance sum SE
[85]	Single antenna radiating to LIS	Receiver	Coverage positioning	Distributed deployments have the ability to expand terminal placement coverage and deliver superior average Cramer–Rao lower bound (CRLBs) in all dimensions.
[124]	MISO	Reflector	Coverage probability and average throughput	Improve system coverage probability and throughput without consuming more energy.
[125]	MISO-OFDM	Reflector	Downlink rate	Downlink rate enhancement despite the lack of independent RIS phase control

(Continues)

TABLE 4 (Continued)

Reference	Communication setup	IRS functionality	Criterion for measuring performance	Design goal
[126]	Single user SISO	Reflector Array	Outage probability and the average bit-error probability	The RIS-assisted system outperforms the AF relay system with fewer reflecting elements
[127]	Single source and two wireless sensor nodes	Reflector	Average symbol error probability (ASER) and the outage probability	As the number of reflecting elements grows, the performance improves
[128]	RIS-assisted NOMA	Forward Relay	Outage probability and ergodic rate	Enhance energy efficiency compared to conventional cooperative communications.

that need to be investigated which are not yet covered properly in the above research like the doppler shift and mobility, practical phase shift models, proper and fast channel estimations, and mutual coupling for the adjacent RIS elements. Table 5 summarizes the work of RIS reflection optimization studies based on the system settings analysis and optimization methodologies used.

4 | CHANNEL ESTIMATION

4.1 | Channel estimation protocol and pilot transmission

To effectively appreciate the performance advantages given by RIS, accurate CSI is necessary, which is a practical obstacle. The challenges can be summarized as follows:

- Aside from having significantly more RIS-induced channel coefficients than a conventional system without RIS, RIS channel estimation has a hurdle in that its cheap reflecting components lack active RF chains and hence are unable to broadcast pilot and training signals to facilitate channel estimate, in contrast to traditional systems' active BSs and user equipment.
- The RIS channel estimation is constructing high-dimensional channels from low-dimensional channels with approximated CSI.
- In broadband systems with frequency-selective fading channels, extra channel coefficients must be estimated due to the multi-path delay spread and subsequent convolution of the User-RIS and RIS-BS multi-path channels in each cascaded User-RIS-BS channel. Additionally, although the channels are frequency-selective, the RIS reflection coefficients are frequency-flat, making it impossible to create flexible various frequencies, such as separate sub-carriers in OFDM communications. In all SISO, MISO, MIMO, single and multi-user scenarios, forecasting the RIS channel for broadband frequency-selective fading channels is much more challenging than estimating the RIS channel for narrow-band flat-fading channels due to these characteristics [3].

To address the challenges, let us consider the downlink wide-band SISO communication. Recall (1) but for the wideband system, The received signal can be represented as:

$$\tilde{z} = F(H_{eq}^T \theta + b_d) \odot x + w \quad (8)$$

Where $F \in \mathbb{C}^{K \times K}$ is the DFT matrix and K is the number of subcarriers, $H_{eq} = [b_{eq1}, b_{eq2}, \dots, b_{eqK}] \in \mathbb{C}^{N \times K}$ is the cascaded channels V and G to and from the RIS, respectively, the configuration of the RIS is given by the diagonal matrix $\theta = \Gamma \Phi$ with $\Phi = \text{diag}(e^{-j\theta_1}, \dots, e^{-j\theta_N})$ and $\Gamma = \text{diag}(\gamma_1, \dots, \gamma_N)$, $b_d = [b_{d1}, \dots, b_{dK}] \in \mathbb{C}^{K \times 1}$ gathers all the uncontrollable channel components and $w \sim \mathcal{N}_{\mathbb{C}}(0, \sigma^2)$ is the receiver noise. Accordingly, the downlink CSI includes the number of channel coefficients to and from the RIS (i.e. V and G) equal to $(NK + NK \times U)$ where $U = 1$ for single user antenna and the number of channel coefficients for the direct link b_d equal to $(U \times K)$. The total number of coefficients is different for TDD and FDD systems. Furthermore, they are substantially more as compared to the conventional systems. It is sufficient to estimate the cascaded BS-RIS-User channel H_{eq} for any RIS configuration ϕ . Suppose pilot signal x is transmitted on each of the S subcarriers. Let the RIS configuration ϕ_i where i is the index of the OFDM block. The received signal:

$$\tilde{z}(i) = F_S H_{eq}^T \theta_{\phi_i} x + \tilde{w}(i) \in \mathbb{C}^S, \quad (9)$$

where F_S contains the S rows of F . There are SN unknown coefficients in H_{eq} but we only get S observations from $\tilde{Z}(i)$. One possible way to get SN linearly independent observations, is to consider a sequence of N OFDM blocks with different configurations (ϕ_1, \dots, ϕ_N) . So, the joint received signal [139]:

$$\tilde{z}[1], \dots, \tilde{z}[N] = F_S H_{eq}^T [\theta_1, \dots, \theta_N] x + \tilde{w}[1], \dots, \tilde{w}[N] \quad (10)$$

Let $\tilde{Z} = \tilde{Z}[1], \dots, \tilde{Z}[N]$, $w_{\theta} = [\theta_1, \dots, \theta_N]$ and $\tilde{W} = \tilde{w}[1], \dots, \tilde{w}[N]$. If w_{θ} is invertible then we can apply the

TABLE 5 Summary of existing work of optimization techniques for narrow and wideband systems

Reference	System model	Algorithm	Algorithm Performance	Work Objective
[79]	Wideband Multiuser SISO-OFDM	Power Method	Heuristic	Maximize Data Rate for 50 Users
[114]	Narrowband Single/Multiuser MISO	AO and SDR	Near Optimal	In an RIS-assisted multiuser system, reduce the transmit power as much as possible
[116]	Narrowband Single User MISO	Fixed point iteration, manifold optimization	Locally Optimal	Maximize Spectral efficiency and lower computational complexity
[117]	Narrowband Single and Multiuser MISO	ZF precoder and MMSE precoder based algorithms	Near Optimal	Combine the AP's continuous transmit precoding with the RIS's discrete reflect phase changes to reduce transmit power at the AP
[118]	Wideband Single User MIMO-OFDM	AO and convex relaxation	Locally Optimal	Capacity enhancement
[119]	Wideband Single user mm-wave MIMO-OFDM	Geometric mean decomposition (GMD) based on beamformer and combiner	Heuristic	Improve BER without sophisticated bit/power allocation
[120]	Narrowband Full-duplex MIMO	Arimoto-Blahut algorithm	Near Optimal	Maximize sum rate
[121]	Wideband Single user SISO-OFDM	SCA, AO	Near Optimal	To optimise the achievable rate, combine the transmit power allocation and the RIS passive array reflection coefficients
[122]	Wideband Single user SISO-OFDM	The strongest-CIR maximization (SCM) method	Near Optimal	Maximize the achievable data rate
[129]	Wideband Single user SIMO-OFDM	SDR, STM	Near Optimal	Improve the maximum achievable rate and data transfer latency
[130]	Wideband Multiuser MISO-OFDM	Three-phase one-dimensional search method	Near Optimal	Determine the wideband MU-MISO-OFDM system's highest average sum-rate
[131]	Wideband Single user SISO-OFDM	AO	/	The necessity of considering practical RIS model for channel estimation
[132]	Wideband Multiuser SISO-OFDM	Quadratic unconstrained binary optimization formulation (QUBO)	/	Assigning each RIS to a maximum of one UE using the allocation scheduling method for each UE
[133]	Wideband Single-user downlink OFDM	AO	High Quality Suboptimal	Optimize the transmission power allocation at the BS and the passive array reflection coefficients at the IRS to boost the user's downlink achievable rate
[134]	Wideband Multi-antenna for eavesdropper MIMOME-OFDM	AO	Approximation and Suboptimal	Maximizing the sum secrecy rate
[135]	Wideband Multicell multiuser MISO OFDMA ultra-reliable low latency (ULLC)	Successive Convex Approximation and iterative rank maximization approach (IRMA)	Iterative Suboptimal	Under QoS constraints, maximise the weighted total throughput
[136]	Wideband RIS-Assisted UAV OFDMA	AO	Approximation	The employment of an RIS in UAV OFDMA transmission can boost the system's sum-rate dramatically
[137]	Wideband Multiuser RIS assisted UAV	Successive Convex Approximation with the Rate restriction penalty	Iterative Suboptimal	Maximize the lowest possible average rate for all users
[138]	Narrowband Single user MISO	Branch and Bound (BnB)	Globally Optimal	Maximize spectral efficiency

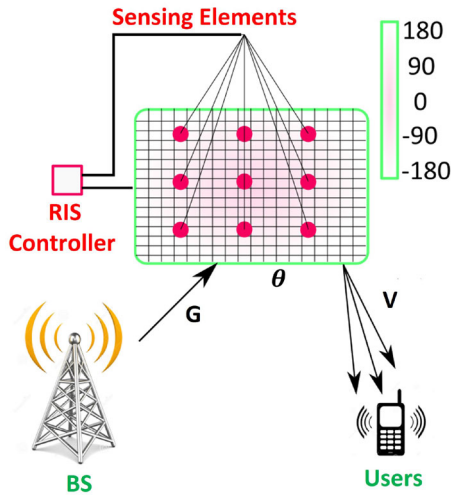


FIGURE 20 RIS assisted wireless communication with sensing elements (nearly passive RIS)

least square (LS) estimate to compute H_{eq} as follows:

$$\underbrace{\frac{1}{x} F_S^{-1} \bar{Z} w_\theta^{-1}}_{\text{Known Signal}} = \underbrace{H_{eq}^T}_{\text{Estimated Composite Channel}} + \underbrace{\frac{1}{x} F_S^{-1} \bar{W} w_\theta^{-1}}_{\text{Noise Signal}} \quad (11)$$

The challenge is when w_θ is non-invertible and the system is overdetermined to solve.

There are two basic methodologies for RIS channel estimates in the available literature, which are based on two alternative RIS configurations, depending on whether it is installed with sensing devices (receive RF chains as per Figure 20) or not, and are referred to as semi-passive RIS and completely passive RIS, respectively. For more details, refer to [140, 141]. One example for the full passive channel estimation method is by employing [142] the ON/OFF based RIS reflection pattern but it requires $N + 1$ channel coefficients and substantial reflection power loss. An other workable method by grouping the neighbouring RIS elements into smaller RIS surfaces so, only the effective cascaded BS-RIS-User channel associated with each smaller surface needs to be estimated, hence significantly reducing the training overhead [108, 143].

In case of MIMO/MISO multi-user systems, the training overhead will be more as compared with single user SISO. To handle this, some RIS channel characteristics (such as spatial correlation, sparsity, and low rank) can be used to make the cascaded channel division easier and decrease the training overhead [144]. The authors in [145] used deep learning and searching algorithms to accelerate the training for channel estimation. The authors in [146] exploited the fact that all users share the same RIS-BS channel in the uplink to get minimum training overhead $U + N + \max(U - 1, \lceil \frac{(U-1)N}{A_B} \rceil)$ where U is the number of active users and A_B is the number of antennas at base station. Moreover, [147] utilized the redundancy of having more OFDM subcarriers than the number of delayed paths

in designing OFDM-based pilot symbols to effectively estimate the channels of multiple users simultaneously. For instance, by exploiting the common BS-RIS channel and the LoS dominant RIS-User channels. It was demonstrated that $N + 1$ OFDM symbols are required to estimate the cascaded channels of up to $\lceil \frac{(N+1)(K-L)}{N+L} \rceil + 1$ users at the same time. Where L is the number of multipath and K is the number of subcarriers.

4.2 | Channel estimation: The state-of-the art

The authors in [149] examines the progression of the reflecting radio idea to RISs, as well as the RIS-assisted MISO communication model and how it differs from traditional multi-antenna communication models. For the design and study of RIS-assisted systems, a MMSE based channel estimate technique was proposed. The BS instructs the microcontroller to keep all RIS elements turned off throughout the channel estimation phase, and the BS estimates the direct channel for all users. The BS then sends a signal to the microcontroller to turn element n of the RIS ON while leaving the other elements OFF, allowing the BS to begin estimating the cascaded channel. As a result, the microcontroller instructs the RIS's control circuit board in Figure 3a to carry out the needed sequence, and so on. The MMSE estimating method is used to calculate the estimations. The BS then computes the optimal beamforming vector using the channel estimates and transmits it to the RIS microcontroller. Using the estimated channels (direct and cascaded), the phase shifts of the RIS are tuned by utilizing a gradient ascent algorithm.

Similar to [149] the authors in [150] describe a unique passive intelligent surface PIS-assisted energy transfer mechanism from a multi-antenna power beacon (PB) to a single-antenna energy harvesting user. A controlled LS Channel estimate protocol with binary reflection was proposed. This binary model is used because it accounts for the fact that a passive intelligent surface (PIS) lacks active components, forcing PB to estimate all the channel vectors on its own. The above-mentioned works require at least $N + 1$ pilot symbols for predicting the total $N + 1$ channel coefficients in the system. Because only one element is turned on at a time, the ON/OFF-based RIS reflection setup suffers from considerable reflection power losses, resulting in a feeble reflected signal.

Different from the above research of work, as shown in Figure 17 (over which the RIS channels are typically spatially correlated), the authors in [122, 148] developed an effective method of grouping adjacent RIS elements into a sub-surface, referred to as RIS element grouping; consequently, only the effective cascaded user RIS-BS channel connected with each sub-surface needs to be calculated, significantly decreasing the training overhead and simplifying RIS reflection configuration for transmitting data. However, it is crucial to mention that the channel coherence time has a significant impact on the appropriate grouping ratio for practical implementation. The upward and downward trend of the achievable data rate in Figure 21 is an obvious example of the effect of the grouping ratio on the data rate at a high SNR regime.

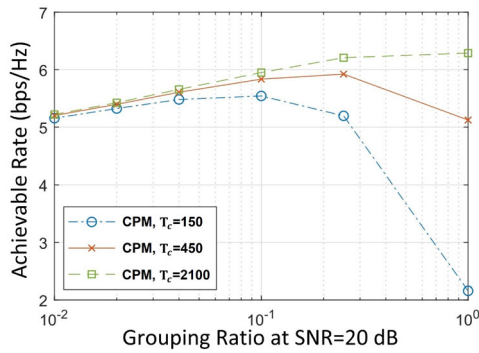


FIGURE 21 Achievable rate versus RIS Grouping [148]

Similar to [122, 148] the authors in [151, 152] studied the channel estimation for the broadband system but for multi-users. The authors in [151] proposed two efficient channel estimate algorithms for various channel configurations in an RIS-assisted multi-user broadband communication system using orthogonal frequency division multiple access (OFDMA). The sequential-user channel estimation (SeUCE) scheme can sustain more users for channel estimation than the simultaneous-user channel estimation (SiUCE) scheme by leveraging the advantage that all users have the same RIS-AP channel, but at the cost of increased channel estimation complexity and some decayed channel estimation performance. The authors in [152] describes a compressive sensing (CS)-based CE solution for RIS-aided mm-Wave massive MIMO systems, whereby the angular channel sparsity of large-scale array at mm-Wave is used for improved CE with reduced pilot overhead. The authors develop pilot signals based on the previous knowing of the line-of-sight-dominated transmitter-to-RIS channel as well as previous experience of the high-dimensional transmitter-to-receiver and RIS-to-receiver channels using compressed sensing techniques. To take advantage of the channel sparsity, a distributed orthogonal matching pursuit method is used. As a result, several writers [153–159] leverage RIS channel features (such as low-rank, sparsity, and spatial correlation) to simplify cascaded channel decomposition and decrease training overhead in RIS-assisted single-user MIMO/MISO systems. On the other hand, the authors in [160–163] used the same channel properties to investigate the channel estimation in the multi-user MISO/MIMO systems.

To speed up the training process in passive RIS-aided MIMO and MISO systems, deep learning and hierarchical searching algorithms have been developed for channel estimation [164–167].

Different from the above-mentioned works, the authors in [168–171] exploited some sensing elements interlaced with the passive RIS elements to provide RIS with sensing capabilities for the channel estimation process as per Figure 20. Unlike the fully passive RIS channel estimation, the nearly passive RIS has two modes of operation. All the reflecting elements are kept OFF in the first mode or called sensing mode, moreover the sensing elements are powered up to receive pilot signals from the BS or users in the downlink or uplink for estimating their

respective channels to RIS, whereas in the second mode or called reflection or transmission mode, the sensors are deactivated, and the RIS reflecting elements are turned on to reflect the data signals from the BS or users for improving downlink and uplink communication in both.

The authors in [168] presented a new deep reinforcement learning framework for estimating RIS reflection matrices by teaching the RIS how to anticipate optimum interaction matrices using sampling channel knowledge on its own. Unlike supervised learning-based methods, this technique does not require an initial dataset gathering step.

4.3 | Discussions and insightful prospect for section IV

- In summary of the above section, a detailed explanation for the various types of channel estimation in different wireless communication system environments was presented. Table 6 summarize to some extent good literature of channel estimation taking into consideration different communication parameters. The pilot transmission and channel estimation are not fully covered in the literature.

5 | RIS DEPLOYMENT

5.1 | Why RIS location is important?

RIS works in FD mode with just passive reflection, avoiding amplification, processing noise and self-interference. These appealing features of RIS have prompted extensive research into using it to largely enhance the performance of wireless systems in a variety of scenarios, including multi-user NOMA, WPT, physical-layer security, multi-carrier communications, multi-antenna, and MEC [3, 6, 13]. In the existing literature, the RIS is usually deployed near the distributed users for the purpose of enhancement the local coverage which is completely different from that for the active relay, almost placed in the middle of the transmitter and receiver for balancing the SNRs of the two-hop links, that process and amplify the source signal before forwarding it to the receiver. Alternatively, the other deployment method is to position the RIS near the base station bearing in mind that both methods of deployments minimize the product distance path loss as per Figures 23a and 23b. It's worth mentioning that RIS might be deployed much more widely across the network, due to its cheap price, to effectively modify signal propagation. However, this creates a considerably larger-scale deployment optimization challenge that is far more difficult to address in addition to the fact that because RIS is passive equipment, the strength of their reflected signals decays fast with distance; consequently, if RISs are placed far enough away, reciprocal interference is essentially non-existent, considerably simplifying their deployment design so, thanks to the RIS passivity.

Another important issue is that for a RIS to be genuinely successful, it must be properly deployed. It should be installed at a place with LoS to the access point, and it may then be set to

TABLE 6 Summary of existing work of channel estimation methods and techniques

Reference	Communication setup	Practical phase shift model	RIS passivity	Channel estimation protocol
[149]	Multi-user MISO	Discrete	Full	Channel estimation procedure based on the minimum mean squared error (MMSE)
[162]	Point to Point MISO	Discrete	Full	LS CE protocol with binary-reflection (full or no)
[88]	Single user RIS-enhanced OFDM	Continuous	Full	Interpolation based on DFT/IDFT to estimate the channel
[87]	Single user RIS based OFDM	Discrete	Full	The RIS's on-and-off state control of reflecting elements
[151]	Multi-user OFDMA Uplink	Continuous	Full	The sequential-user channel estimation
[152]	Multi-user mm-Wave massive MIMO	Continuous	Full	Compressive sensing (CS)-based CE solution
[153]	Single user mm-wave MISO	Continuous	Full	Compressed-sensing-based channel estimation
[154]	Single-user LIM-assisted massive MIMO system	Continuous	Full	a two-stage mixed channel estimate. The JBF-MC method (joint bilinear factorization and matrix completion)
[155]	Single-user RIS-assisted MIMO system	Continuous	Full	a tensor model with parallel factors (PARAFAC) that may be used to estimate the communication channels involved
[156]	Single-user RIS-enabled MIMO system	Continuous	Full	A bilinear adaptive vector approximate message passing (BADVAMP) method with a traditional training uplink technique
[157]	Single-user RIS-aided mm-Wave MIMO system	Continuous	Full	The channel parameters are successively estimated using an iterative reweighted technique
[158]	RIS assisted SISO	Continuous	Full	a low complexity channel information acquisition method using the channel sparsity and the position of the UE
[159]	Single-user MISO	Continuous	Full	Method for channel estimate based on compressed sensing
[160]	A RIS aided multi-user MIMO system	Continuous	Full	CS approaches are used to solve a sparse channel matrix recovery problem
[161]	An RIS aided multi-user MIMO system	Continuous	Full	a dual-link pilot transmission scheme
[162]	Multi-user MIMO	Continuous	Full	a matrix-calibration based sparse matrix factorization
[163]	Multi-user MISO	Continuous	Full	a method based on the parallel factor (PARAFAC) decomposition
[164]	Single-user massive MIMO assisted RIS	Continuous	Full	Design of a hierarchical search codebook (low-complexity basis of beam training)
[165]	Multi-user massive MIMO assisted RIS	Continuous	Full	a beam training-based cooperative channel estimation approach for RIS-assisted MIMO systems
[166]	Single-user RIS assisted MISO	Continuous	Full	Deep Learning DL-based detector, called (Deep RIS) for channel estimates
[167]	Multi-user mm-Wave massive MIMO	Continuous	Full	Deep learning bases scheme (A twin convolutional neural network (CNN))
[168–170]	Single-user OFDM based system	Continuous	Nearly passive	Deep Reinforcement Learning and compressive sensing Based RIS
[171]	Single user SISO	Discrete	Nearly Passive	a method for explicit channel estimation that uses alternating optimization

substantially boost the information rate for users inside LoS. The authors in [139] compared the cases of LoS and NLoS between the transmitter and the RIS. By considering the strongest tap maximization approach to select the value of θ_l that maximizes the magnitude of each channel tap l :

$$\theta_l = \underset{\theta}{\operatorname{argmax}} \left| b_d[l] + H_{eq}^T \theta \right|, \quad l = 0, \dots, M-1, \quad (12)$$

where M is the channel taps. The authors proved in the case of LoS that the RIS can boost the data rate by 2.7–2.9 times, which make a huge improvements when there is NLoS case.

5.2 | RIS deployment: The state-of-the art

In this part of the paper, we look at the new RIS deployment problems in a variety of scenarios to get valuable insights into practical design, beamforming performance, and coverage.

The authors in [172] tackles the critical topic of how to place RISs in a wireless communication network for maximum performance. In terms of different communication performance metrics, the two traditional techniques of installing RIS at the BS or at distributed users are evaluated, and then suggest a novel hybrid RIS deployment approach that combines their cooperative benefits. An inter-RIS reflective link between both

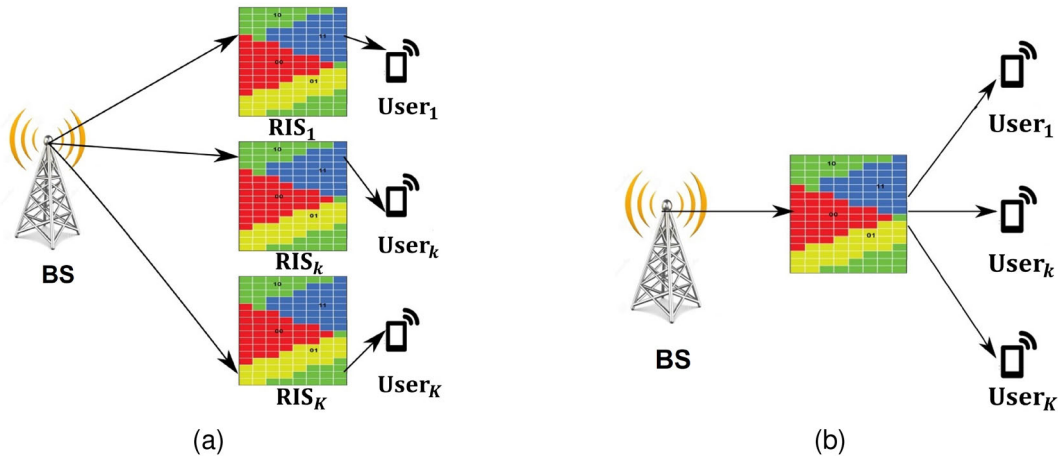


FIGURE 22 RIS Deployment methods, (a) Centralized RIS Deployment, (b) Distributed RIS Deployment

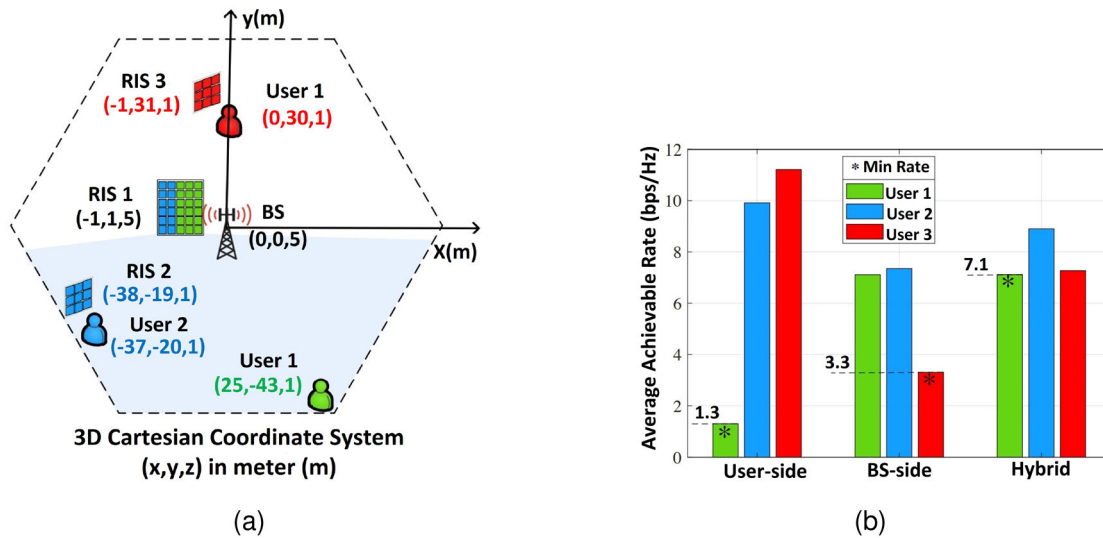


FIGURE 23 The three typical users' achievable rates, as well as their minimum rate, given various RIS deployment techniques [172], (a) System simulation setup, (b) Achievable Rate versus Deployment method

the BS-side RIS and each of the user-side RIS is included in the hybrid RIS installation proposal. When both direct and single-reflection links between the BS and its served users are significantly obstructed, the double-reflection links can be leveraged to provide alternative accessible LoS pathways between them. The double-reflection path may achieve a significantly larger asymptotic passive beamforming gain than the single-reflection channel. Given the same total number of reflecting elements N despite the fact that N increase of $\mathcal{O}(N^4)$ versus $\mathcal{O}(N^2)$. The simulation results show the superior performance of the proposed deployment over the conventional ones as per Figure 23. Because all users may be served by at least one RIS, located whether user or BS side, under the hybrid RIS deployment, it demonstrates its increased efficacy in terms of network coverage.

The authors [173–176] employed the cooperative RIS method in their work to reap the advantages of placing more

than one RIS near the users or base stations and to overcome the standalone RIS which suffers from gain loss if it is located far away from the base station or user equipment. As per Figure 24, in the case of standalone RIS, when situating the RIS near the user or AP it provides the highest SNR however, placing it in the midway between the user and the AP yields the lowest SNR meanwhile the two cooperative RIS case obtains a significant SNR boost. When compared to the highest SNR in the single-RIS scenario.

The authors in [173] contribute to current research by proposing and assessing a wireless communication system with the double-RIS communication system. On the reasonable premise that the reflection channel from the first RIS to the second RIS is of rank one, a combined passive beamforming design for the two RISs was developed. A power increase of order $\mathcal{O}(N^4)$, may be achieved by deploying two cooperative RIS with a total of N components, which is superior than

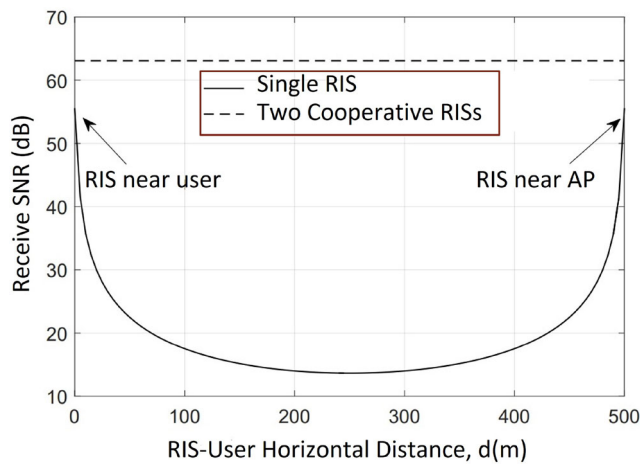


FIGURE 24 Received SNR versus d (m) [3]

installing one ordinary RIS with a power gain of level $\mathcal{O}(N^2)$. Simulated findings demonstrate that establishing two cooperative RISs performs much better than deploying one RIS with the same total number of elements. The simulation shows that when two cooperative RISs are deployed, their performance is lower than when only one RIS is deployed. However, when the total number of elements is big, such as $N = 1600$, using two cooperatives' RISs instead of one can result in substantial performance gains. Another point to notice is that increasing the total number of elements by a factor of two, for example, from $N = 800$ to $N = 1600$, raises the received SNR of the benchmark case with one RIS by 6 dB, while increasing the received SNR of the two-RIS case with $N_1 = N_2 = N/2$ by 12 dB.

Similar to [173], the authors in [175] investigate effective channel estimation and passive beamforming solutions for a single and multiuser communication system helped by a double-RISs. In [174] the authors consider a cooperative passive beamforming design for a double-RIS assisted multiuser MIMO that catches the inter-RIS channel's multiplication beamforming gain. The constructive received beamforming at the BS and the cooperative passive reflected beamforming at the two distributed RISs, positioned near the BS and users, respectively, are optimised in a general channel structure with both dual and single-reflection links to increase the minimum SINR of all users equipment. In the simulation, the maximum power $P = 30$ dBm was adopted to investigate the influence of channel ranking and spatially multiplexing gain on system performance for multi-users and found the superiority of the doubled RIS over the single in relation to achievable max-min rate data rate for the users.

The researchers in [176] proposed a wireless network consists of multiple reconfigurable intelligent surfaces RISs, which would help transmission between a multi-antenna base station and a large number of single-antenna cell-edge users. The authors aim to optimise the weighted sum rate of all cell-edge users by adjusting the BS's transmit beamforming and RIS's phase shifts together. For several schemes, the simulation results display the transmit power versus the weighted sum rate (WSR). To begin, all systems' WSR grows in lockstep with BS power,

and when BS has a larger transmit power budget, the proposed multi-RIS with continuous phase shifts outperforms the single RIS with continuous phase shifts in terms of WSR. This is because, in multi-RIS systems, having the RIS close to the users minimises pathloss propagation, allowing the users' data rate to increase due to the RIS' passive beamforming gain. This exemplifies the value of using several RISs to increase system performance.

More inter-RIS reflections are created as the number of RISs in the User-AP connection grows, resulting in increased pathloss, backhaul cost, and complexity in the aforementioned activities. However, bigger multiplicative beamforming benefits may be obtained by performing cooperative passive beamforming across a large number of RISs.

The researchers in [80, 177] considered two workable RIS deployment methods that correspond to various effective channels between users and the AP: scattered deployment, in which the N elements form two RISs, each placed near one user, and centrally managed deployment, in which all of the N elements are deployed near the AP. The capacity and achievable rate regions for both deployment methods using various multiple-access algorithms are calculated considering the uplink multiple access channel (MAC). It is shown that in symmetric channel settings, the centrally controlled deployment beats the scattered deployment in terms of achievable user rates and capacity region. By exploiting the MAC broadcast (BC) duality, the results were extended to the downlink RIS-aided broadcast channel BC, where the performance advantage of centralized over distributed RIS deployment was also proven to be true. The advantages of centralized vs scattered RIS deployment is particularly apparent when the two users have asymmetric rate demands and channel conditions, according to numerical results. However, in practical scenarios, the assumption of the uplink and downlink channel duality for both RIS deployments may change in terms of the LoS and the NLoS which it will by return impact performance gain of the system.

The uplink power control of an RIS-aided IoT network under the QoS limitations at each user is investigated in [178]. The objective is to reduce total user power by simultaneously optimizing RIS reflecting element phase shifts and receiving beamforming at the BS, while considering each user's unique SINR restriction. The authors used the environment diversity by installing several RISs to produce considerable improvements in energy efficiency through combined optimization of RIS phase shifts and reception beamforming. Specifically, Each RIS is made up of N reflecting components that may independently reflect the incident signal with an adjustable phase shift. The simulation results reveal that when the number of RIS units rises from 1 to 8, the Riemannian manifold based alternating optimization (RM-AO) algorithm saves about 4 dBm transmit power in the single-user situation. Furthermore, as the number of users grows, more transmission power can be conserved. Despite the above-mentioned efforts and advancements in link-level performance optimization for different RIS-aided wireless systems, the large-scale deployment of RISs in large size wireless networks require methods and tools to optimize the huge deployments of the multiple RIS units in the wireless network.

TABLE 7 Summary of existing work of RIS deployment

Reference	RIS deployment method	Users	Achievement
[168]	Hybrid by adopting IA-MS design (distributed near the users and base station)	Multi-users SISO	Minimum data rate significant improvement over the methods of placing the RIS near users or near the base station
[173]	Cooperative double RIS (near base station and user)	Single-user SISO	Improvement of the power gain of order $\mathcal{O}(N^4)$ instead of $\mathcal{O}(N^2)$
[174]	Cooperative double RIS (near base station and users)	Multi-user MIMO	maximize the minimum SINR among all users
[175]	Cooperative double RIS (near base station and user)	Single-user SISO	The training overhead and channel estimate error are taken into consideration, resulting in significant rate improvement
[176]	Four numbers of RIS distributed uniformly at the cell edge of the base station vicinity	Multi-user MISO	maximisation of the cell-edge users' weighted sum rate
[80, 177]	Both Distributed and Centralized	Two users SISO	the centralized deployment beats the distributed deployment in terms of possible user rates Under symmetric channel setups
[178]	Multiple RIS near the users	Multi-user SIMO	By combining the phase shifts of RIS reflecting components with receiving beamforming at the BS, the overall user power is reduced
[179]	Hybrid active and passive OFDMA wireless network	Multi-user	maximizes the hybrid network throughput

The authors in [78, 179, 180] offer an analytical framework for the RIS assisted hybrid network relied on stochastic geometry while the authors in [181, 182] rely on machine learning algorithms in resolving the problems joint RIS deployments, phase shift design, and power allocation in a MISO NOMA network to increase energy efficiency while considering the data needs of each individual user.

5.3 | Discussions and insightful prospect for section V

Table 7 summarize the different RIS deployments for various communication system models for single and multiple users in addition to the purpose and the achievement of the RIS deployments. It was shown that different deployments methods can achieve tradeoff between performance improvements from one side and complexity/budget/training overhead/optimization from the other side. Moreover, the dimensional size (number of RIS elements) of RIS and the LoS path between the transmitter and the RIS are essential parameters that should be taken into account in the RIS designs and deployments to ensure achieving performance gain and better channel conditions.

6 | FUTURE RESEARCH DIRECTIONS

Various techniques, examined in this research, represent that RIS-assisted wireless networks can strongly improve the received signal power, boost the capacity and sum rate, expand network coverage, minimize transmit power, reduce interference, and provide better security layer and Quality of service supply to multiple users. However, from a communication aspect, the design of RIS-aided wireless communication has novel and unique issues, which are outlined below:

1) The passive reflections of all reflective elements at each RIS must be constructed in such a way that they enable

coordinated signal focusing and interference elimination at the RIS's location. Meanwhile, whether or not an associated RIS is located near every user, the RIS passive reflections must be built in tandem with the BSs or users' transmissions in order to enhance their end-to-end communications across the RISs re-designed wireless channels.

- 2) Lacking RF chains makes it difficult to obtain the CSI between RIS and its feeding BSs or users, which is necessary for the RIS reflection optimization mentioned earlier. This is especially true given that RIS typically has a high percentage of reflecting elements and consequently related channel coefficients to calculate.
- 3) Due to their different array structures, passive versus active, operating mechanisms, and reflect versus transmit or receive, the best possible implementation method for RISs in wireless networks to achieve maximum network capacity is observed to be extremely different from that for traditional wireless networks with active BSs, APs, and relays, and thus needs to be thoroughly re-tested. In conclusion, integrating RISs into wireless networks effectively brings both new possibilities and problems, both of which need further exploration.

In this section, we will try to present some challenges of the RIS that we think that still need more studying and investigations.

- **Scaling laws and beyond far-field regime:** When narrow-band capacity increased, the SNR with an RIS grows as $N^2 G \theta V$ at the time when N paths have the same propagation loss [16]. The quadratic SNR scaling does not imply that a higher SNR may be achieved than if the RIS were replaced with an equitable antenna array broadcasting at the same power level as the RIS. The SNR would be proportional to NV in the latter scenario. The SNR scaling can be factorized obtained by the RIS as $(NG\theta)(NV)$ to recognize the difference. The first term accounts for the proportion of the transmitter's signal power reflected by the RIS, which is

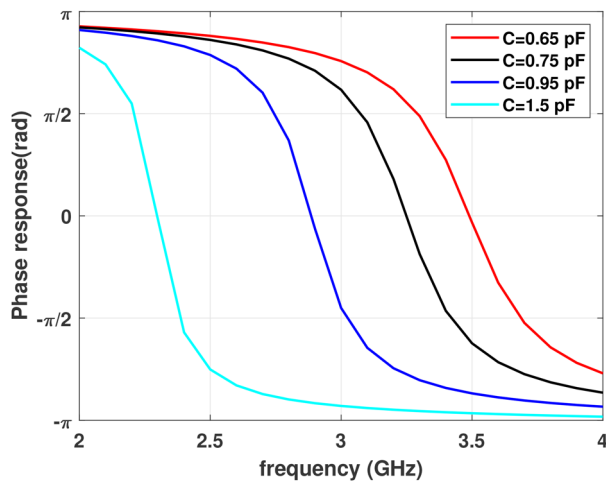


FIGURE 25 The frequency response adjustment when employing a varactor to change the effective capacitance

a relatively tiny amount even when N is big. As a result, the RIS can't get a higher SNR than NV . Consequently, the RIS must be large to be competitive with another enabling technology [183]. Far-field assumptions have been used in the majority of current research on RIS-enabled SRE. RISs, on the other hand, can be composed of a few square metres of geometrically large surfaces. This means that inappropriate application settings, such as interior environments, RISs can function in the near-field regime. The usage of large RISs allows for the creation of novel wireless networks that function in the near-field domain, which is not a common design assumption in wireless communications since the RIS elements incur substantial variations in propagation loss due to the different propagation distances and angles. More significantly, the near field allows the RIS to focus signals not only in a certain direction but also at a specific location within that direction, making it superior to a mirror [184]. This feature can also be exploited for enhanced localization [185]. The basic performance restrictions, design requirements, and possible uses and advantages of near-field transmissions in RIS-enabled SREs have received little attention thus far. The near-field regime is deserving of greater research because of the possible uses that may be unlocked, such as highly focused capabilities.

- Mutual coupling:** When the RIS sections on the substrate material are near together, separating them appropriately is challenging. This causes mutual coupling, in which one element's impedance is linked to the impedances of its neighbours. As a result, whereas Figure 25 depicts how a RIS element acts in isolation, the frequency response will change based on the arrangement of the adjacent elements. The mutual impedance is determined using full-wave simulations, such as the method of moments, and is reliant on the physical characteristics of the components. A RIS constructed of patch or slot antennas effectively decouples the reflected wave's amplitude and phase, providing complete two-phase control. The trade-off between complexity and performance

when the RIS is densified cannot be determined without adequate modelling of the mutual impedance. As a result, to capture the behaviour of RISs with closely spaced components, new modelling approaches that do not rely on the canonical minimum-scattering (CMS) assumption must be devised. Machine learning methods could be useful to solve the problem of system identification if accurate models are difficult to develop [16]. The mutual coupling will affect both algorithmic design from one side and communication and localization performance from the other side. The effect of Mutual coupling on RIS-aided IoT-based applications is inevitable. The RIS is most beneficial when the number of its elements is large however when the surface is quite big (e.g. 4096 elements, i.e. 2Mtrs X 2Mtrs), the mutual coupling between the adjacent elements will impact the actual response of the reflection coefficients of all elements which will end eventually in losing the reward of RIS technology in beamforming or steering the beam direction towards the intended receiver. For example, if the RIS is deployed in LoS with the energy transmitters and receivers in addition to utilising their big aperture and excellent passive beamforming gains, the received power of neighbouring IoT devices can be greatly improved nevertheless, such power enhancement cannot be achieved when mutual coupling affecting the beamforming capability of the RIS.

- Electromagnetic Interference (EMI):** Many researches are ignoring the electromagnetic interference (EMI) that is unavoidably present in any environment and instead focus only on the signals produced by the system [186]. The EMI may result from a range of natural, purposeful, or unintentional factors, such as man-made devices and background radiation from the environment. In general, every unregulated wireless transmission generates EMI [187]. The energy of the EMI waves that strike the RIS in the space in front of it is proportional to its area. When the EMI energy is radiated again by the RIS, it will reach the intended receiver resulting in degrading the end-to-end SNR of the wireless networks which are unaware of such interference effects. The SNR decline is attributed to the fact that such wireless networks/systems are simply designed to deliberately act against only the thermal noise generated by the receiver. As a result, the RIS must be aware of such damaging EMI effect by designing beamforming RIS assisted algorithms that take into consideration the uncontrollable EMI. For example, many authors [188] studied the potential of an RIS assisted wireless powered sensor networks (WPSN) where the RIS is deployed to help multiple IOT devices to enhance their energy harvesting and data transmission capabilities with intelligently adjustable phase shifts. Consequently, we will not get considerable improved throughput performance with the presence of EMI and mutual coupling effects.
- Deployment of large-scale wireless networks:** Due to the extensive deployment of reconfigurable metasurfaces on diverse objects in the future smart radio environment, wireless networks can benefit from a decentralized RIS system with individually programmable RIS units. The great bulk of previous research activities have focused on optimizing

small scale networks, which are often networks consisting of a single RIS. This is a natural growth to start when evaluating the potential advantages of new technology. Furthermore, the evaluation of these fundamental conditions is dependent on modelling hypotheses that may or may not be realistic enough for the evaluation of sub-wavelength meta-materials. However, quantifying the performance constraints of SREs in large-scale installations is critical. This creates a difficult scenario for real-time allocation and optimization of different RISs in dynamic and heterogeneous networks to service diverse data streams. Individual transceivers can adjust their operating parameters in response to the channel state, which is determined by a stochastic model and can be predicted or estimated via a training procedure. Because of the RIS's reconfigurability, the radio environment becomes programmable and non-stationary. As a result, understanding the CSI via training becomes more challenging for individual transceivers. This suggests that the RIS-assisted networks, at least for the scattered RIS units, will be coordinated from a central location. The wireless environment becomes tractable and controlled as a result. To efficiently allocate and associate RIS units to service numerous users at the same time, a joint control method is necessary [13]. Consequently, deploying large density RISs in a big industrial plant or even in a city's Centre to improve coverage probability or energy efficiency are becoming necessary in future wireless systems.

- Sensing and estimation of energy-efficient channels:** The RIS's supremacy is based on its ability to reconfigure the phase shift of each scattering element based on the channel circumstances from the transmitter to the receiver. This necessitates channel sensing and signal processing capabilities, which are difficult to come by without specific signal processing capacity at the passive scattering components. Channel estimation in an RIS-assisted system is often performed at one side of the communication process, such as the BS with superior computing capabilities or the receiver end. In channel estimation section IV, we overview the different existing RIS channel estimate techniques, For instance, the paper in [150], assumes that only one scattering element is active at any one time, with the rest inert. An element-by-element ON/OFF-based channel estimation technique is fundamentally too costly for a sizable RIS with massive scattering components. The RIS is underutilized because only a tiny percentage of the scattering components is active at any given moment. This reduces the precision of the channel estimate and causes a significant estimation delay. Despite the tremendous efforts exerted in [122, 151, 154, 189–191] in creating robust channel estimation algorithms to reduce the training overhead and enhancing the estimation accuracy by deviating from the ON/OFF technique and proposing other effective ones, we think that still feasible, efficient, and long-term channel estimation methods are needed to alleviate the pressure on requesting more energy consumption for exchange of information, signal processing, and computing. Consequently, the authors in [192–194] resolved the optimization problems by considering schemes without the need for computing the channel state information

calculating the convex optimizations. For example, the authors in [192] optimizes beamforming without CSI at the BS and RIS by decreasing transmit power while maintaining a minimal signal-to-noise ratio SNR by proposing a particle swarm optimization (PSO) technique which is a stochastic optimization method inspired by some animal species' social behaviour based on updating the varying velocity and positions of the particles and then , for each particle, comparing the SNR at the user equipment with threshold to update its state and so on. While the researcher in [194] solved the optimization problem by proposing cosine similarity based low complexity algorithm to avoid the complex iterations and the huge overhead needed when using convex optimization techniques. Despite, the proposed algorithm is not powerful in comparison to convex, it is still very simple and does not require many iterations to adjust the phases of the RIS elements.

- RIS configuration under mobility:** Many characteristics of communication systems have been investigated under the idea that the channel is approximately piecewise time-invariant, allowing the use of linear time-invariant (LTI) system theory, in the majority of the research employing the RIS to aid transmission however, the wireless channels are time-variant because of the mobility of the transmitter/receiver. The authors in [16, 195, 196] revealed the importance of using the RIS in reducing the delay spread and eliminating additional Doppler spread. However, the results in [195] were based on hypothetical RISs which create specular reflections with a single and very large conducting elements. While in [196] the inclusion of statistical channel model that accounts for atmospheric effects and line of sight outage were not considered in the system model and optimization of the RIS assisted LEO satellite communications. Consequently, the literature is still lacking to be enriched with practical communication models that take into consideration real and practical assumptions and parameters.

In the above-mentioned points, we tried to summarize some challenges that have been noticed while preparing this survey and the purpose of referring to them is to ensure that the research is still in its infancy and herculean efforts are required to establish strong foundation research to create strong enabling RIS technologies for beyond 5G and 6 G wireless standards so, this paper suggests some study directions for future investigation based on the existing literature review and the thorough system analysis of the present volume of researches.

- Machine learning for passive beamforming:** Machine learning techniques, rather than the alternating optimization techniques often used in the literature, may be more appealing to the RIS in terms of achieving flexible and lightweight phase management dependent on locally obtained radio environment data. This might reduce the quantity of data shared between the RIS and active transceivers [13, 160, 161, 173–175].
- mm-Wave and THz communications:** Mm-Wave communications cannot give gigabit-per-second data rates in the

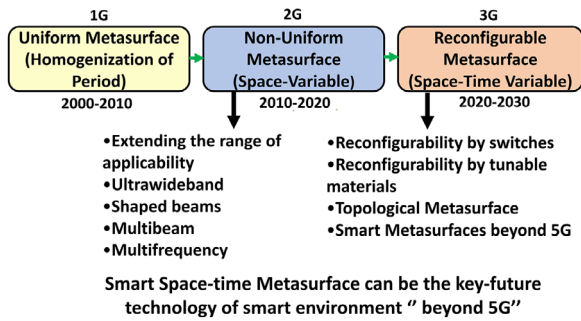


FIGURE 26 3G Metasurfaces [6]

future, enabling rate-demanding wireless applications (augmented/virtual reality (AR/VR) and online gaming, because of the large bandwidth available at mm-Wave frequencies (i.e. 30–300 GHz). However, because of the growing figure of operating antennas and RF chains, mm-Wave communications have significantly higher energy consumption and hardware costs [3]. Furthermore, mm-Wave communication channels are more prone to obstruction and suffer from greater propagation loss overall. When RISs are installed between base stations and end-users, the RIS's two key EM features of reflection and refraction may be leveraged to address the critical problem of dead spots by establishing line-of-sight channels between the AP and the user equipment, allowing for high SE and data rates [197–199]. It is predicted that the RIS will be integrated with the beyond 5G, Figure 26, networks and the current massive MIMO and the mm-wave and THz networks to enhance the network coverage and increase the capacity.

- **Multiple access MEC:** The core premise of the MEC is that network congestion is minimized, and applications function better when applications and related processing activities are executed closer to consumers. The MEC technology is intended for use at cellular base stations and other edge nodes. It helps clients to deploy new applications and services in a flexible and timely manner, in addition, to assisting in offloading computing workloads from mobile devices to reduce latency and energy consumption. Some academics have been looking into the use of RISs in this setting recently [200–204] to enhance the computing performance gains and optimize the computing and communication operations.
- **Advanced applications of RISs in wireless communications:** In the above discussions, the applications of RISs in wireless communications are focused on controlling the wireless channels and improving the wireless environment by reconfiguring the beam directions and beam coverages, in which the metasurfaces are not involved in the digital information modulations. Recently, digital coding and programmable metasurfaces have been presented [205–212], in which the metasurfaces are characterized digital states and controlled by FPGA. On one hand, the digital coding and programmable metasurfaces can manipulate the beam directions, beam coverages, number of beams [205–207], polarization states [208], and the waveforms like cone beams [209] and orbital-angular-momentum vortex beams

[210–212] in real time and in programmable way; and on the other hand, they can directly modulate the digital information. More recently, time-domain digital coding metasurfaces have been developed, which increase an additional degree of freedom to control the EM waves - the frequency spectral distributions [213, 214]. In this manner, the general space-time-coding digital metasurfaces have the capabilities in engineering both spatial beams and the frequency spectra simultaneously and independently, and directly modulating the digital information [215, 216]. Hence, the digital coding and programmable metasurfaces are also called as information metasurfaces [217–219], which have set up a broad link between the EM physical world and the digital world. The information metasurfaces can be regarded as advanced RISs, which will have deeper applications in wireless communications. For example, the information metasurfaces can be utilized to construct new architectures of the wireless communication systems, in which the digital-analog converters, mixers, RF devices, and antennas in the traditional transmitters are no longer required [220–226]; and the information metasurfaces can also be used to develop the EM information theory to combine the Shannon information theory and the Maxwell's equations, in which both EM information and bit-stream information are considered simultaneously [227, 228]. Based on the information metasurfaces, ambient backscatter communications were demonstrated by manipulating the commodity Wi-Fi signals, making it possible to realize secure wireless communications without any active radio components [224]. In the future, we expect that the information metasurfaces, or the advanced RISs, will push revolutionary advances of the wireless communications in basic theories, system levels and communication security for future wireless generations.

The literature is full of interesting and promising future research directions, however, this study concentrates on the conceptual and the techniques of analysis and optimization for RIS more than investigating each RIS assisted application individually.

7 | CONCLUSION

This paper provided a thorough overview of the RIS's architecture and uses in wireless communication networks. In the beginning, we have presented the RIS principles to throw new light on the RIS design and different types of control mechanisms that show the applied tuning methods used in various communication models. In addition to the channel correlation fading and practical pathloss models which characterize the signal and channel model in RIS-aided communications. Then, the optimization frameworks and performance analysis methodologies for RIS, are discussed. The methods have shown promises in increasing the spectral efficiency of wireless networks because of their capacity to modify the behaviours of the interacting EM waves through intelligent manipulations of the reflections phase shifts under different wireless communication scenarios,

including the SNR/data rate/secret rate maximization, transmit power minimization and EE/SE maximization. The paper afterwards gives various relevant RIS deployments strategies and channel estimation algorithms to teach the RIS how to recognize the surrounding environments and enhance the system performance despite its passiveness. Finally, this work paves the way for some research limitations and future directions.

This survey encompasses a wide range of research topics related to RIS and its uses in wireless communication, from its physical tuning, channel modelling, digital coding and information modulations to research issues from a wireless communication viewpoint, with a key goal on the optimization techniques and solution approaches for RIS-assisted wireless systems. The presented methods in the current research are still limited to certain assumptions and dropping some practical parameters and limitations. For example, the mutual coupling between the adjacent RIS elements, the impractical phase shift resolution models that describe the reflection coefficients of all RIS elements and the uncontrollable EM interference are vital, crucial and essential factors in limiting and degrading the RIS performance. In addition to the scaling laws in the near/far-field regime and the time-variant channel mobility which are still required to be explored thoroughly due to their significant effects on the performance of RIS-aided communication. The current solutions mentioned in the literature is depending mainly on the alternating optimization methods and grouping the elements to reduce the overhead and guarantee the convergence of the algorithms to locally optimal solutions nevertheless, the computational complexity and the elapsed run time are still substantially high. In the future work, by analyzing low complex and run time RIS-based algorithms using the machine learning methods for acceleration the phase management, the RIS-aided wireless systems are predicted to attain not only a higher performance gain but also it will establish for more refined and realistic communication models. Furthermore, the RIS must be aware of the mutual coupling, the uncontrollable electromagnetic interference and the practical phase shift models for the RIS coefficients to guarantee remarkable and optimum RIS performance outcome in their beamforming algorithms. Besides, the RISs provide LOS channels which can be exploited to enhance the coverage in the dead spot zones of the mm-wave communication channels and the MEC computing performance gains in congested networks. However, the research of RIS-enhanced networks is still full of challenges and future directions not only from controlling the wireless channel and the smart radio environment perspective but also when the RIS is involved in digital coding and information modulations which will push for revolutionary advances in security communication based RIS systems.

LIST OF ABBREVIATIONS

SRE	Smart Radio Environments
AF/DF	Amplify Forward/Decode Forward
CSI	Channel State Information
FSS	Frequency Selective Surface

PWE	Programmable Wireless Environments
SMM	Spatial Microwave Modulators
FSO	Free Space Optical
MU	Multiuser
UAV	Unmanned Aerial Vehicle
MEC	Mobile Edge Computing
FPGA	Field Programmable Gate Array
MEMS	Micro Electromechanical Systems
HIS	High Impedance Surfaces
LOS	Line of Sight
PEC	Perfect Electric Conductor
IID	Independent and identically distributed
VBLAST	Vertical Bell Labs Layered Space Time
NOMA	Non-Orthogonal Multiple Access
MRT	Maximum Ratio Transmission
LIS	Large Intelligent Surfaces
ZF	Zero Forcing
MMSE	Minimum Mean Square Error
CIR	Channel Impulse Response
SCA	Successive Convex Approximation
BCD	The Block Coordinate Descent
MSE	Mean Square Error
AO	Alternating Optimization
SDR	Semidefinite Relaxation
STM	Strongest Tap Maximization
GMD	Geometric Mean Decomposition
LS	Least Square
CE	Channel Estimate
SeUCE	Sequential User Channel Estimation
SiUCE	Simultaneous User Channel estimation
DFT/IDFT	Discrete Fourier Transform
PARAFAC	Parallel Factor
JBF MC	Joint Bilinear and Matrix Completion
BADV AMP	Bilinear Adaptive Vector Approximate Message Passing
FD	Full Duplex
WPT	Wireless Power Transfer
IoT	Internet of Things
MISO	Multiple-Input Single-Output
SISO	single-input and single-output
RF	Radio frequency
BER	Bit Error Rate
UE	User Equipment
SNR	Signal-to-noise-ratio
SINR	Signal-to-Interference-plus-Noise ratio
QAM	Quadrature Amplitude Modulation
BPSK	Binary Phase Shift Keying
SEP	Symbol Error Probability
CR	Cognitive Radio
AP	Access Point
SU/PU	Secondary/Primary Users
BS	Base Station
PIN	A Positive-Intrinsic-Negative
LoS	Line of Sight
EM	Electromagnetic
MRC	Maximum Ratio Combining
FDD/TDD	Frequency/Time Division Duplexing

AUTHOR CONTRIBUTIONS

Saber Hassouna: Writing - original draft. Muhammad Ali Jamshed: Investigation, supervision. James Rains : Data curation. Jalil ur Rehman Kazim: Data curation. Masood Ur Rehman: Supervision. Muhammad abualhayja: Visualization. Lina mohjazi: Visualization. Tiejun Cui: Conceptualization, data curation. Muhammad Imran: Supervision. Qammer Abbasi: Conceptualization, supervision, validation.

ACKNOWLEDGEMENT

This work was supported in parts by Engineering and Physical Sciences Research Council (EPSRC) grants: EP/T021063/1.

CONFLICT OF INTEREST

The authors declare that there is no conflict of Interest.

DATA AVAILABILITY STATEMENT

Data sharing not applicable to this article as no datasets were generated or analyzed during the current study.

ORCID

Saber Hassouna  <https://orcid.org/0000-0002-3178-1677>

Masood Ur Rehman  <https://orcid.org/0000-0001-6926-7983>

Qammer H. Abbasi  <https://orcid.org/0000-0002-7097-9969>

REFERENCES

- 3GPP: First 5G nr specs approved. <https://www.3gpp.org/news-events/3gpp-news/1929-nsa>. Accessed January 2022
- Saad, W., Bennis, M., Chen, M.: A vision of 6g wireless systems: Applications, trends, technologies, and open research problems. *IEEE Network* 34(3), 134–142 (2019)
- Wu, Q., Zhang, S., Zheng, B., You, C., Zhang, R.: Intelligent reflecting surface aided wireless communications: A tutorial. *IEEE Trans. Commun.* (2021)
- Samsung NewsRoom. (2020, July) The vision of 6g. [samsungresearch. https://news.samsung.com/global/samsungs-6g-white-paper-lays-out-the-companys-vision-for-the-nextgeneration-of-communications-technology](https://news.samsung.com/global/samsungs-6g-white-paper-lays-out-the-companys-vision-for-the-nextgeneration-of-communications-technology). Accessed 11 July 2020.
- Goldsmith, A.: *Wireless Communications*. Cambridge University Press, Cambridge (2005).
- Di Renzo, M., Zappone, A., Debbah, M., Alouini, M.-S., Yuen, C., De Rosny, J., Tretyakov, S.: Smart radio environments empowered by reconfigurable intelligent surfaces: How it works, state of research, and the road ahead. *IEEE J. Sel. Areas Commun.* 38(11), 2450–2525 (2020)
- Subrt, L., Pechac, P.: Controlling propagation environments using intelligent walls. In: 2012 6th European Conference on Antennas and Propagation (EUCAP), pp. 1–5. IEEE, Piscataway (2012)
- Welkie, A., Shangquan, L., Gummesson, J., Hu, W., Jamieson, K.: Programmable radio environments for smart spaces. In: Proceedings of the 16th ACM Workshop on Hot Topics in Networks, 2017, pp. 36–42. ACM, New York (2017)
- Liaskos, C., Nie, S., Tsioliaridou, A., Pitsillides, A., Ioannidis, S., Akyildiz, I.: A new wireless communication paradigm through software-controlled metasurfaces. *IEEE Commun. Mag.* 56(9), 162–169 (2018)
- Liaskos, C., Tsioliaridou, A., Nie, S., Pitsillides, A., Ioannidis, S., Akyildiz, I.F.: On the network-layer modeling and configuration of programmable wireless environments. *IEEE/ACM Trans. Netw.* 27(4), 1696–1713 (2019)
- Dunna, M., Zhang, C., Sievenpiper, D., Bharadia, D.: Scattermimo: Enabling virtual mimo with smart surfaces. In: Proceedings of the 26th Annual International Conference on Mobile Computing and Networking, pp. 1–14. ACM, New York (2020)
- Liu, Y., Liu, X., Mu, X., Hou, T., Xu, J., Di Renzo, M., Al-Dhahir, N.: Reconfigurable intelligent surfaces: Principles and opportunities. *IEEE Commun. Surv. Tutorials* 23(3), 1546–1577 (2021)
- Gong, S., Lu, X., Hoang, D.T., Niyato, D., Shu, L., Kim, D.I., Liang, Y.-C.: Toward smart wireless communications via intelligent reflecting surfaces: A contemporary survey. *IEEE Commun. Surv. Tutorials* 22(4), 2283–2314 (2020)
- Alghamdi, R., Alhadrami, R., Alhothali, D., Almorad, H., Faisal, A., Helal, S., Shalabi, R., Asfour, R., Hammad, N., Shams, A., Saeed, N., Dahrouj, H., Al-Naffouri, T.Y., Alouini, M.-S.: Intelligent surfaces for 6g wireless networks: A survey of optimization and performance analysis techniques. *IEEE Access* 8, 202795–202818 (2020)
- Zhao, J.: A survey of intelligent reflecting surfaces (irs): Towards 6g wireless communication networks. *arXiv preprint arXiv:1907.04789*, 2019.
- Björnson, E., Wymeersch, H., Matthiesen, B., Popovski, P., Sanguinetti, L., de Carvalho, E.: Reconfigurable intelligent surfaces: A signal processing perspective with wireless applications. *arXiv preprint arXiv:2102.00742*, 2021.
- Chen, H.-T., Taylor, A.J., Yu, N.: A review of metasurfaces: physics and applications. *Rep. Prog. Phys.* 79(7), 076401 (2016)
- Liu, F., Ptilakis, A., Mirmoosa, M.S., Tsilipakos, O., Wang, X., Tasolamprou, A.C., Abadal, S., Cabellos-Aparicio, A., Alarcón, E., Liaskos, C., Kantartzis, N.V., Kafesaki, M., Economou, E.N., Soukoulis, C.M., Tretyakov, S.: Programmable metasurfaces: State of the art and prospects. In: 2018 IEEE International Symposium on Circuits and Systems (ISCAS), pp. 1–5. IEEE, Piscataway (2018)
- Turpin, J.P., Bossard, J.A., Morgan, K.L., Werner, D.H., Werner, P.L.: Reconfigurable and tunable metamaterials: a review of the theory and applications. *Int. J. Antennas Propag.* 2014, 429837 (2014)
- Costa, F., Monorchio, A., Talarico, S., Valeri, F.M.: An active high-impedance surface for low-profile tunable and steerable antennas. *IEEE Antennas Wirel. Propag. Lett.* 7, 676–680 (2008)
- Huang, D., Poutirina, E., Smith, D.R.: Analysis of the power dependent tuning of a varactor-loaded metamaterial at microwave frequencies. *Appl. Phys. Lett.* 96(10), 104104 (2010)
- Katko, A.R., Hawkes, A.M., Barrett, J.P., Cummer, S.A.: Rf limiter metamaterial using pin diodes. *IEEE Antennas Wirel. Propag. Lett.* 10, 1571–1574 (2011)
- Nayeri, P., Yang, F., Elsherbeni, A.Z.: *Reflectarray antennas: theory, designs, and applications*. (2018)
- Abeywickrama, S., Zhang, R., Wu, Q., Yuen, C.: Intelligent reflecting surface: Practical phase shift model and beamforming optimization. *IEEE Trans. Commun.* 68(9), 5849–5863 (2020)
- Kaina, N., Dupré, M., Leroose, G., Fink, M.: Shaping complex microwave fields in reverberating media with binary tunable metasurfaces. *Sci. Rep.* 4(1), 1–8 (2014)
- Tan, X., Sun, Z., Jornet, J.M., Pados, D.: Increasing indoor spectrum sharing capacity using smart reflect-array. In: 2016 IEEE International Conference on Communications (ICC), pp. 1–6, IEEE (2016)
- Hu, S., Rusek, F., Edfors, O.: The potential of using large antenna arrays on intelligent surfaces. In: 2017 IEEE 85th Vehicular Technology Conference (VTC Spring), pp. 1–6. IEEE (2017)
- Liaskos, C., Nie, S., Tsioliaridou, A., Pitsillides, A., Ioannidis, S., Akyildiz, I.: A novel communication paradigm for high capacity and security via programmable indoor wireless environments in next generation wireless systems. *Ad Hoc Networks* 87, 1–16 (2019)
- Nie, S., Akyildiz, I.F.: Beamforming in intelligent environments based on ultra-massive mimo platforms in millimeter wave and terahertz bands. In: ICASSP 2020-2020 IEEE International Conference on Acoustics, Speech and Signal Processing (ICASSP), pp. 8683–8687. IEEE, Piscataway (2020)

30. Najafi, M., Schmauss, B., Schober, R.: Intelligent reflecting surfaces for free space optical communication systems. *IEEE Trans. Commun.* 69(9), 6134–6151 (2021)
31. del Hougne, P., Fink, M., Lerosey, G.: Optimally diverse communication channels in disordered environments with tuned randomness. *Nat. Electron.* 2(1), 36–41 (2019)
32. Karasik, R., Simeone, O., Di Renzo, M., Shitz, S.S.: Beyond max-snr: Joint encoding for reconfigurable intelligent surfaces. In: 2020 IEEE International Symposium on Information Theory (ISIT), pp. 2965–2970. IEEE, Piscataway (2020)
33. Zappone, A., Di Renzo, M., Shams, F., Qian, X., Debbah, M.: Overhead-aware design of reconfigurable intelligent surfaces in smart radio environments. *IEEE Trans. Wireless Commun.* 20(1), 126–141 (2020)
34. Tang, W., Dai, J.Y., Chen, M.Z., Wong, K.-K., Li, X., Zhao, X., Jin, S., Cheng, Q., Cui, T.J.: MIMO transmission through reconfigurable intelligent surface: System design, analysis, and implementation. *IEEE J. Sel. Areas Commun.* 38(11), 2683–2699 (2020)
35. Kern, D., Wilhelm, M., Werner, D., Werner, P.: A novel design technique for ultra-thin tunable ebga surfaces. In: IEEE Antennas and Propagation Society Symposium, 2004, vol. 2, pp. 1167–1170. IEEE, Piscataway (2004)
36. Sheng, Z., Varadan, V.V.: Tuning the effective properties of metamaterials by changing the substrate properties. *J. Appl. Phys.* 101(1), 014909 (2007)
37. Lu, H., Zeng, Y., Jin, S., Zhang, R.: Enabling panoramic full-angle reflection via aerial intelligent reflecting surface. In: 2020 IEEE International Conference on Communications Workshops (ICC Workshops), pp. 1–6. IEEE, Piscataway (2020)
38. Björnson, E., Sanguinetti, L.: Rayleigh fading modeling and channel hardening for reconfigurable intelligent surfaces. *IEEE Wireless Commun. Lett.* 10(4), 830–834 (2020)
39. Wu, Q., Zhang, R.: Towards smart and reconfigurable environment: Intelligent reflecting surface aided wireless network. *IEEE Commun. Mag.* 58(1), 106–112 (2019)
40. Yu, X., Xu, D., Schober, R.: MISO wireless communication systems via intelligent reflecting surfaces. In: 2019 IEEE/CIC International Conference on Communications in China (ICCC), pp. 735–740. IEEE, Piscataway (2019)
41. Huang, C., Zappone, A., Alexandropoulos, G.C., Debbah, M., Yuen, C.: Reconfigurable intelligent surfaces for energy efficiency in wireless communication. *IEEE Trans. Wireless Commun.* 18(8), 4157–4170 (2019)
42. Basar, E., Di Renzo, M., De Rosny, J., Debbah, M., Alouini, M.-S., Zhang, R.: Wireless communications through reconfigurable intelligent surfaces. *IEEE Access* 7, 116 753–116 773 (2019)
43. Tang, W., Chen, M.Z., Chen, X., Dai, J.Y., Han, Y., Di Renzo, M., Zeng, Y., Jin, S., Cheng, Q., Cui, T.J.: Wireless communications with reconfigurable intelligent surface: Path loss modeling and experimental measurement. *IEEE Trans. Wireless Commun.* 20(1), 421–439 (2020)
44. Tang, W., Chen, X., Chen, M.Z., Dai, J.Y., Han, Y., Di Renzo, M., Jin, S., Cheng, Q., Cui, T.J.: Path loss modeling and measurements for reconfigurable intelligent surfaces in the millimeter-wave frequency band. arXiv preprint arXiv:2101.08607 (2021)
45. Özdogan, Ö., Björnson, E., Larsson, E.G.: Intelligent reflecting surfaces: Physics, propagation, and pathloss modeling. *IEEE Wireless Commun. Lett.* 9(5), 581–585 (2019)
46. Di Renzo, M., Danufane, F.H., Xi, X., De Rosny, J., Tretyakov, S.: Analytical modeling of the path-loss for reconfigurable intelligent surfaces—anomalous mirror or scatterer? In: 2020 IEEE 21st International Workshop on Signal Processing Advances in Wireless Communications (SPAWC), pp. 1–5. IEEE, Piscataway (2020)
47. Garcia, J.C.B., Sibille, A., Kamoun, M.: Reconfigurable intelligent surfaces: Bridging the gap between scattering and reflection. *IEEE J. Sel. Areas Commun.* 38(11), 2538–2547 (2020)
48. Ellingson, S.W.: Path loss in reconfigurable intelligent surface-enabled channels. In: 2021 IEEE 32nd Annual International Symposium on Personal, Indoor and Mobile Radio Communications (PIMRC), pp. 829–835. IEEE, Piscataway (2021)
49. Khawaja, W., Ozdemir, O., Yapici, Y., Erden, F., Guvenc, I.: Coverage enhancement for nlos mmwave links using passive reflectors. *IEEE Open J. Commun. Soc.* 1, 263–281 (2020)
50. Usman, M., Rains, J., Cui, T.J., Khan, M.Z., Imran, M.A., Abbasi, Q.H.: Intelligent wireless walls for contactless in-home monitoring. *Light Sci. Appl.* 11(1), 1–13 (2022)
51. Cui, M., Zhang, G., Zhang, R.: Secure wireless communication via intelligent reflecting surface. *IEEE Wireless Commun. Lett.* 8(5), 1410–1414 (2019)
52. Yu, X., Xu, D., Sun, Y., Ng, D.W.K., Schober, R.: Robust and secure wireless communications via intelligent reflecting surfaces. *IEEE J. Sel. Areas Commun.* 38(11), 2637–2652 (2020)
53. Björnson, E., Özdogan, Ö., Larsson, E.G.: Intelligent reflecting surface versus decode-and-forward: How large surfaces are needed to beat relaying? *IEEE Wireless Commun. Lett.* 9(2), 244–248 (2019)
54. Sharma, S.K., Patwary, M., Chatzinotas, S., Ottersten, B., Abdel-Maguid, M.: Repeater for 5g wireless: A complementary contender for spectrum sensing intelligence. In: 2015 IEEE International Conference on Communications (ICC), pp. 1416–1421. IEEE, Piscataway (2015)
55. Liu, R., Wu, Q., Di Renzo, M., Yuan, Y.: A path to smart radio environments: An industrial viewpoint on reconfigurable intelligent surfaces. *IEEE Wireless Commun.* 29(1), 202–208 (2022)
56. Xu, C., Yang, L., Zhang, P.: Practical backscatter communication systems for battery-free internet of things: A tutorial and survey of recent research. *IEEE Signal Process Mag.* 35(5), 16–27 (2018)
57. Zhao, H., Shuang, Y., Wei, M., Cui, T.J., del Hougne, P., Li, L.: Metasurface-assisted massive backscatter wireless communication with commodity wi-fi signals. *Nat. Commun.* 11(1), 1–10 (2020)
58. Nemat, M., Ding, J., Choi, J.: Short-range ambient backscatter communication using reconfigurable intelligent surfaces. In: 2020 IEEE Wireless Communications and Networking Conference (WCNC), pp. 1–6. IEEE, Piscataway (2020)
59. Di Renzo, M., Ntontin, K., Song, J., Danufane, F.H., Qian, X., Lazarakis, F., De Rosny, J., Phan-Huy, D.-T., Simeone, O., Zhang, R., Debbah, M., Lerosey, G., Fink, M., Tretyakov, S., Shamai, S.: Reconfigurable intelligent surfaces vs. relaying: Differences, similarities, and performance comparison. *IEEE Open J. Commun. Soc.* 1, 798–807 (2020)
60. Khaleel, A., Basar, E.: Reconfigurable intelligent surface-empowered mimo systems. *IEEE Syst. J.* 15(3), 4358–4366 (2020)
61. Di Renzo, M., Song, J.: Reflection probability in wireless networks with metasurface-coated environmental objects: An approach based on random spatial processes. *Eurasip J. Wirel. Commun. Netw.* 2019(1), 1–15 (2019)
62. Tan, X., Sun, Z., Koutsonikolas, D., Jornet, J.M.: Enabling indoor mobile millimeter-wave networks based on smart reflect-arrays. In: IEEE INFOCOM 2018-IEEE Conference on Computer Communications, pp. 270–278. IEEE, Piscataway (2018)
63. Guo, C., Cui, Y., Yang, F., Ding, L.: Outage probability analysis and minimization in intelligent reflecting surface-assisted miso systems. *IEEE Commun. Lett.* 24(7), 1563–1567 (2020)
64. Narayanan, A., Sreejith, T., Ganti, R.K.: Coverage analysis in millimeter wave cellular networks with reflections. In: GLOBECOM 2017-2017 IEEE Global Communications Conference, pp. 1–6. IEEE, Piscataway (2017)
65. Lu, B., Wang, R., Liu, Y.: Outage probability of intelligent reflecting surface assisted full duplex two-way communications. *IEEE Commun. Lett.* 26(2), 286–290 (2021)
66. Wang, J., Zhang, W., Bao, X., Song, T., Pan, C.: Outage analysis for intelligent reflecting surface assisted vehicular communication networks. In: GLOBECOM 2020-2020 IEEE Global Communications Conference, pp. 1–6. IEEE, Piscataway (2020)
67. Ferreira, R.C., Facina, M.S., De Figueiredo, F.A., Fraidenraich, G., De Lima, E.R.: Bit error probability for large intelligent surfaces under double-nakagami fading channels. *IEEE Open J. Commun. Soc.* 1, 750–759 (2020)
68. Basar, E.: Transmission through large intelligent surfaces: A new frontier in wireless communications. In: 2019 European Conference on Networks and Communications (EuCNC), pp. 112–117. IEEE, Piscataway (2019)

69. Assaf, T., Al-Dweik, A.J., El Moursi, M.S., Zeineldin, H., Al-Jarrah, M., Exact bit error-rate analysis of two-user noma using qam with arbitrary modulation orders. *IEEE Commun. Lett.* 24(12), 2705–2709 (2020)
70. Thirumavalavan, V.C., Jayaraman, T.S.: Ber analysis of reconfigurable intelligent surface assisted downlink power domain noma system. In: 2020 International Conference on COMMunication Systems & NETWORKS (COMSNETS), pp. 519–522. IEEE, Piscataway (2020)
71. Jung, M., Saad, W., Debbah, M., Hong, C.S.: Asymptotic optimality of reconfigurable intelligent surfaces: Passive beamforming and achievable rate. In: ICC 2020-2020 IEEE International Conference on Communications (ICC), pp. 1–6. IEEE, Piscataway (2020)
72. Li, J., Hong, Y.: Intelligent reflecting surface aided communication systems: Performance analysis. In: 2021 IEEE 32nd Annual International Symposium on Personal, Indoor and Mobile Radio Communications (PIMRC), pp. 519–524. IEEE, Piscataway (2021)
73. Salhab, A.M., Samuh, M.H.: Accurate performance analysis of reconfigurable intelligent surfaces over rician fading channels. *IEEE Wireless Commun. Lett.* 10(5), 1051–1055 (2021)
74. He, J., Wymeersch, H., Sanguanpuak, T., Silvén, O., Juntti, M.: Adaptive beamforming design for mmwave ris-aided joint localization and communication. In: 2020 IEEE Wireless Communications and Networking Conference Workshops (WCNCW), pp. 1–6. IEEE, Piscataway (2020)
75. Özdogan, Ö., Björnson, E., Larsson, E.G.: Using intelligent reflecting surfaces for rank improvement in mimo communications. In: ICASSP 2020-2020 IEEE International Conference on Acoustics, Speech and Signal Processing (ICASSP), pp. 9160–9164. IEEE, Piscataway (2020)
76. Zhang, H., Di, B., Song, L., Han, Z.: Reconfigurable intelligent surfaces assisted communications with limited phase shifts: How many phase shifts are enough? *IEEE Trans. Veh. Technol.* 69(4), 4498–4502 (2020)
77. Alegria, J.V., Rusek, F.: Achievable rate with correlated hardware impairments in large intelligent surfaces. In: 2019 IEEE 8th International Workshop on Computational Advances in Multi-Sensor Adaptive Processing (CAMSAP), pp. 559–563. IEEE, Piscataway (2019)
78. Lyu, J., Zhang, R.: Spatial throughput characterization for intelligent reflecting surface aided multiuser system. *IEEE Wireless Commun. Lett.* 9(6), 834–838 (2020)
79. Björnson, E., Optimizing a binary intelligent reflecting surface for ofdm communications under mutual coupling. arXiv preprint arXiv:2106.04280 (2021)
80. Zhang, S., Zhang, R.: Intelligent reflecting surface aided multi-user communication: Capacity region and deployment strategy. *IEEE Trans. Commun.* 69(9), 5790–5806 (2021)
81. Papazafeiropoulos, A., Pan, C., Elbir, A., Kourtessis, P., Chatzinotas, S., Senior, J.M.: Coverage probability of distributed irs systems under spatially correlated channels. *IEEE Wireless Commun. Lett.* 10(8), 1722–1726 (2021)
82. Jung, M., Saad, W., Jang, Y., Kong, G., Choi, S.: Performance analysis of large intelligent surfaces (liss): Asymptotic data rate and channel hardening effects. *IEEE Trans. Wireless Commun.* 19(3), 2052–2065 (2020)
83. Hu, S., Rusek, F., Edfors, O.: Capacity degradation with modeling hardware impairment in large intelligent surface. In: 2018 IEEE Global Communications Conference (GLOBECOM), pp. 1–6. IEEE, Piscataway (2018)
84. Papazafeiropoulos, A., Pan, C., Kourtessis, P., Chatzinotas, S., Senior, J.M.: Intelligent reflecting surface-assisted mu-miso systems with imperfect hardware: Channel estimation, beamforming design. arXiv preprint arXiv:2102.05333 (2021)
85. Hu, S., Rusek, F., Edfors, O.: Beyond massive mimo: The potential of positioning with large intelligent surfaces. *IEEE Trans. Signal Process.* 66(7), 1761–1774 (2018)
86. Basar, E., Wen, M., Mesleh, R., Di Renzo, M., Xiao, Y., Haas, H.: Index modulation techniques for next-generation wireless networks. *IEEE Access* 5, 16 693–16 746 (2017)
87. Phan-Huy, D.-T., Kokar, Y., Rachedi, K., Pajusco, P., Mokh, A., Magounaki, T., Masood, R., Buey, C., Ratajczak, P., Malhouroux-Gaffet, N., Conrat, J.-M., Prévotet, J.-C., Ourir, A., De Rosny, J., Crussière, M., Héléard, M., Gati, A., Sarrebourg, T., Di Renzo, M.: Single-carrier spatial modulation for the internet of things: Design and performance evaluation by using real compact and reconfigurable antennas. *IEEE Access* 7, 18 978–18 993 (2019)
88. Van Huynh, N., Hoang, D.T., Lu, X., Niyato, D., Wang, P., Kim, D.I.: Ambient backscatter communications: A contemporary survey. *IEEE Commun. Surv. Tutorials* 20(4), 2889–2922 (2018)
89. Guan, X., Wu, Q., Zhang, R.: Joint power control and passive beamforming in irs-assisted spectrum sharing. *IEEE Commun. Lett.* 24(7), 1553–1557 (2020)
90. Wu, W., Wang, Z., Yuan, L., Zhou, F., Lang, F., Wang, B., Wu, Q.: Irs-enhanced energy detection for spectrum sensing in cognitive radio networks. *IEEE Wireless Commun. Lett.* 10(10), 2254–2258 (2021)
91. Mahmoud, A., Muhaidat, S., Sofotasios, P., Abualhaol, I., Dobre, O.A., Yanikomeroglu, H.: Intelligent reflecting surfaces assisted uav communications for iot networks: Performance analysis. *IEEE Trans. Green Commun. Networking* 5(3), 1029–1040 (2021)
92. Al-Jarrah, M., Alsusa, E., Al-Dweik, A., So, D.K.: Capacity analysis of irs-based uav communications with imperfect phase compensation. *IEEE Wireless Commun. Lett.* 10(7), 1479–1483 (2021)
93. Al-Jarrah, M., Al-Dweik, A., Alsusa, E., Iraqi, Y., Alouini, M.-S.: On the performance of irs-assisted multi-layer uav communications with imperfect phase compensation. *IEEE Trans. Commun.* 69(12), 8551–8568 (2021)
94. Zhang, S., Zhang, R.: Capacity characterization for intelligent reflecting surface aided mimo communication. *IEEE J. Sel. Areas Commun.* 38(8), 1823–1838 (2020)
95. Huang, C., Alexandropoulos, G.C., Yuen, C., Debbah, M.: Indoor signal focusing with deep learning designed reconfigurable intelligent surfaces. In: 2019 IEEE 20th International Workshop on Signal Processing Advances in Wireless Communications (SPAWC), pp. 1–5. IEEE, Piscataway (2019)
96. Ye, J., Guo, S., Alouini, M.-S.: Joint reflecting and precoding designs for ser minimization in reconfigurable intelligent surfaces assisted mimo systems. *IEEE Trans. Wireless Commun.* 19(8), 5561–5574 (2020)
97. Huang, C., Zappone, A., Alexandropoulos, G.C., Debbah, M., Yuen, C.: Reconfigurable intelligent surfaces for energy efficiency in wireless communication. *IEEE Trans. Wireless Commun.* 18(8), 4157–4170 (2019)
98. Wu, Q., Zhang, R.: Beamforming optimization for wireless network aided by intelligent reflecting surface with discrete phase shifts. *IEEE Trans. Commun.* 68(3), 1838–1851 (2019)
99. Yu, X., Xu, D., Schober, R.: Miso wireless communication systems via intelligent reflecting surfaces. In: 2019 IEEE/CIC International Conference on Communications in China (ICCC), pp. 735–740. IEEE, Piscataway (2019)
100. Wu, Q., Zhang, R.: Intelligent reflecting surface enhanced wireless network: Joint active and passive beamforming design. In: 2018 IEEE Global Communications Conference (GLOBECOM), pp. 1–6. IEEE, Piscataway (2018)
101. Chen, W., Ma, X., Li, Z., Kuang, N.: Sum-rate maximization for intelligent reflecting surface based terahertz communication systems. In: 2019 IEEE/CIC International Conference on Communications Workshops in China (ICCC Workshops), pp. 153–157. IEEE, Piscataway (2019)
102. Guo, H., Liang, Y.-C., Chen, J., Larsson, E.G.: Weighted sum-rate maximization for reconfigurable intelligent surface aided wireless networks. *IEEE Trans. Wireless Commun.* 19(5), 3064–3076 (2020)
103. Huang, C., Zappone, A., Debbah, M., Yuen, C.: Achievable rate maximization by passive intelligent mirrors. In: 2018 IEEE International Conference on Acoustics, Speech and Signal Processing (ICASSP), pp. 3714–3718. IEEE, Piscataway (2018)
104. Mu, X., Liu, Y., Guo, L., Lin, J., Al-Dhahir, N.: Exploiting intelligent reflecting surfaces in noma networks: Joint beamforming optimization. *IEEE Trans. Wireless Commun.* 19(10), 6884–6898 (2020)
105. Guo, H., Liang, Y.-C., Chen, J., Larsson, E.G.: Weighted sum-rate optimization for intelligent reflecting surface enhanced wireless networks. arXiv preprint arXiv:1905.07920 (2019)

106. Yu, X., Xu, D., Schober, R.: Optimal beamforming for miso communications via intelligent reflecting surfaces. In: 2020 IEEE 21st International Workshop on Signal Processing Advances in Wireless Communications (SPAWC), pp. 1–5. IEEE, Piscataway (2020)
107. Perović, N.S., Tran, L.-N., Di Renzo, M., Flanagan, M.F.: Achievable rate optimization for mimo systems with reconfigurable intelligent surfaces. *IEEE Trans. Wireless Commun.* 20(6), 3865–3882 (2021)
108. Yang, Y., Zheng, B., Zhang, S., Zhang, R.: Intelligent reflecting surface meets ofdm: Protocol design and rate maximization. *IEEE Trans. Commun.* 68(7), 4522–4535 (2020)
109. Björnson, E.: Optimizing a binary intelligent reflecting surface for ofdm communications under mutual coupling. arXiv preprint arXiv:2106.04280 (2021)
110. Yang, Y., Zhang, S., Zhang, R.: Irs-enhanced ofdma: Joint resource allocation and passive beamforming optimization. *IEEE Wireless Commun. Lett.* 9(6), 760–764 (2020)
111. Yang, Y., Zhang, S., Zhang, R.: Irs-enhanced ofdm: Power allocation and passive array optimization. In: 2019 IEEE Global Communications Conference (GLOBECOM), pp. 1–6. IEEE, Piscataway (2019)
112. Björnson, E., Wymeersch, H., Matthiesen, B., Popovski, P., Sanguinetti, L., de Carvalho, E.: Reconfigurable intelligent surfaces: A signal processing perspective with wireless applications. *IEEE Signal Process. Mag.* 39(2), 135–158 (2022)
113. Nuti, P., Balti, E., Evans, B.L.: Spectral efficiency optimization for mmwave wideband mimo ris-assisted communication. arXiv preprint arXiv:2201.01739 (2021)
114. Wu, Q., Zhang, R.: Intelligent reflecting surface enhanced wireless network via joint active and passive beamforming. *IEEE Trans. Wireless Commun.* 18(11), 5394–5409 (2019)
115. Björnson, E., Sanguinetti, L.: Demystifying the power scaling law of intelligent reflecting surfaces and metasurfaces. In: 2019 IEEE 8th International Workshop on Computational Advances in Multi-Sensor Adaptive Processing (CAMSAP), pp. 549–553. IEEE, Piscataway (2019)
116. Yu, X., Xu, D., Schober, R.: Miso wireless communication systems via intelligent reflecting surfaces. In: 2019 IEEE/CIC International Conference on Communications in China (ICCC), pp. 735–740. IEEE, Piscataway (2019)
117. Wu, Q., Zhang, R.: Beamforming optimization for wireless network aided by intelligent reflecting surface with discrete phase shifts. *IEEE Trans. Commun.* 68(3), 1838–1851 (2019)
118. Zhang, S., Zhang, R.: Capacity characterization for intelligent reflecting surface aided mimo communication. *IEEE J. Sel. Areas Commun.* 38(8), 1823–1838 (2020)
119. Ying, K., Gao, Z., Lyu, S., Wu, Y., Wang, H., Alouini, M.-S.: Gmd-based hybrid beamforming for large reconfigurable intelligent surface assisted millimeter-wave massive mimo. *IEEE Access* 8, 19 530–19 539 (2020)
120. Zhang, Y., Zhong, C., Zhang, Z., Lu, W.: Sum rate optimization for two way communications with intelligent reflecting surface. *IEEE Commun. Lett.* 24(5), 1090–1094 (2020)
121. Yang, Y., Zheng, B., Zhang, S., Zhang, R.: Intelligent reflecting surface meets ofdm: Protocol design and rate maximization. *IEEE Trans. Commun.* 68(7), 4522–4535 (2020)
122. Zheng, B., Zhang, R.: Intelligent reflecting surface-enhanced ofdm: Channel estimation and reflection optimization. *IEEE Wireless Commun. Lett.* 9(4), 518–522 (2019)
123. Björnson, E.: Configuring an intelligent reflecting surface for wireless communications. arXiv preprint arXiv:2106.03497 (2021)
124. Yang, Z., Feng, L., Zhou, F., Qiu, X., Li, W.: Analytical performance analysis of intelligent reflecting surface aided ambient backscatter communication network. *IEEE Wireless Commun. Lett.* 10(12), 2732–2736 (2021)
125. He, M., Xu, W., Shen, H., Xie, G., Zhao, C., Di Renzo, M.: Cooperative multi-ris communications for wideband mmwave miso-ofdm systems. *IEEE Wireless Commun. Lett.* 10(11), 2360–2364 (2021)
126. Du, H., Zhang, J., Cheng, J., Ai, B.: Millimeter wave communications with reconfigurable intelligent surfaces: Performance analysis and optimization. *IEEE Trans. Commun.* 69(4), 2752–2768 (2021)
127. El Bouanani, F., Muhaidat, S., Sofotasios, P.C., Dobre, O.A., Badarneh, O.S.: Performance analysis of intelligent reflecting surface aided wireless networks with wireless power transfer. *IEEE Commun. Lett.* 25(3), 793–797 (2020)
128. Yue, X., Liu, Y.: Performance analysis of intelligent reflecting surface assisted noma networks. *IEEE Trans. Wireless Commun.* 21(4), 2623–2636 (2021)
129. Lin, S., Zheng, B., Alexandropoulos, G.C., Wen, M., Chen, F., Smumtaz, S.: Adaptive transmission for reconfigurable intelligent surface-assisted ofdm wireless communications. *IEEE J. Sel. Areas Commun.* 38(11), 2653–2665 (2020)
130. Li, H., Cai, W., Liu, Y., Li, M., Liu, Q., Wu, Q.: Intelligent reflecting surface enhanced wideband mimo-ofdm communications: From practical model to reflection optimization. *IEEE Trans. Commun.* 69(7), 4807–4820 (2021)
131. Yang, W., Li, H., Li, M., Liu, Y., Liu, Q.: Channel estimation for practical irs-assisted ofdm systems. In: 2021 IEEE Wireless Communications and Networking Conference Workshops (WCNCW), pp. 1–6. IEEE, Piscataway (2021)
132. Ohyama, T., Kawamoto, Y., Kato, N.: Intelligent reflecting surface (irs) allocation scheduling method using combinatorial optimization by quantum computing. *IEEE Trans. Emerging Top. Comput.* 10(3), 1633–1644 (2021)
133. Yang, Y., Zhang, S., Zhang, R.: Irs-enhanced ofdm: Power allocation and passive array optimization. In: 2019 IEEE Global Communications Conference (GLOBECOM) pp. 1–6. IEEE, Piscataway (2019)
134. Jiang, W., Chen, B., Zhao, J., Xiong, Z., Ding, Z.: Joint active and passive beamforming design for the irs-assisted mimome-ofdm secure communications. *IEEE Trans. Veh. Technol.* 70(10), 10 369–10 381 (2021)
135. Ghanem, W.R., Jamali, V., Schober, R.: Joint beamforming and phase shift optimization for multicell irs-aided ofdma-urllc systems. In: 2021 IEEE Wireless Communications and Networking Conference (WCNC), pp. 1–7. IEEE, Piscataway (2021)
136. Wei, Z., Cai, Y., Sun, Z., Ng, D.W.K., Yuan, J., Zhou, M., Sun, L.: Sum-rate maximization for irs-assisted uav ofdma communication systems. *IEEE Trans. Wireless Commun.* 20(4), 2530–2550 (2020)
137. Pan, Y., Wang, K., Pan, C., Zhu, H., Wang, J.: Uav-assisted and intelligent reflecting surfaces-supported terahertz communications. *IEEE Wireless Commun. Lett.* 10(6), 1256–1260 (2021)
138. Yu, X., Xu, D., Schober, R.: Optimal beamforming for miso communications via intelligent reflecting surfaces. In: 2020 IEEE 21st International Workshop on Signal Processing Advances in Wireless Communications (SPAWC), pp. 1–5. IEEE, Piscataway (2020)
139. Björnson, E., Wymeersch, H., Matthiesen, B., Popovski, P., Sanguinetti, L., de Carvalho, E.: Reconfigurable intelligent surfaces: A signal processing perspective with wireless applications. *IEEE Signal Process. Mag.* 39(2), 135–158 (2022)
140. Wu, Q., Zhang, S., Zheng, B., You, C., Zhang, R.: Intelligent reflecting surface-aided wireless communications: A tutorial. *IEEE Trans. Commun.* 69(5), 3313–3351 (2021)
141. Björnson, E., Özdogan, Ö., Larsson, E.G.: Reconfigurable intelligent surfaces: Three myths and two critical questions. *IEEE Commun. Mag.* 58(12), 90–96 (2020)
142. Mishra, D., Johansson, H.: Channel estimation and low-complexity beamforming design for passive intelligent surface assisted miso wireless energy transfer. In: ICASSP 2019-2019 IEEE International Conference on Acoustics, Speech and Signal Processing (ICASSP), pp. 4659–4663. IEEE, Piscataway (2019)
143. Zheng, B., Zhang, R.: Intelligent reflecting surface-enhanced ofdm: Channel estimation and reflection optimization. *IEEE Wireless Commun. Lett.* 9(4), 518–522 (2019)
144. He, Z.-Q., Yuan, X.: Cascaded channel estimation for large intelligent metasurface assisted massive mimo. *IEEE Wireless Commun. Lett.* 9(2), 210–214 (2019)
145. Elbir, A.M., Papazafeiropoulos, A., Kourtessis, P., Chatzinotas, S.: Deep channel learning for large intelligent surfaces aided mm-wave

- massive mimo systems. *IEEE Wireless Commun. Lett.* 9(9), 1447–1451 (2020)
146. Wang, Z., Liu, L., Cui, S.: Channel estimation for intelligent reflecting surface assisted multiuser communications: Framework, algorithms, and analysis. *IEEE Trans. Wireless Commun.* 19(10), 6607–6620 (2020)
 147. Zheng, B., You, C., Zhang, R.: Intelligent reflecting surface assisted multi-user ofdma: Channel estimation and training design. *IEEE Trans. Wireless Commun.* 19(12), 8315–8329 (2020)
 148. Yang, Y., Zheng, B., Zhang, S., Zhang, R.: Intelligent reflecting surface meets ofdm: Protocol design and rate maximization. *IEEE Trans. Commun.* 68(7), 4522–4535 (2020)
 149. Nadeem, Q.-U.-A., Kammoun, A., Chaaban, A., Debbah, M., Alouini, M.-S.: Intelligent reflecting surface assisted wireless communication: Modeling and channel estimation. *arXiv preprint arXiv:1906.02360* (2019)
 150. Mishra, D., Johansson, H.: Channel estimation and low-complexity beamforming design for passive intelligent surface assisted miso wireless energy transfer. In: *ICASSP 2019-2019 IEEE International Conference on Acoustics, Speech and Signal Processing (ICASSP)*, pp. 4659–4663. IEEE, Piscataway (2019)
 151. Zheng, B., You, C., Zhang, R.: Intelligent reflecting surface assisted multi-user ofdma: Channel estimation and training design. *IEEE Trans. Wireless Commun.* 19(12), 8315–8329 (2020)
 152. Wan, Z., Gao, Z., Alouini, M.-S.: Broadband channel estimation for intelligent reflecting surface aided mmwave massive mimo systems. In: *ICC 2020-2020 IEEE International Conference on Communications (ICC)*, pp. 1–6. IEEE, Piscataway (2020)
 153. Wang, P., Fang, J., Duan, H., Li, H.: Compressed channel estimation for intelligent reflecting surface-assisted millimeter wave systems. *IEEE Signal Process Lett.* 27, 905–909 (2020)
 154. He, Z.-Q., Yuan, X.: Cascaded channel estimation for large intelligent metasurface assisted massive mimo. *IEEE Wireless Commun. Lett.* 9(2), 210–214 (2019)
 155. de Araújo, G.T., de Almeida, A.L.: Parafac-based channel estimation for intelligent reflective surface assisted mimo system. In: *2020 IEEE 11th Sensor Array and Multichannel Signal Processing Workshop (SAM)*, pp. 1–5. IEEE, Piscataway (2020)
 156. Mirza, J., Ali, B.: Channel estimation method and phase shift design for reconfigurable intelligent surface assisted mimo networks. *IEEE Trans. Cognit. Commun. Networking* 7(2), 441–451 (2021)
 157. He, J., Leinonen, M., Wymeersch, H., Juntti, M.: Channel estimation for ris-aided mmwave mimo systems. In: *GLOBECOM 2020-2020 IEEE Global Communications Conference*, pp. 1–6. IEEE, Piscataway (2020)
 158. Cui, Y., Yin, H.: An efficient csi acquisition method for intelligent reflecting surface-assisted mmwave networks. *arXiv preprint arXiv:1912.12076* (2019)
 159. Wang, P., Fang, J., Duan, H., Li, H.: Compressed channel estimation for intelligent reflecting surface-assisted millimeter wave systems. *IEEE Signal Process Lett.* 27, 905–909 (2020)
 160. Chen, J., Liang, Y.-C., Cheng, H.V., Yu, W.: Channel estimation for reconfigurable intelligent surface aided multi-user mimo systems. *arXiv preprint arXiv:1912.03619* (2019)
 161. Hu, C., Dai, L., Han, S., Wang, X.: Two-timescale channel estimation for reconfigurable intelligent surface aided wireless communications. *IEEE Trans. Commun.* 69(11), 7736–7747 (2021)
 162. Liu, H., Yuan, X., Zhang, Y.-J.A.: Matrix-calibration-based cascaded channel estimation for reconfigurable intelligent surface assisted multiuser mimo. *IEEE J. Sel. Areas Commun.* 38(11), 2621–2636 (2020)
 163. Wei, L., Huang, C., Alexandropoulos, G.C., Yuen, C.: Parallel factor decomposition channel estimation in ris-assisted multi-user miso communication. In: *2020 IEEE 11th Sensor Array and Multichannel Signal Processing Workshop (SAM)*, pp. 1–5. IEEE, Piscataway (2020)
 164. Ning, B., Chen, Z., Chen, W., Du, Y.: Channel estimation and transmission for intelligent reflecting surface assisted thz communications. In: *ICC 2020-2020 IEEE International Conference on Communications (ICC)*, pp. 1–7. IEEE, Piscataway (2020)
 165. Ning, B., Chen, Z., Chen, W., Du, Y., Fang, J.: Terahertz multi-user massive mimo with intelligent reflecting surface: Beam training and hybrid beamforming. *IEEE Trans. Veh. Technol.* 70(2), 1376–1393 (2021)
 166. Khan, S., Khan, K.S., Haider, N., Shin, S.Y.: Deep-learning-aided detection for reconfigurable intelligent surfaces. *arXiv preprint arXiv:1910.09136* (2019)
 167. Elbir, A.M., Papazafeiropoulos, A., Kourtessis, P., Chatzinotas, S.: Deep channel learning for large intelligent surfaces aided mm-wave massive mimo systems. *IEEE Wireless Commun. Lett.* 9(9), 1447–1451 (2020)
 168. Taha, A., Zhang, Y., Mismar, F.B., Alkhateeb, A.: Deep reinforcement learning for intelligent reflecting surfaces: Towards standalone operation. In: *2020 IEEE 21st International Workshop on Signal Processing Advances in Wireless Communications (SPAWC)*, pp. 1–5. IEEE (2020)
 169. Taha, A., Alrabeiah, M., Alkhateeb, A.: Deep learning for large intelligent surfaces in millimeter wave and massive mimo systems. In: *2019 IEEE Global Communications Conference (GLOBECOM)*, pp. 1–6. IEEE, Piscataway (2019)
 170. Taha, A., Alrabeiah, M., Alkhateeb, A.: Enabling large intelligent surfaces with compressive sensing and deep learning. *IEEE Access* 9, 44 304–44 321 (2021)
 171. Alexandropoulos, G.C., Vlachos, E.: A hardware architecture for reconfigurable intelligent surfaces with minimal active elements for explicit channel estimation. In: *ICASSP 2020-2020 IEEE International Conference on Acoustics, Speech and Signal Processing (ICASSP)*, pp. 9175–9179. IEEE, Piscataway (2020)
 172. You, C., Zheng, B., Zhang, R.: How to deploy intelligent reflecting surfaces in wireless network: Bs-side, user-side, or both sides? *arXiv preprint arXiv:2012.03403* (2020)
 173. Han, Y., Zhang, S., Duan, L., Zhang, R.: Cooperative double-irs aided communication: Beamforming design and power scaling. *IEEE Wireless Commun. Lett.* 9(8), 1206–1210 (2020)
 174. Zheng, B., You, C., Zhang, R.: Double-irs assisted multi-user mimo: Cooperative passive beamforming design *IEEE Trans. Wireless Commun.* 20(7), 4513–4526 (2021)
 175. You, C., Zheng, B., Zhang, R.: Wireless communication via double irs: Channel estimation and passive beamforming designs. *IEEE Wireless Commun. Lett.* 10(2), 431–435 (2020)
 176. Li, Z., Hua, M., Wang, Q., Song, Q.: Weighted sum-rate maximization for multi-irs aided cooperative transmission. *IEEE Wireless Commun. Lett.* 9(10), 1620–1624 (2020)
 177. Zhang, S., Zhang, R.: Intelligent reflecting surface aided multi-user communication: Capacity region and deployment strategy. *IEEE Trans. Commun.* (2021)
 178. Wu, J., Shim, B.: Power minimization of intelligent reflecting surface-aided uplink iot networks. In: *2021 IEEE Wireless Communications and Networking Conference (WCNC)*, pp. 1–6. IEEE, Piscataway (2021)
 179. Lyu, J., Zhang, R.: Hybrid active/passive wireless network aided by intelligent reflecting surface: System modeling and performance analysis. *IEEE Trans. Wireless Commun.* 20(11), 7196–7212 (2021)
 180. Kishk, M.A., M.-S. Alouini: Exploiting randomly located blockages for large-scale deployment of intelligent surfaces. *IEEE J. Sel. Areas Commun.* 39(4), 1043–1056 (2020)
 181. Liu, X., Liu, Y., Chen, Y., Poor, H.V.: Ris enhanced massive non-orthogonal multiple access networks: Deployment and passive beamforming design. *IEEE J. Sel. Areas Commun.* 39(4), 1057–1071 (2020)
 182. Jia, C., Gao, H., Chen, N., He, Y.: Machine learning empowered beam management for intelligent reflecting surface assisted mmwave networks. *China Commun.* 17(10), 100–114 (2020)
 183. Björnson, E., Sanguinetti, L.: Power scaling laws and near-field behaviors of massive mimo and intelligent reflecting surfaces. *IEEE Open J. Commun. Soc.* 1, 1306–1324 (2020)
 184. Björnson, E., Özdoğan, Ö., Larsson, E.G.: Reconfigurable intelligent surfaces: Three myths and two critical questions. *IEEE Commun. Mag.* 58(12), 90–96 (2020)
 185. Elzanaty, A., Guerra, A., Guidi, F., Alouini, M.-S.: Reconfigurable intelligent surfaces for localization: Position and orientation error bounds. *IEEE Trans. Signal Process.* 69, 5386–5402 (2021)

186. Loyka, S.: Electromagnetic interference in wireless communications: behavioral-level simulation approach. In: IEEE 60th Vehicular Technology Conference, VTC2004-Fall, vol. 6, pp. 3945–3949. IEEE, Piscataway (2004)
187. de Jesus Torres, A., Sanguinetti, L., Björnson, E.: Electromagnetic interference in ris-aided communications. *IEEE Wireless Commun. Lett.* 11(4), 668–672 (2021)
188. Chu, Z., Zhu, Z., Zhou, F., Zhang, M., Al-Dhahir, N.: Intelligent reflecting surface assisted wireless powered sensor networks for internet of things. *IEEE Trans. Commun.* 69(7), 4877–4889 (2021)
189. Guan, X., Wu, Q., Zhang, R.: Anchor-assisted intelligent reflecting surface channel estimation for multiuser communications. In: GLOBECOM 2020-2020 IEEE Global Communications Conference, pp. 1–6. IEEE, Piscataway (2020)
190. Xia, S., Shi, Y.: Intelligent reflecting surface for massive device connectivity: Joint activity detection and channel estimation. In: ICASSP 2020-2020 IEEE International Conference on Acoustics, Speech and Signal Processing (ICASSP), pp. 5175–5179. IEEE, Piscataway (2020)
191. Jensen, T.L., De Carvalho, E.: An optimal channel estimation scheme for intelligent reflecting surfaces based on a minimum variance unbiased estimator. In: ICASSP 2020-2020 IEEE International Conference on Acoustics, Speech and Signal Processing (ICASSP), pp. 5000–5004. IEEE, Piscataway (2020)
192. Souto, V.D.P., Souza, R.D., Uchôa-Filho, B.F., Li, A., Li, Y.: Beamforming optimization for intelligent reflecting surfaces without CSI. *IEEE Wireless Commun. Lett.* 9(9), 1476–1480 (2020)
193. Abrardo, A., Dardari, D., Di Renzo, M.: Intelligent reflecting surfaces: Sum-rate optimization based on statistical position information. *IEEE Trans. Commun.* 69(10), 7121–7136 (2021)
194. Yigit, Z., Basar, E., Altunbas, I.: Low complexity adaptation for reconfigurable intelligent surface-based mimo systems. *IEEE Commun. Lett.* 24(12), 2946–2950 (2020)
195. Basar, E.: Reconfigurable intelligent surfaces for doppler effect and multipath fading mitigation. *arXiv preprint arXiv:1912.04080* (2019)
196. Matthiesen, B., Björnson, E., De Carvalho, E., Popovski, P.: Intelligent reflecting surface operation under predictable receiver mobility: A continuous time propagation model. *IEEE Wireless Commun. Lett.* 10(2), 216–220 (2020)
197. Tan, X., Sun, Z., Koutsonikolas, D., Jornet, J.M.: Enabling indoor mobile millimeter-wave networks based on smart reflect-arrays. In: IEEE INFOCOM 2018-IEEE Conference on Computer Communications, pp. 270–278. IEEE, Piscataway (2018)
198. Jamali, V., Tulino, A.M., Fischer, G., Müller, R.R., Schober, R.: Intelligent surface-aided transmitter architectures for millimeter-wave ultra massive mimo systems. *IEEE Open J. Commun. Soc.* 2, 144–167 (2020)
199. Wang, P., Fang, J., Yuan, X., Chen, Z., Li, H.: Intelligent reflecting surface-assisted millimeter wave communications: Joint active and passive precoding design. *IEEE Trans. Veh. Technol.* 69(12), 14 960–14 973 (2020)
200. Mao, Y., You, C., Zhang, J., Huang, K., Letaief, K.B.: A survey on mobile edge computing: The communication perspective. *IEEE Commun. Surv. Tutorials* 19(4), 2322–2358 (2017)
201. Cao, Y., Lv, T.: Intelligent reflecting surface enhanced resilient design for MEC offloading over millimeter wave links. *arXiv preprint arXiv:1912.06361* (2019)
202. Liu, Y., Zhao, J., Xiong, Z., Niyato, D., Yuen, C., Pan, C., Huang, B.: Intelligent reflecting surface meets mobile edge computing: Enhancing wireless communications for computation offloading. *arXiv preprint arXiv:2001.07449* (2020)
203. Bai, T., Pan, C., Deng, Y., Elkashlan, M., Nallanathan, A., Hanzo, L.: Latency minimization for intelligent reflecting surface aided mobile edge computing. *IEEE J. Sel. Areas Commun.* 38(11), 2666–2682 (2020)
204. Hua, S., Zhou, Y., Yang, K., Shi, Y., Wang, K.: Reconfigurable intelligent surface for green edge inference. *IEEE Trans. Green Commun. Networking* 5(2), 964–979 (2021)
205. Cui, T.J., Qi, M.Q., Wan, X., Zhao, J., Cheng, Q.: Coding metamaterials, digital metamaterials and programmable metamaterials. *Light Sci. Appl.* 3(10), e218–e218 (2014)
206. Liu, S., Cui, T.J., Zhang, L., Xu, Q., Wang, Q., Wan, X., Gu, J.Q., Tang, W.X., Qing, Q., Han, J.G., et al.: Convolution operations on coding metasurface to reach flexible and continuous controls of terahertz beams. *Adv. Sci.* 3(10), 1600156 (2016)
207. Li, L., Jun Cui, T., Ji, W., Liu, S., Ding, J., Wan, X., Bo, Li, Y., Jiang, M., Qiu, C.-W., Zhang, S.: Electromagnetic reprogrammable coding-metasurface holograms. *Nat. Commun.* 8(1), 1–7 (2017)
208. Ma, Q., Shi, C.B., Bai, G.D., Chen, T.Y., Noor, A., Cui, T.J.: Beam-editing coding metasurfaces based on polarization bit and orbital-angular-momentum-mode bit. *Adv. Opt. Mater.* 5(23), 1700548 (2017)
209. Liu, S., Cui, T.J.: Flexible controls of terahertz waves using coding and programmable metasurfaces. *IEEE J. Sel. Top. Quantum Electron.* 23(4), 1–12 (2016)
210. Zhang, L., Liu, S., Li, L., Cui, T.J.: Spin-controlled multiple pencil beams and vortex beams with different polarizations generated by pancharatnam-berry coding metasurfaces. *ACS Appl. Mater. Interfaces* 9(41), 36447–36455 (2017)
211. Shuang, Y., Zhao, H., Ji, W., Cui, T.J., Li, L.: Programmable high-order oam-carrying beams for direct-modulation wireless communications. *IEEE J. Emerging Sel. Top. Circuits Syst.* 10(1), 29–37 (2020)
212. Zhang, X.G., Jiang, W.X., Jiang, H.L., Wang, Q., Tian, H.W., Bai, L., Luo, Z.J., Sun, S., Luo, Y., Qiu, C.-W., et al.: An optically driven digital metasurface for programming electromagnetic functions. *Nat. Electron.* 3(3), 165–171 (2020)
213. Zhao, J., Yang, X., Dai, J.Y., Cheng, Q., Li, X., Qi, N.H., Ke, J.C., Bai, G.D., Liu, S., Jin, S., et al.: Programmable time-domain digital-coding metasurface for non-linear harmonic manipulation and new wireless communication systems. *Nat. Sci. Rev.* 6(2), 231–238 (2019)
214. Dai, J.Y., Zhao, J., Cheng, Q., Cui, T.J.: Independent control of harmonic amplitudes and phases via a time-domain digital coding metasurface. *Light Sci. Appl.* 7(1), 1–10 (2018)
215. Zhang, L., Chen, X.Q., Liu, S., Zhang, Q., Zhao, J., Dai, J.Y., Bai, G.D., Wan, X., Cheng, Q., Castaldi, G., et al.: Space-time-coding digital metasurfaces. *Nat. Commun.* 9(1), 1–11 (2018)
216. Zhang, L., Chen, X.Q., Shao, R.W., Dai, J.Y., Cheng, Q., Castaldi, G., Galdi, V., Cui, T.J.: Breaking reciprocity with space-time-coding digital metasurfaces. *Adv. Mater.* 31(41), 1904069 (2019)
217. Cui, T.-J., Liu, S., Li, L.-L.: Information entropy of coding metasurface. *Light Sci. Appl.* 5(11), e16 172–e16 172 (2016)
218. Cui, T.J., Liu, S., Zhang, L.: Information metamaterials and metasurfaces. *J. Mater. Chem. C* 5(15), 3644–3668 (2017)
219. Cui, T.J., Li, L., Liu, S., Ma, Q., Zhang, L., Wan, X., Jiang, W.X., Cheng, Q.: Information metamaterial systems. *Iscience* 23(8), 101403 (2020)
220. Dai, J.Y., Tang, W.K., Zhao, J., Li, X., Cheng, Q., Ke, J.C., Chen, M.Z., Jin, S., Cui, T.J.: Wireless communications through a simplified architecture based on time-domain digital coding metasurface. *Adv. Mater. Technol.* 4(7), 1900044 (2019)
221. Wan, X., Zhang, Q., Chen, T.Y., Zhang, L., Xu, W., Huang, H., Xiao, C.K., Xiao, Q., Jun Cui, T.: Multichannel direct transmissions of near-field information. *Light Sci. Appl.* 8(1), 1–8 (2019)
222. Cui, T.J., Liu, S., Bai, G.D., Ma, Q.: Direct transmission of digital message via programmable coding metasurface. *Research* 2019, 2584509 (2019)
223. Dai, J.Y., Tang, W., Yang, L.X., Li, X., Chen, M.Z., Ke, J.C., Cheng, Q., Jin, S., Cui, T.J.: Realization of multi-modulation schemes for wireless communication by time-domain digital coding metasurface. *IEEE Trans. Antennas Propag.* 68(3), 1618–1627 (2019)
224. Zhao, H., Shuang, Y., Wei, M., Cui, T.J., Hougné, P.D., Li, L.: Metasurface-assisted massive backscatter wireless communication with commodity wi-fi signals. *Nat. Commun.* 11(1), 1–10 (2020)
225. Zhang, L., Chen, M.Z., Tang, W., Dai, J.Y., Miao, L., Zhou, X.Y., Jin, S., Cheng, Q., Cui, T.J.: A wireless communication scheme based on space- and frequency-division multiplexing using digital metasurfaces. *Nat. Electron.* 4(3), 218–227 (2021)

226. Chen, M.Z., Tang, W., Dai, J.Y., Ke, J.C., Zhang, L., Zhang, C., Yang, J., Li, L., Cheng, Q., Jin, S., et al.: Accurate and broadband manipulations of harmonic amplitudes and phases to reach 256 qam millimeter-wave wireless communications by time-domain digital coding metasurface. *Natl. Sci. Rev.* 9(1), nwab134 (2022)
227. Wu, H., Bai, G.D., Liu, S., Li, L., Wan, X., Cheng, Q., Cui, T.J.: Information theory of metasurfaces. *Natl. Sci. Rev.* 7(3), 561–571 (2020)
228. Wu, H., Gao, X.X., Zhang, L., Bai, G.D., Cheng, Q., Li, L., Cui, T.J.: Harmonic information transitions of spatiotemporal metasurfaces. *Light Sci. Appl.* 9(1), 1–13 (2020)

How to cite this article: Hassouna, S., Jamshed, M.A., Rains, J., Kazim, J.R., Rehman, M.U., Abualhayja, M., Mohjazi, L., Cui, T.J., Imran, M.A., Abbasi, Q.H.: A survey on reconfigurable intelligent surfaces: Wireless communication perspective. *IET Commun.* 17, 497–537 (2023). <https://doi.org/10.1049/cmu2.12571>